To the Graduate Council:

I am submitting herewith a thesis written by Marc A. Klingshirn entitled "Synthesis, Characterization, and Performance Studies of Novel Anionic and Cationic Ion Exchange Resins." I have examined the final copy of this thesis for form and content and recommend that it be accepted in partial fulfillment of the requirements for the degree of Master of Science, with a major in Chemistry.

Spiro D. Alexandratos, Major Professor

We have read this thesis
and recommend its acceptance:

Accepted for the Council:

Associate Vice Chancellor and
Dean of the Graduate School

SYNTHESIS, CHARACTERIZATION, AND PERFORMANCE STUDIES OF NOVEL ANIONIC AND CATIONIC ION EXCHANGE RESINS

A Thesis

Presented for the

Master of Science

Degree

The University of Tennessee, Knoxville

Marc A. Klingshirn

May 2000

To Jennifer

ACKNOWLEDGEMENTS

I would like to thank first and foremost, Professor Spiro D. Alexandratos, for his guidance throughout the course of this work, and for his endless encouragement with my academic studies and for being a personal friend and confidant in difficult times. I would also like to thank Dr. Bruce A. Moyer and Wally Porter of the Oak Ridge National Laboratory for allowing me to perform work within their labs, and for their insightful thoughts and discussions about this work. In addition, I would like to thank Dr. Doug Gilman and Dr. Georges Guiochon for serving as my committee members.

The work contained here also would not have been possible without the help and support of my fellow group members Christy, Bob, Min, Stephanie, Subu, and Chris. You have all been great friends and co-workers. This work also would not have been possible without the love, support and encouragement of my parents and my other family members. A special acknowledgement is made to Jay, a friend who has given so much in so many times of need. Finally, I would like to thank the University of Tennessee, Department of Chemistry and the Department of Energy for financial support.

ABSTRACT

Binding constants were calculated for a novel class of ketophosphonate coordinating resins and their interactions with Eu (III) in 1 N HNO_3. These resins include α-ketophosphonic acid, β-ketophosphonic acid, γ-ketophosphonic acid and the parent phosphonic acid resin. Calculated binding constants indicate that as the length of the carbon spacer between the carbonyl and phosphoryl moieties is increased, the binding strength decreases. This is due to unstable ring formation upon chelation. The phosphonic acid resin gave results similar to those of the γ-ketophosphonate resin even though a ring is not formed upon complexation. This lack of ring formation is due to the absence of the carbonyl group.

Another aspect of the work involves studies with a novel class of quaternary ammonium resins. These resins possess quaternized trimethyl, triethyl, tributyl, and trihexyl groups. A bifunctional resin was also studied which utilized both quaternized trihexyl and triethyl groups. Contact studies were carried out with pertechnetate, perrhenate, iodide, nitrate, bromide, selenate and sulfate in various chloride and nitrate background matrices. Interactions with the monovalent anions showed that the resins with increased alkyl chain length favored ion exchange with the larger anions. This is due to the soft-soft interaction between the ligand and anion. Interactions with divalent anions showed a reversed trend having the trimethyl resin exchanging more than the trihexyl resin. This is due to the hard ligand, hard anion interaction. Uptake for the divalent anions was found to be low regardless of the resin used, since two active sites are needed for exchange rather than just one with the monovalent anions.

Previous studies conducted with these anion exchange resins showed that as the alkyl chain length within the resin is increased, the rate of exchange decreases. This was believed to be due to lack of hydration of the active site due to the increased hydrophilicity as the alkyl chain length is increased. Thermogravimetric analysis of the resins indicated that as the alkyl chain length is increased, the amount of water associated with the site is reduced. A correlation between exchange capacity and amount of water associated with the ligand was found. The amount of water associated with the active site was also found to change as the degree of functionalization and counter-ion is varied.

Even though these results prove our original hypothesis of active site hydration, kinetic studies in high ionic strength solutions showed that each of the resins, regardless of alkyl chain length, exhibited fast kinetics. This is believed to be due to the increased concentration of co-ion within the pores and their ability to help facilitate movement of the exchanging ion within the pores.

TABLE OF CONTENTS

LIST OF TABLES

LIST OF FIGURES

CHAPTER 1

INTRODUCTION

Due to their great versatility, ion exchange resins see use in many operations such as water purification, catalysis, decontamination of water-cooling systems, and separation science techniques such as chromatography. By far, though, ion exchange resins still have their most prominent use in purification of contaminated water and in environmental applications.[1]

The concept of ion exchange is by no means a new idea or concept. The technique has biblical references in Exodus 15: 23-25 when Moses implies the making of brackish water into that which is suitable for drinking. In more recent times, substances such as sand and soils have been found to be able to undergo ion exchange.[1] Substances such as these can be classified as inorganic ion exchangers. Another class of synthetic exchangers has also been developed. This class will be discussed later.

Contamination of the environment by hazardous substances has had a long history. It is believed that water contamination by lead may have caused the demise of the Roman Empire, since many of the wealthy emperors suffered from lead-induced psychoses.[2] However, it was not until the advent of the industrial revolution that the problem began to escalate and reach a severe level. With the onset of the Industrial Revolution and advances in medical science and public health, the population began to grow. Along with the population growth came increased industrial production and consumption, which also lead to, increased waste, some of which included toxic substances, both the inorganic and organic type.[2]

Mercury is one of the most toxic inorganic substances known to man. Depending on its form, it can cause paralysis and sensory loss, along with causing other illnesses such as Mad Hatter's Disease.[2] Other toxic species such as chlorinated organics have been used as pesticides and herbicides and have thus made their way into water supply.[2] Contaminants such as these have caused research to expand in the areas of water purification. The two most common methods used to deal with contaminated ground water systems include ion exchange resins and solvent extraction.

Ion exchange resins are commonly produced by suspension polymerization, quite often with polystyrene or divinylbenzene backbones. These supports are then reacted with various ligands. This allows for the ligand (extractant) to be covalently bound to the support. The contaminated water is then contacted with the resin, which then allows for the ion exchange or coordination of the toxic species. Ion exchange or coordination will occur depending on the type of ligand utilized and the matrix conditions. The metal ion can then be stripped from the resin with a suitable stripping agent.[3] In solvent extraction, an organic phase and the contaminated aqueous phase are present in a biphasic system.[4,5] Through agitation of the two phases, partitioning of the toxic substance from the aqueous phase into the organic phase is carried out. This is possible due the presence of an extractant within the organic phase that has a high affinity for the toxic substance of interest. The substance of interest can then be back extracted to reuse the receptor.

While both ion exchange and solvent extraction are common in environmental remediation, many advantages of ion exchange can be seen over solvent extraction. The first advantage is that the extractant is immobilized within the resin. It therefore cannot

gradually leach into the aqueous phase of the system. This is a problem in solvent extraction due to the extractants finite solubility in water. Another advantage is that ion exchange resins do not utilize large amounts of volatile, organic compounds, which must then be disposed of after treatment. This in turn creates large amounts of waste, which if not handled properly, may in itself pose an environmental threat. Finally, since the water in need of remediation usually possesses dilute quantities of toxic substances, solvent extraction is not practical due to the need for large amounts of extractant.[6] While the use of ion exchange resins has seen widespread use for the removal of toxic metal cations, not as much attention has been devoted to the removal of toxic metal and organic anions.

The first synthetic organic type ion exchange resins were developed by Adams and Holmes, two English chemists, and were found to possess better properties than any other products ever created or used. These resins were first improved upon by the Germans followed by the Americans and the English. The development and applications of ion exchange resins grew at such a rapid pace that theory was slow to be developed. In turn, the resins were used on an empirical basis, without knowing how to optimize selectivity, efficiency, or operating conditions.[1]

Two types of ion exchange resins are possible, anion and cation. In the work presented here, both types will be investigated. The cationic resins studied belong to a ketophosphonic acid resin family that operates by a coordination mechanism. The anion exchange resins belong to a strong base, quaternary ammonium family that have already seen use in environmental separations. Resins of the anionic exchange type, which primarily consists of amine-based ligands, will be discussed below for the separation of

noble metal ion, inorganic anion, and organic species. Prior to this, a presentation of the basics of anion exchange resins will be discussed.

Introduction to Anion Exchange Resins

Anion exchange resins are those resins that take part in removal of anions from solution. The anions may be of the common inorganic type, anionic noble metal complexes, or even ionized organics. They typically possess the following functionalities: $-NH_3^+$, $>NH_2^+$, $>N^+<$, or $>S-^+$,[1] although quaternary phosphonium groups are also possible.[7,8] Other ligands are capable of sorbing anions as well, but through coordination rather than ion exchange. Some examples of this coordination phenomenon are with various transition metal ions with ethylene diamine and p-dichlormethyl benzene copolymers[9] and with various transition metals with pendant N-sulfonyl-ethylenebis(dithiocarbamate) ligands bound to a polystyrene divinyl benzene support.[10] In some instances though, ion exchange groups can help facilitate coordination by allowing for ionization of other parts of the ligand.[11] The ligands can also be modified accordingly to enhance kinetics and selectivity. Selectivity is defined as the ability for the resin to preferentially choose one ion over another when in competition for the active site.

The resins can be of two broad structural types: gel or macroporous. Gel beads contain less crosslinking (lowest being 2 %) and are microporous. Macroporous resins possess a higher degree of crosslinking (lowest being 5 %) and contain large pores (on the order of 500Å). Resins can be designed with either structure, but this may play a role

in kinetics and capacity. Gel resins tend to have larger capacities due to lower crosslinking levels.

Anion Exchange Resins for Noble Metal Ion Separation

Sorptions of dicyanoaurate ($Au(CN)_4^{2-}$) anions have been studied extensively due to the desire for precious metal recovery. Two resins found to be selective for this anion use poly(vinylbenzyl chloride) crosslinked with 2 wt % divinylbenzene polymeric backbones. The first resin contained the N, N' –substituted amide of malonic acid with terminal guanidyl groups.[12](Fig. 1.1), while the second contained the N, N' –substituted amide of malonic acid with terminal imidazole groups.[12] (Fig. 1.2). The resin with terminal guanidyl groups was found to be selective for gold cyano complexes over silver (I) cyano complexes, zinc (II) cyano complexes, and copper (II) cyano complexes. The only metal cyano complex that showed any uptake besides the gold is the iron (II) and iron (III) cyano complexes. The resin containing the terminal imidazole groups was found to show selectivity for the gold cyano complex over all the metal cyano complexes mentioned previously.

An anion exchange resin has been developed by reacting tris (2,6, -dimethoxyphenyl) phosphine with chloromethylated polystyrene, that has been crosslinked with 3 % divinylbenzene. (Figure 1.3) The ligand was chosen due to its behavior in extraction systems.[13] Upon reaction with the polymer support, the resin utilizes a quaternary phosphonium group as the anion exchange site. The resin has shown selectivity toward noble metal anions such as $AuCl_4^-$ and $PtCl_6^-$ in 0.1 M

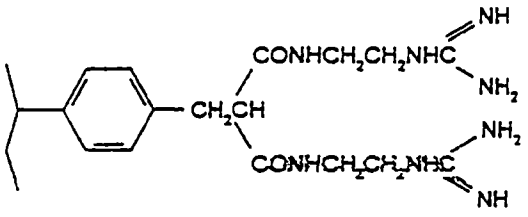

Figure 1.1 N, N' – substituted amide of malonic acid with terminal guanidyl groups

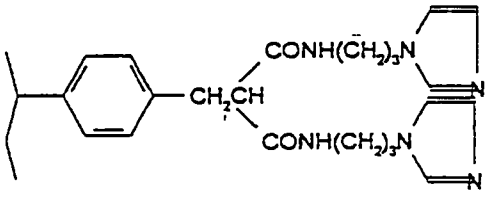

Figure 1.2 N, N' – substituted amide of malonic acid with terminal imidazole groups

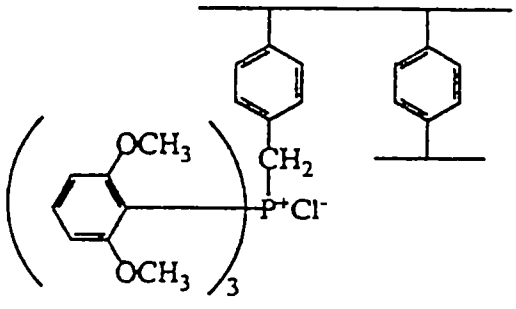

Figure 1.3 Immobilized tris(2, 6, - dimethoxyphenyl) phosphine on polystyrene

hydrochloric acid. Column studies were carried out, and it was found that $AuCl_4^-$ could be selectively separated from other complexes such as $CuCl_4^{2-}$ in 0.1 M hydrochloric acid solutions.

A novel 1,2,4,5 – tetrazine functionalized polymer has also been designed for removal of chloro complexes of the noble metals. (Figure 1.4) The resin utilizes an aminomethylated macroporous polystyrene copolymer crosslinked with divinyl benzene.[14] The resin acts as a weak base anion exchanger due to the protonation of the secondary amine group in the spacer chain under acidic conditions. The resin was found to show selectivity for common anions in the following order: $SO_4^{2-} > NO_3^- > PO_4^{3-} > Cl^- > F^-$. The resin also showed favorable sorption of metal chloro complexes due to the formation of ion pairs on the protonated secondary amine. In 1 M hydrochloric acid solutions, and a concentration of 1.0×10^{-3} M of each metal, the resin displayed the following selectivities for the metals respective chloro complex: Pd (II) > Au (II) >> Ir (IV) > Os (IV) > Pt (IV) > Ru (III) > Rh (III). In 1 M hydrochloric acid, approximately 93 % of the palladium complex had been removed, while only 20% had been removed of the rhodium complex. This selectivity was also seen in 0.1 M and 3.5 M hydrochloric acid solutions. Kinetic studies indicated that equilibrium is reached in about 24 hours after contact with the resin.[14]

Anion Exchange Resins for Inorganic Anion Removal

Polymer supported mercaptoacetimide on a polyethyleneimine backbone (Figure 1.5) has been found to interact with various arsenic anions, common byproducts of many

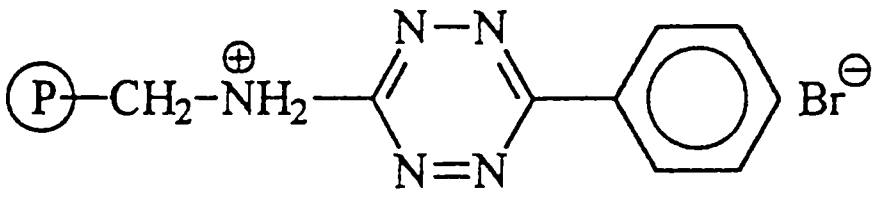

Figure 1.4 1, 2, 4, 5 – tetrazine modified ion exchange resin

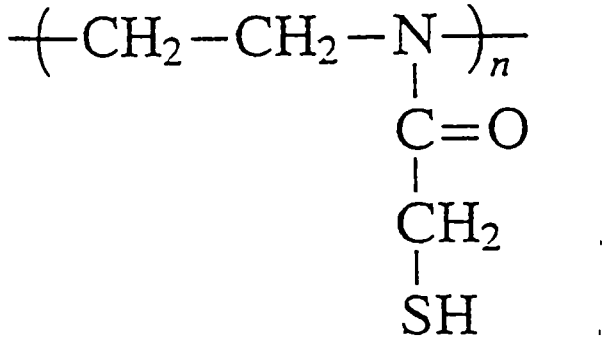

Figure 1.5 Poly(ethylene mercaptoacetimide)

different industrial processes. Sorption was found to occur by two different methods.[15] In basic conditions, arsenite anions are complexed by the terminal thiol groups. In acidic conditions, where the tertiary amine of the polymeric backbone is protonated, the resin is not only able to complex arsenic by the terminal thiol groups, but also by ion pair formation with the protonated amine. However, when salts are present in solution, the sorption of arsenate and arsenite are both dramatically reduced. Regeneration of the resin can be carried out by elution with 0.2 M NH_4OH. The oxidized thiol groups (disulfide) can be changed back to their original thiol groups by reduction with a 10 % sodium bisulfite solution.

Marsh et al. have designed a series of bifunctional anion exchange resins that have been found to be effective for the separation of plutonium in nitric acid matrices.[16] (Figure 1.6). These bifunctional resins differ in their design as compared to those developed by Alexandratos et al.[17] Alexandratos' resins are designed in such a way that two different ligands interact with one another in a synergistic fashion and are located on discrete pendent groups. Marsh's design is a derivative of Reillex 402, a poly 4-vinyl pyridine resin. Bifunctionality involves quaternizing the nitrogen of the pyridine ring with a spacer arm followed by an additional cationic site. Both cationic sites are capable of ion exchange.

The resins have been found to be selective for the di-anionic hexanitrato plutonium (IV) complex.[16] All of the resins showed greater uptake than the initial base poly 4 – vinylpyridine resin, while the ligands, which utilized longer spacer chains,

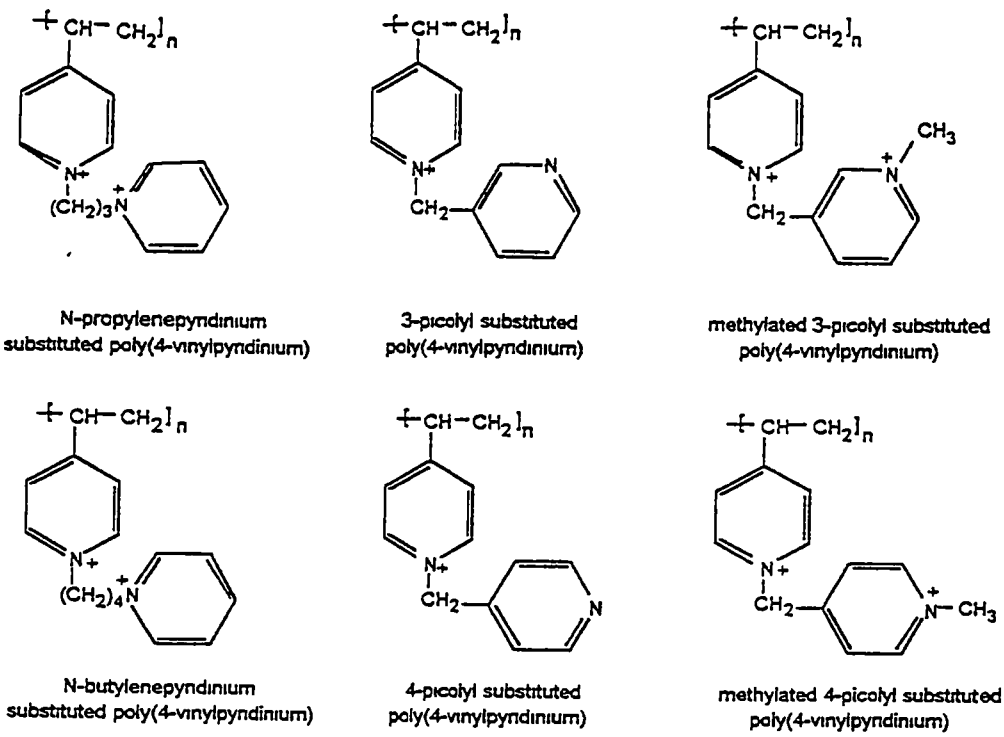

Figure 1.6 Bifunctional resins derived from poly(4 – vinylpyridine)

showed greater uptake of the plutonium complex. This is attributed to optimal energy configurations with less strain being present upon exchange.

Another interesting resin has been developed for the binding of the uranyl ion as $UO_2(CO_3)_3^{4-}$ in seawater. This has been reported by Jang et al.[11] Based from extraction behavior of 2, 2' –dihydroxyazobenzene (DHAB) and uranium species, DHAB and triethylamine groups were incorporated onto a partially chloromethylated polystyrene support. (Figure 1.7). While the quaternary amine groups do not appear to take part in the removal of the uranium carbonate complex, coordination of negatively charged carbonate complex takes place through the phenol groups and nitrogen groups of the DHAB species. The role of the quaternary amine groups are believed to help ionize the phenol groups of the DHAB moiety.

Natural seawater is approximately 1.4×10^{-8} M in the uranium carbonate ion and 2.5 mM in bicarbonate. Studies indicated that as the bicarbonate concentration is raised in the presence of 0.55 M chloride, affinity for the uranium ion increases. This is partially due to the loss of original chloride counter ion of the quaternary amine groups and replacement with bicarbonate ions. While results only indicated that approximately 10 μg of uranium ion per 1 g of resin could be removed, it is believed that the resin will need to be further modified to be more efficient.[11]

Ashley et al found that Reillex HPQ (Reilly Industries) is selective for the pertechnetate ion.[18] Reillex HPQ is made from a styrene and vinyl pyridine backbone. The pyridine is then methylated to create a strong base cationic site. The resin used in the studies consisted of 75 % strong base methylated pyridinium sites and 25 % weak base,

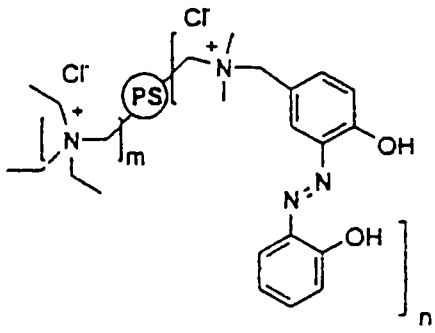

Figure 1.7 DHAB and triethyl amine groups incorporated onto a polystyrene support

protonated pyridinium sites. (Figure 1.8) The resin was initially in its chloride form but was converted to the nitrate form with 0.1 M nitric acid. Kinetic studies showed equilibrium being reached between 10 and 30 minutes from a 3.75×10^{-6}M pertechnetate solution in 2 M nitric acid. Kd values (distribution coefficients) were found to increase by a factor of 300 as the molar concentration of nitric acid decreased to 0.001 N. Distribution coefficients are ratios of the moles of sorbed species per gram of dry resin to moles of species remaining per mL of solution.

Wu et al. expanded the scope of anion interactions with Reillex HPQ by studying its interaction with various halide ions in nitric acid concentrations of 0.01 M to 1.00 M.[19] The results were then compared to those of pertechnetate to determine if the presence of halide ions would interfere with the sorption of pertechnetate. Studies with chloride (resin in nitrate form) indicated that no measurable uptake of chloride was seen in nitric acid concentrations above 0.01 M with a chloride concentration of 2.50×10^{-4} M. Uptake in 0.01 M nitric acid was minimal. Studies with bromide and iodide in three different experiments using three different concentrations in each experiment indicated that as the concentration of halide ions increased, the distribution coefficient decreased. It was also found that as the nitric acid concentration was increased from 0.01 M to 1.00 M, the distribution coefficients decreased. This exhibits the same trend as seen with pertechnetate, but distribution coefficients for pertechnetate exceed those of bromide and iodide in the most concentrated halide solution and weakest acid concentration by a factor of nearly 500. Based on these experiments, it can be concluded that the presence of halide ions will not interfere with the uptake of pertechnetate.[19] Studies have also been

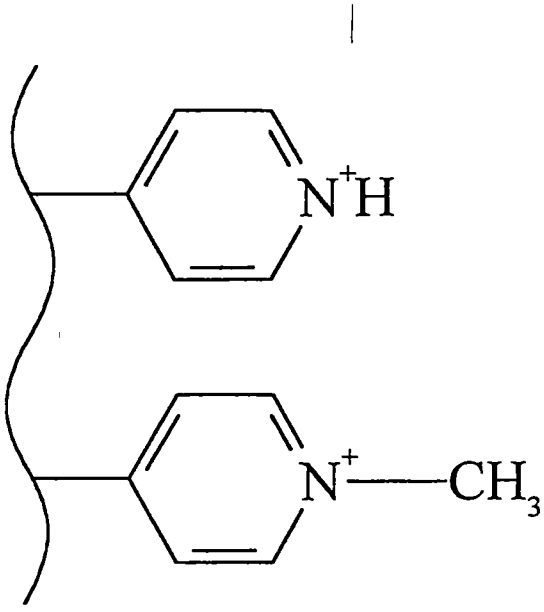

Figure 1.8 Methylated/ protonated poly(4-vinylpyridine)

carried out that analyze for the interaction of the resin with perrhenate and oxochromium (VI) species.[20] Kd values indicate that selectivity will follow the following order: TcO_4^-, ReO_4^-, chromium (VI) species, and halides.

Anion Exchange Resins for Organic Species Separation

Organic species separations by anion exchange resins have not been studied extensively. However, certain types of organic compounds are well suited for separation by ion exchange. Gaikar and Maiti reported that napthenic acids are capable of being recovered by using weak base anion exchange resins and also a strong base anion exchange resin with a quaternary ammonium group.[21] While the weak base resin permitted adsorption through the mechanism of hydrogen bonding, the strong base resin allowed for uptake by utilizing an ion-dipole interaction. Their studies concluded, though, that even though equilibrium constants were higher for the strong base resin indicating a stronger interaction, the use of the weak base resin is more suited for use in this recovery. This was found due to a higher loading capacity of the resin, which allowed twice the amount of loading as compared to the quaternary amine resin.[21]

Phenols exist in wastewater due to industrial settings such as oil refineries, coke plants, and phenolic resin plants.[22] Phenols are toxic compounds but are suitable for separation by the use of anion exchange resins. Lee and Ku reported that Purolite A-510 is effective in the separation of various types of phenols.[22] Purolite A-510 incorporates a quaternary ammonium site onto a polystyrene- divinylbenzene macroreticular resin. The quaternized ammonium group is formed with the following features:

$R(CH_3)_2(C_2H_4OH)N+$, where R designates the polymeric backbone. The following were studied: phenol, 2-chlorophenol, 2, 4-dichlorophenol, and 2, 4, 6-trichlorophenol. Studies showed effective removal under alkaline conditions leading toward the ion exchange with the deprotonated phenol and also hydrophobic interactions between the phenol and the styrene backbone. The extent of ion exchange was followed by determining the increase in free chloride content in solution, while it was assumed that the remaining uptake of phenol was through physical adsorption onto the resin. It was found that uptake increased as the degree of chlorine substitution upon the substrate increased. When background salt was introduced into the matrix, the background chloride interfered with the ion exchange mechanism, thus forcing the adsorption of the phenols to take place through the physical adsorption mechanism.[22]

A resin containing a quaternary ammonium group consisting of $(CH_3)_2(C_2H_4OH)N+$ was also shown to be effective in the separation of carboxylic acids.[23] The salt forms of butyric, hexanoic, octanoic, nonanoic, and decanoic acid was used for equilibration studies. Experiments involved equilibration with low concentrations of the respective salt, followed by gradual increases in salt concentrations allowing for equilibration at each step. Results indicate that the resin showed greater affinity for those acids with longer carbon chains. This is believed to occur due to structural differences in the water inside the resin and in the bulk solution, and also due to hydrophobic interactions between the long carbon chains and the styrenic backbone. Hydrophobic interaction between the chains may also play a role in their increased uptake.[23]

Presentation/ Goals of the Project

Our project encompasses the use of resins that are effective for the removal of both anions and cations. A new family of coordinating resins that possesses ketophosphonate ligands has been developed. This type of ligand utilizes a phosphoryl and carbonyl moiety for complexation. Studies with soluble ketophosphonates have been found to act as strong metal ion-complexing agents. To further understand the binding abilities of each of these resins in a more quantitative and thermodynamic nature, a method has been developed which quantifies the binding strength in terms of a binding constant. The studies involve the complexation of europium in 1 N HNO_3. We plan to prove in a quantitative manner, that as the spacer chain between the phosphoryl and carbonyl moieties increases, the stability of the resulting complex decreases.

Another aspect of our study deals with anionic exchange resins. Amine-based anion exchange resins are abundant in their use in environmental remediation. However, many of these resins have poor selectivity. The amine resins described here couple high selectivity with good kinetics. A series of monofunctional resins have been synthesized with trimethyl, triethyl, tributyl and trihexyl amine groups. A special bifunctional resin derived from a triethyl amine and a trihexyl amine has also been developed and has been found to possess excellent selectivity and fast kinetics. Initial studies with the bifunctional amine resin and pertechnetate showed favorable results.[24] The resin has been found to perform better than any other resin that is currently commercially available. It is believed that the incorporation of the long trihexyl groups allow for greater selectivity, while the presence of triethyl groups help to improve kinetics. Promising results from

previous studies with pertechnetate and this particular bifunctional resin have led to more investigations with other anionic species. These species include both monovalent and divalent type anions.

We plan to synthesize all the monofunctional resins mentioned previously along with the bifunctional resin discussed. Tests will be carried out with various anions in different chloride matrices. A comparison of sorption abilities will be presented along with determination of trends.

As mentioned before, problems with kinetics are seen with resins that contain long alkyl groups within the ligands, while fast kinetics are seen with short alkyl chains. The reason for this is believed to be the amount of hydration of the active sites. Short alkyl chains are more hydrophilic allowing for the presence of water to be favorable. Conversely, long alkyl chains create a more hydrophobic environment. There is believed to be a direct correlation between the hydration of the active site and the rate of kinetics. We plan to study the family of monofuctional resins along with the bifunctional resin described previously for their water content. The experiments will be carried out using thermogravimetric analysis.

Our main goal is to design an experiment that will allow for the determination of different water types within the resin. It is thought that at least two major types of water are present, the first which fills the macropores of the resin, and the second type that hydrates the active site and the polymeric backbone. We plan to show a correlation between the length of alkyl chain and the amount of water within the resin and also to gain a better understanding of the overall water structure within the resin. In addition, the

effect of ligand density and counter ion will be studied. Results will be discussed thoroughly.

CHAPTER 2

Adsorption Isotherm Studies: The Determination of Binding Constants for Ketophosphonate Cation Exchange Resins

Introduction

Ion exchange isotherms are the most common experimental technique used to study the binding strength of ion exchangers. These isotherms have been applied to many different materials including synthetic zeolites, minerals and ion exchange resins to calculate the equilibrium constants of the systems. It is important to understand the exchange properties of these substances since the information gained can ultimately be applied to problems such as separation, strategic recovery, or sorption of radionuclides.[25] These isotherms can be also used to study the ligand-substrate interaction or to probe the effect of various microenvironments on the ligand-substrate interactions.[26]

Recently, Alexandratos, et al. have studied the interaction of various substrates with the ligand bound to various types of polymer supports with the use of Langmuir isotherms. It was found that the binding constants varied with the type of substrate studied and the type of polymer backbone used. The conclusions were drawn by comparing the binding constants with the Hammett constants of the different species, which gives a measure of the ability of each substrate to act as an electron donor or acceptor. A linear correlation of the binding constant with the Hammett constants gives a slope that is a measure of the effect of the different polymeric backbones on the ligand-substrate interaction. Polymeric backbone flexibility, polarity and other parameters were

found to influence the substrate-ligand interaction. In all experiments correlations of 0.99 or greater were found when the Langmuir isotherms were applied.[26]

In this work we studied a novel class of coordinating resins that possessed keto-phosphonate groups (see Figure 2.1 for resin structures). Previous work with these resins involved determining the affinity for various metal ions (Eu (III), Cu (II), Pb (II), Cd (II), Co (II), and Ag (I) in different concentrations of nitric acid (0.01 N, 0.10 N, and 1.0 N). In dilute concentrations of nitric acid, it was determined that ion exchange was the predominant sorption mechanism. However, when the concentration of nitric acid was increased to 1.0 N, the ion-exchange mechanism was negated, and coordination became the sole mechanism of sorption. At this concentration, the background acidity is high enough to counter the ion exchange mechanism, but low enough that protons were not coordinated to the carbonyl and phosphoryl moieties. The high concentration of protons shifts the equilibrium of the phosphonic acid group back to its unionized form. Under these conditions, Eu (III) exhibited the highest uptake with the α-ketophosphonic acid resin, followed by the β-ketophosphonic acid, γ-ketophosphonic acid and finally the phosphonic acid resin. This trend was seen in all instances regardless of the metal ion or nitric acid concentration studied.[27] The affinities of the resins can be explained by the stability of the rings formed upon complexation of the metal ion. The α-keto resin forms a stable five membered ring upon complexation, followed by the β-keto forming a six membered ring and finally with the γ-keto resin forming an unstable seven membered ring. The poor phosphonic acid complexation ability is due to the sole existence of the phosphoryl moiety and the lack of ring formation.

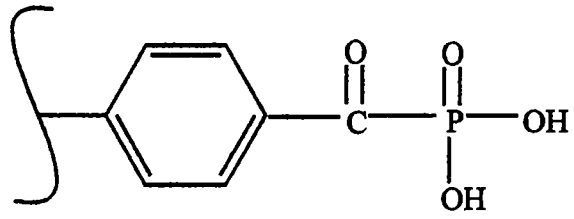

alpha-ketophosphonic acid

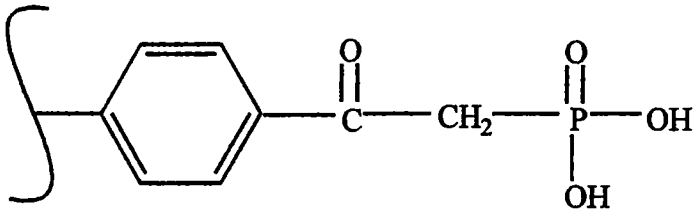

beta-ketophosphonic acid

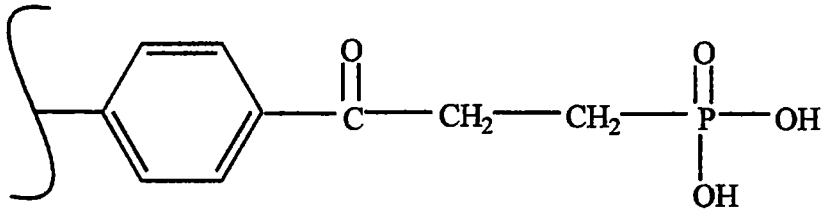

gamma-ketophosphonic acid

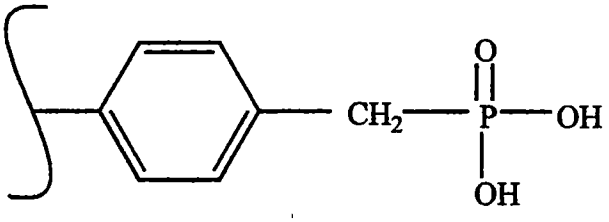

phosphonic acid

Figure 2.1 Polymer supported phosphonic acid resins

In this work, we plan to further quantify the complexing abilities of each of these resins with Eu (III) in 1 N nitric acid. We will do this by applying various types of Langmuir isotherms to each of the resin systems and determining the binding constants. It is expected that the binding constants will reiterate the trend seen before in terms of removal, with the α-keto resin exhibiting the highest binding constant and the phosphonic acid resin exhibiting the lowest binding constant.

Mathematical Background

Binding constants between various ketophosphonic acid resins were calculated to help determine subtle changes within the microenvironment of the resins. The binding constant represents the equilibrium constant for the interaction between the ligand and the substrate, in this case, europium ions. This is shown by the following equation:

$$L + S \Leftrightarrow LS \qquad (2.1)$$

with the equilibrium constant for a 1:1 complex represented as

$$K = [LS] / ([L][S]) \qquad (2.2)$$

where [LS] is the equilibrium concentration of the ligand-substrate complex, [L] is the concentration of unbound ligand, and [S] is the concentration of unbound substrate.

A method for equilibrium constant determination involves contacting a given amount of ligand with various concentrations of substrate in solution.[28] Upon equilibration, the remaining substrate is quantified to determine the amount of substrate bound by the ligand. Once the solution is analyzed, r (mequiv bound per gram of dry resin), and c (mequiv free per mL of solution) are calculated and later used for binding

constant determination. An r vs. c plot represents the binding isotherm for the system. This binding isotherm, commonly referred to as a Langmuir isotherm,[29] is expressed mathematically by the following equation:

$$r = Kc / (1+ Kc) \qquad (2.3)$$

This isotherm represents a portion of the rectangular hyberbola,[29] which is described mathematically by the following equation:

$$r = (S_t c)/ (K^{-1} + c) \qquad (2.4)$$

where S_t represents the saturation capacity (r_{max}) of the resin. The saturation capacity represents the total number of ligands available, complexed and noncomplexed (assuming 1:1 stoichiometry), and can be expressed by the following:

$$S_t = [L] + r \qquad (2.5)$$

A significant portion of the isotherm must be examined in order to estimate the saturation capacity.[30] By using the iterative solution of the rectangular hyperbolic equation and fitting the experimental points to the curve, the binding constant can be determined.

Deranleau suggests that only 20 %-80 % of the S_t should be used to calculate the binding constant, since the degree of saturation dictates the relative error. It has been shown that the relative error increases significantly when the 20 %-80 % constraint is not followed.[30] Upon evaluation of the binding constants for these studies, it has been found though, that this may not represent the best treatment since non-converging values were obtained.

An assumption made when using the Langmuir isotherm is that all of the binding sites within the resin behave in the same manner. Although theoretically this assumption

can be made, it is highly improbable that this is the case. Let us consider the environment created during the polymerization process. Cross-linking differences, different reactivity ratios of monomers (if copolymers are being used), and porosity variations within the resin will all play a role in the accessibility of the ligand. Ligands within heavily cross-linked areas may not be able to obtain the proper orientations necessary for the interaction with the metal ion to occur. Also, if copolymers consisting of two or more types of monomers are used as the backbone for the ligand, regions of greater hydrophobicity may be formed which would not allow proper solvent stabilization of the ligand. This, in turn, will cause a decrease in interaction strength with the metal ion. Porosity variations within resins, or from batch to batch, may also dictate the interaction of the ligand with the substrate. When considering each of these factors, it is logical to believe that each ligand has its own specific binding constant due to its slightly different microenvironment.

The presence of non-uniform ligand behavior cannot be seen directly by simple inspection of the binding isotherm (r vs. c plot). X- reciprocal plots (r/c vs. r), however, can be used to distinguish the weaker interacting ligands.[29,31] The equilibrium expression can be restated mathematically in the following manner:

$$K = r/([L]\,c) \qquad (2.6)$$

where [LS] has been replaced by r and [S] has been replaced by c. This equation can then be rearranged to give the following expression:

$$r/c = K\,[L] \qquad (2.7)$$

By substituting the saturation capacity expression into the above, the rearranged equilibrium expression is given as:

$$r/c = K(S_t - r) \qquad (2.8)$$

or

$$r/c = -Kr + KS_t \qquad (2.9)$$

If all the ligands within the resin behave identically, a straight line with a slope of -K is obtained from the x-reciprocal plot. The saturation capacity can be obtained from - intercept/slope.

If the ligands do not behave in a similar manner, then a curved line is found. This curved line can be expressed by the following equation

$$r = \Sigma \{(K_i c) / (1 + K_i c)\} \qquad (2.10)$$

where there are i sites with binding constant K_i. If a tangent is drawn to each point on the curve, the negative slope of each tangent would represent the binding constant for that particular site. Since the determination of an infinite number of binding constants would yield useless information in terms of a general characterization parameter, a different treatment is performed.

In these plots, a curve is obtained that consists of two portions that run asymptotically with the x and y axis. This curve can be reduced into two major portions representing a general class of strong binding sites and a general class of weak binding sites within the resin.[29,31] The curved x-reciprocal plot can be described mathematically by a double rectangular hyperbola which is given by the following equation

$$r = [(S_{t1}\, c) / (K_1^{-1} + c)] + [(S_{t2}\, c) / (K_2^{-1} + c)] \qquad (2.11)$$

S_{t1} and S_{t2} represent the saturation capacities for the two binding sites, and K_1 and K_2 (the respective binding constants). The binding constants and saturation capacities can be

determined from the iterative solution of the double rectangular hyperbolic equation. When treated graphically, the binding constant and saturation capacities can be determined by creating two intersecting straight lines from the curve, which best approximates the two sets of binding sites.

The binding constants can also be determined from the iterative solution of triple or quadruple rectangular hyperbolic equations. When treated in this manner, three and four different classes of binding constants and saturation capacities can be calculated respectively. It is reasonable to believe that this treatment may allow one to better classify the different interactions between the ligand and metal ion and this was examined with the data generated in the experiments reported in this thesis.

Experimental

Resin Synthesis

See experimental section for complete synthesis procedures.

Binding Constant Studies

Enough buchner dried resin to give 1 mequiv of active site was weighed into an appropriately labeled 25 mL scintillation vial. The following equation was used to calculate the appropriate amount of wet resin

$$(1 \text{ mequiv } (\text{Phosphorus Capacity})^{-1})/ (\%\text{-solids}/ 100)$$

where the phosphorus capacity is in mequiv/ g. This was repeated for twelve separate vials. The resin in each of the vials was then solvent exchanged 3 times with 1 N nitric

acid. This was done by adding approximately 10 mL of acid to each of the vials containing the resin. The resin was agitated thoroughly by placement on a wrist action shaker for 15 minutes. The acid was then carefully removed by using a small, glass, disposable pipette and suction, taking care not to remove any resin in the process. Approximately 10 mL of acid was again added to the resin and the procedure repeated 2 additional times.

A 10 mL volume of the metal ion solution (europium in these studies) was volumetrically pipeted onto each of the resins. The concentrations used were: 0.005 N, 0.01 N, 0.025 N, 0.04 N, 0.06 N, 0.075 N, 0.1 N, 0.15 N, 0.175 N, 0.2 N, 0.25 N and 0.3 N. These twelve concentrations were chosen to cover a range of concentrations, both dilute and concentrated. The vials were placed on a wrist action shaker to allow for agitation for 17 hours. Following contact, the metal ion solutions were carefully drawn off each of the resins and placed into a new, clean, appropriately labeled 25 mL scintillation vial. These solutions were diluted as needed to fit within the linear range of the atomic absorption spectrometer (Perkin-Elmer 3100). Absorbance readings were used to determine the percent metal absorbed in each of the solutions.

Ten-fold Dilution Studies

The procedure was followed as described above, except the 1 mequiv of resin was accurately weighed into a 100 mL jar rather than a 25 mL scintillation vial. The metal ion solution was prepared in the following manner. A 10 mL volume of the respective metal ion solution (once again europium) was volumetrically pipeted into a 100 mL volumetric

flask. The flask and was diluted to the mark with 1 N nitric acid and mixed thoroughly. The solution was then poured into the jar containing the resin and placed on the wrist action shaker for 17 hours. After contact, the contacted metal ion solution was drawn off, diluted as needed with the remaining europium concentration determined by atomic absorption.

Mathematical Procedure for Calculation of Binding Constants

A modified version of Sigma Plot was used to determine the saturation capacities and binding constants for each of the systems. The initial ratios, wet weight of resin, and percent absorbed were initially entered into the spreadsheet. Various transforms, which were specifically written for the program, were then used to calculate the dry weight of the resin, mequiv absorbed, mequiv free, r, c, c/r and r/c. This data was then subjected to various curve fits that included single, double, triple and quadruple Langmuir isotherms. X-reciprocal plots were also plotted for each of the systems.

Results

It must be noted that since double, triple and quadruple Langmuir isotherms give 2, 3 and 4 binding constants and saturation capacities respectively, only the first binding constant will be discussed for the resins. Indeed, the first binding constant represents the strongest binding sites within the resin and is of greatest interest if it represents a significant portion of the saturation capacity. The latter constants that are calculated represent the rest of the sites that are weakly complexing.

α-Ketophosphonic Acid Resin

The α-ketophosphonic acid resin showed the greatest affinity for europium of all the resins studied. The complexation abilities of the resin are due to the electron donating abilities of the carbonyl and phosphoryl oxygen, and the close proximity of the two groups to one another. Upon complexation, the complex formed between the metal ion and the two oxygen moieties allow for the formation of a stable, 5 membered, ring which is entropically favorable[32]. Tables 2.1 and 2.2 show percent absorbed and raw data for each of the data sets. Percent absorbed ranged from approximately 97 % for the 0.005 N solution to approximately 29 % for the 0.3 N solution. Two different batches of resins were used for the two trials with reproducibility between trials yielding percent absorbed values that were within 10% of each other.

Tables 2.3 and 2.4 show the binding constants, saturation capacities and correlations when the various Langmuir treatments are applied. As can be seen, the first binding constant calculated using the single Langmuir isotherm is very low when compared to the other treatments. It is also important to notice the poor correlation. This observation indicates that using the single Langmuir isotherm does not best represent the data. However, the correlation increases when higher order isotherms are applied. Also, the binding constant and saturation capacities calculated are nearly identical for the double, triple and quadruple Langmuir treatments. As can be seen in this data set, and as will be seen in other data sets, the binding constants, saturation capacities, and correlations do not improve once triple and quadruple Langmuir

Table 2.1 Raw Data for Alpha-ketophosphonic acid (Trial 1)
Run Code: MK-01-062

initial ratio	dry wt. (g)	% absorbed	r (mequiv./g)	c (mequiv/mL)
0.05	0.3194	96.48	0 1510	1 7600E-04
0 10	0.3194	93 61	0 2930	6.3900E-04
0 25	0 3195	81 32	0.6363	4.6700E-03
0 40	0.3195	67 11	0.8402	0 0132
0 60	0.3194	55.96	1 0511	0.0264
0 75	0 3195	56.36	1.3229	0 0327
1 00	0 3195	42 37	1 3261	0.0576
1 50	0.3195	44 12	2.0715	0 0838
1.75	0.3196	30 32	1 6604	0.1219
2.00	0 3195	29 33	1 8361	0 1413
2 50	0 3194	23 58	1.8457	0.1911
3.00	0 3195	28 67	2.6922	0.2140

Table 2.2 Raw Data for Alpha-ketophosphonic acid (Trial 2)
Run Code: MK-01-065

initial ratio	dry wt. (g)	% absorbed	r (mequiv./g)	c (mequiv/mL)
0.05	0.3247	96.61	0.1488	1 6950E-04
0.10	0.3247	94 22	0.2902	5.7800E-04
0.25	0 3246	84.97	0.6544	3.7575E-03
0 40	0 3247	72.71	0.8957	0 0109
0.60	0.3246	58 44	1 0801	0.0249
0 75	0.3246	58.67	1.3555	0.0310
1 00	0.3247	43 99	1 3549	0.0560
1.50	0.3247	34.56	1 5967	0.0982
1.75	0.3246	33.29	1 7946	0 1167
2 00	0.3246	27 04	1 6661	0 1459
2.50	0 3246	28.02	2.1578	0 1800
3 00	0 3247	28.47	2.6307	0.2146

Table 2.3 Binding Constants and Saturation Capacities of MK-01-035 (Trial 1)

Mathematical Treatment	K_1 (N^{-1})	St_1 (mequiv/ g)	Correlation
Single Langmuir	35.5	2.39	0.867
Double Langmuir	227	1.18	0.905
Triple Langmuir	253	1.14	0.905
Quadruple Langmuir	231	1.17	0.905

(See Figure 2.2 for Saturation Curves and X-reciprocal Plot)

Table 2.4 Binding Constant and Saturation Capacities of MK-01-054 (Trial 2)

Mathematical Treatment	K_1 (N^{-1})	St_1 (mequiv/ g)	Correlation
Single Langmuir	41.6	2.30	0.865
Double Langmuir	612 *	0.989 *	0.969
Triple Langmuir	612 *	0.989 *	0.969
Quadruple Langmuir	612 *	0.989 *	0.969

* Non-converging value.

(See Figure 2.3 for Saturation Curves and X-reciprocal Plot)

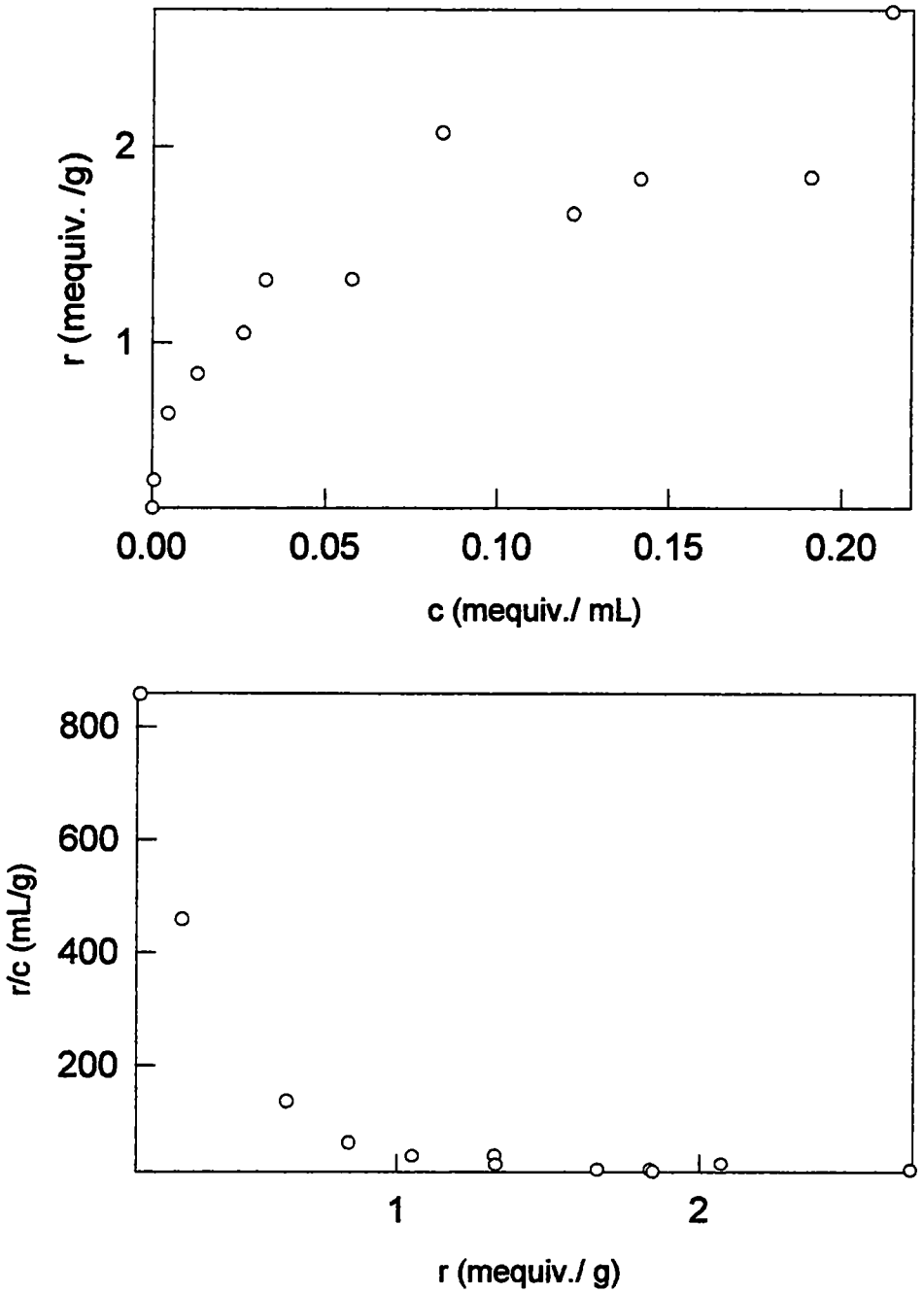

Figure 2.2 Alpha-keto Phosphonic Acid (Trial 1)

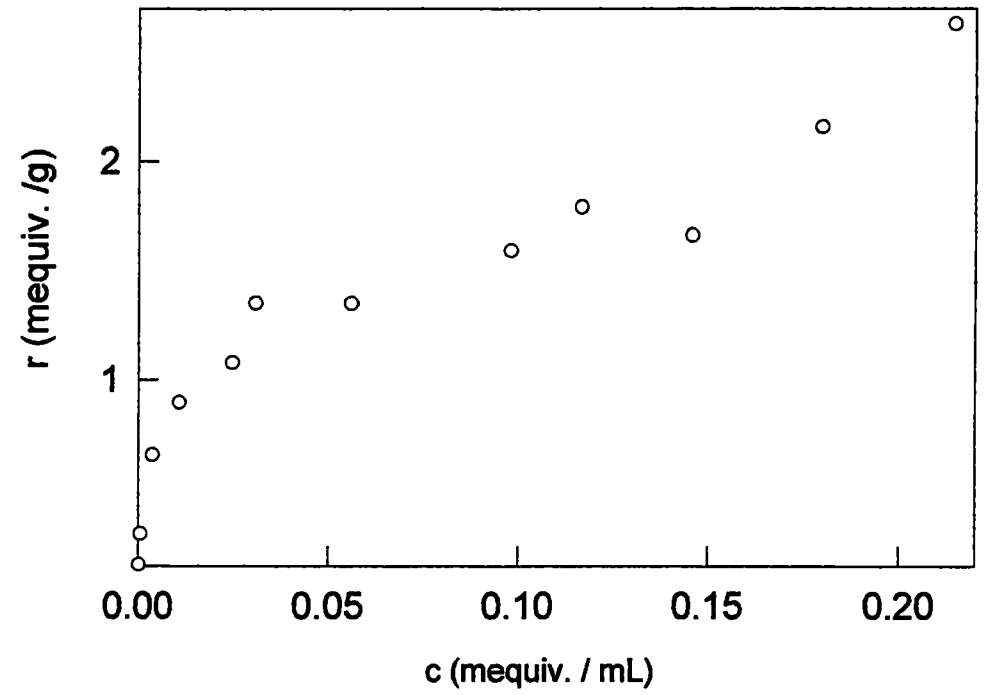

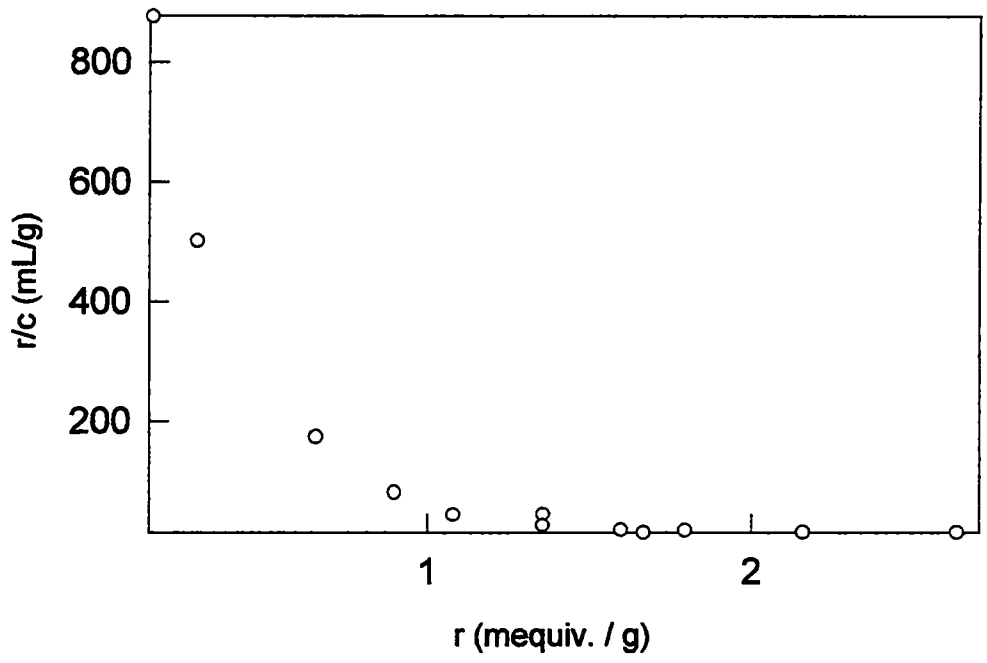

Figure 2.3 Alpha-keto Phosphonic Acid (Trial 2)

isotherms are applied. Consistency is seen with those calculated using the double Langmuir, with the exception being with the phosphonic acid resin. This gives an indication that the double Langmuir treatment best represents the data since it is the simplest isotherm that can be applied. Since this trend is seen, results from the triple and quadruple Langmuir treatments will be omitted for the beta and gamma-keto resins. It is still unclear at this time why the computer is incapable of converging in certain calculations. If it is recalled that the method of computing the binding constant is through an iterative process and fitting the data to the respective equation, the error indicates the computer's lack of convergence on a final value. While it is not evident with this particular resin, it will be seen with other resins that values very similar to non-converging values for higher ordered isotherms will be found. This gives an indication that these non-converging values are indeed good representations of the resin's binding ability. Overlooking these errors, if the binding constants and saturation capacities are compared individually, reproducibility does not appear to have been achieved. However, if the binding constants are coupled with the their respective saturation capacity, the lower saturation capacity gives the higher respective binding constant which corresponds to the steeper slope of the drawn tangent. It must be noted that the binding constant and respective saturation capacity must be considered together. If this is not done, a false interpretation of the resin's performance will be made.

If the x-reciprocal plots are examined, smooth curves are seen which would indicate that a single Langmuir would not best represent the data, rather some higher

order isotherm. The shape of the curve is very important since it shows the many different types of actives sites within the resin.

Ten-fold dilution studies were carried out to determine if non-ideal solutions were the cause of non-reproducibility. To test this hypothesis, 10-fold dilution experiments were carried out with the normal –40 + 60 mesh width (425μm-250μm) along with –100 + 200 mesh width (150μm-75μm). The total volume contacted with 1 mequiv of active site was 100 mL. Unlike previous experiments, the results obtained indicated that equilibrium was not reached during the normal contact time. (See Tables 2.5 for percent absorbed values.) In the study which tested the –40 + 60 mesh resins, percent absorbed of europium metal was about half what was seen in the original study for the more concentrated solutions. This indicates that the ability of the resin to cover the ten-fold increase in volume decreases the ability to complex the metal within a 17 hour contact time. To test if further metal uptake was found at longer contact times, four solutions were chosen and allowed to contact for an extended period of time. Gradual increases in uptake were seen for these samples contacted for extended periods. Because of these results, the binding constant calculations were not carried out.

The studies that utilized the –100 + 200 mesh size beads showed equally perplexing results (Table 2.6). The purpose of decreasing the mesh size was to increase the surface area of the bead and to decrease the amount of diffusion needed to reach the active site within the pores. This decrease in size should allow for faster kinetics. This however was not found. It must be noted that the copolymer used for the synthesis of the

Table 2.5 Raw Data for Alpha-ketophosphonic acid (10-fold dilution/ - 40+60 mesh)

Run Code: MK-01-132

initial ratio	dry wt. (g)	% absorbed*
0.05	0 3081	53 48
0.10	0 3083	53.22
0.25	0 3081	37 50
0.40	0.3082	30.52
0.60	0.3081	23 45
0.75	0.3081	17 22
1.00	0 3081	22 78
1.50	0 3082	17 81
1 75	0 3082	11 89
2.00	0 3082	10 92
2.50	0.3082	16.93
3.00	0.3082	12 32

initial ratio	dry wt. (g)	% absorbed**
0.05	0 3080	79.11

initial ratio	dry wt. (g)	% absorbed***
0 05	0.3080	84 15

*contact time of 17 hours

**contact time of 7 days

***contact time of 14 days

Table 2.6 Raw Data for Alpha-ketophosphonic acid (10-fold dilution/ - 100+200 mesh)

Run Code: MK-01-158

initial ratio	dry wt. (g)	% absorbed*
0.05	0 3227	54.95
0 10	0.3227	46 34
0.25	0.3228	30 77
0 40	0.3226	23.71
0 60	0.3227	12.31
0 75	0.3227	13 34
1.00	0 3228	8.91
1.50	0 3227	9.90
1.75	0.3225	2 43
2.00	0.3227	4 58
2.50	0 3228	0 22
3.00	0.3227	2.20

initial ratio	dry wt. (g)	% absorbed**
0 05	0.3227	74.89
0 40	0.3228	33 14
1.50	0.3227	10.20
3 00	0 3225	3.11

*contact time of 17 hours

**contact time of 7days

resin was structured differently than normal copolymer resins. During the copolymerization process, the diluent needed to make the large macropores within the resin was lost during the reaction. This in turn may have created a less porous material than desired. Uptake and kinetics would obviously be more favorable when the active site is made more accessible to the metal cation. The low porosity may be the cause of the lower than expected uptake. It was anticipated that the uptake would mimic that seen in previous studies, with the difference between runs seen in kinetics. Because of these results, as well, the binding constant calculations were not carried out. It was also drawn from the results that the lack of reproducibility is not due to non-ideal solutions.

β-Ketophosphonic Acid Resin

The β-ketophosphonic acid resin performed well, but showed less complexation ability than the α-ketophosphonate resin. This phenomenon is partly due to the methylene moiety separating the phosphoryl and carbonyl oxygens. The addition of the methylene group allows for the formation of a six membered ring with the metal ion that is entropically less stable.[32] Tables 2.7 and 2.8 show percent absorbed values for the β-ketophosphonic acid resin. Values ranged from approximately 84 % for the 0.005 N contact solution and approximately 23 % for the 0.3 N contact. This shows a decrease of about 12 % in the most dilute solution when compared to the α-ketophosphonic acid resins. Reproducibility between trials (same resin batch for both trials) yielded differences between percent absorbed that were less than five percent from one another.

Table 2.7 Raw Data for Beta-ketophosphonic acid (Trial 1)
Run Code: MK-01-101

initial ratio	dry wt. (g)	% absorbed	r (mequiv./g)	c (mequiv/mL)
0.05	0 3345	84 15	0 1258	7.9250E-04
0.10	0.3344	79.21	0.2368	2.0790E-03
0.25	0.3344	68.49	0 5120	7 8775E-03
0.40	0.3343	59.37	0 7104	0.0163
0 60	0.3343	51 13	0 9175	0.0293
0.75	0 3346	45 48	1 0195	0.0409
1.00	0.3346	39.08	1 1680	0.0609
1.50	0.3346	31.00	1.3898	0.1035
1.75	0.3345	29.04	1.5193	0.1242
2 00	0.3343	24 38	1.4586	0 1512
2.50	0.3343	23.28	1.7409	0.1918
3 00	0 3346	22.15	1.9861	0.2336

Table 2.8 Raw Data for Beta-ketophosphonic acid (Trial 2)
Run Code: MK-01-102

initial ratio	dry wt. (g)	% absorbed	r (mequiv./g)	c (mequiv/mL)
0.05	0.3344	83.18	0.1244	8.4100E-04
0 10	0.3344	78 15	0.2337	2 1850E-03
0.25	0 3345	67.11	0.5016	8.2225E-03
0.40	0.3343	59.41	0 7108	0.0162
0.60	0 3343	52 95	0.9502	0.0282
0 75	0.3343	47 91	1 0747	0.0391
1 00	0.3345	41 32	1 2353	0 0587
1.50	0 3344	35 31	1 5837	0.0970
1.75	0.3344	32.60	1 7061	0.1180
2 00	0 3344	26 81	1.6033	0 1464
2.50	0 3345	24 40	1.8234	0 1890
3.00	0.3345	25 67	2 3020	0.2230

The trends exhibited with the α-keto phosphonic acid resin can also be seen with the β-ketophosphonic acid resin. These can be seen in Table 2.9 and 2.10. When the single Langmuir isotherm is applied to the data, a smaller binding constant in comparison to the other treatments is found. Again, when the higher order isotherms are applied, the binding constants calculated increase dramatically and remain nearly constant whether a double, triple or quadruple Langmuir isotherm is applied. An interesting observation can be made though when comparing the triple Langmuir and quadruple Langmuir isotherm of trial 1. The triple Langmuir gives a non-converging value; whereas, the quadruple Langmuir does not. Both treatments produced binding constants of 122 N^{-1}. If the binding constants and saturation capacities are compared for these two trials, it can be seen that they are nearly identical. The binding constants and saturation capacities for trial 1 and trial 2 are 122 N^{-1}, 1.01 mequiv/ g and 86.8 N^{-1}, 1.15 mequiv/ g respectively. These values remain consistent for the double, triple and quadruple Langmuir treatments. The fact that the values are so close to one another, and that three of the six trials show a lack of convergence, indicates that they may be more reliable than originally anticipated. It can be seen by the improvement of the correlations, that the higher order isotherms represent the data better than the single
Langmuir treatment.

The shape of the saturation and x-reciprocal plots still indicate the resin's relatively high efficiency in coordinating europium from solution. This is mostly seen in the saturation curve, while the x-reciprocal plot still shows strong and weak binding sites within the resin.

Table 2.9 Binding Constants and Saturation Capacities of MK-01-094 (Trial 1)

Mathematical Treatment	K_1 (N^{-1})	St_1 (mequiv/ g)	Correlation
Single Langmuir	28.1703	2.0021	0.9564
Double Langmuir	121.8082 *	1.0137 *	0.9933

* Non-converging value.
(See Figure 2.4 for Saturation Curves and X-reciprocal Plot)

Table 2.10 Binding Constants and Saturation Capacities of MK-01-094 (Trial 2)

Mathematical Treatment	K_1 (N^{-1})	St_1 (mequiv/ g)	Correlation
Single Langmuir	22.3821	2.3655	0.9558
Double Langmuir	86.8090 *	1.1472 *	0.9809

* Non-converging value.
(See Figure 2.5 for Saturation Curves and X-reciprocal Plot)

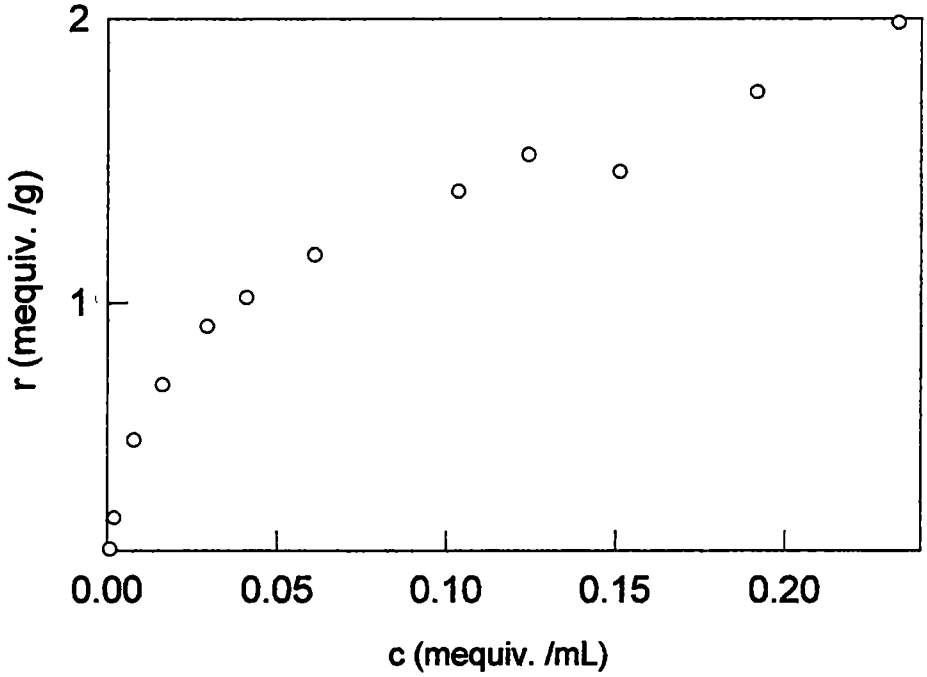

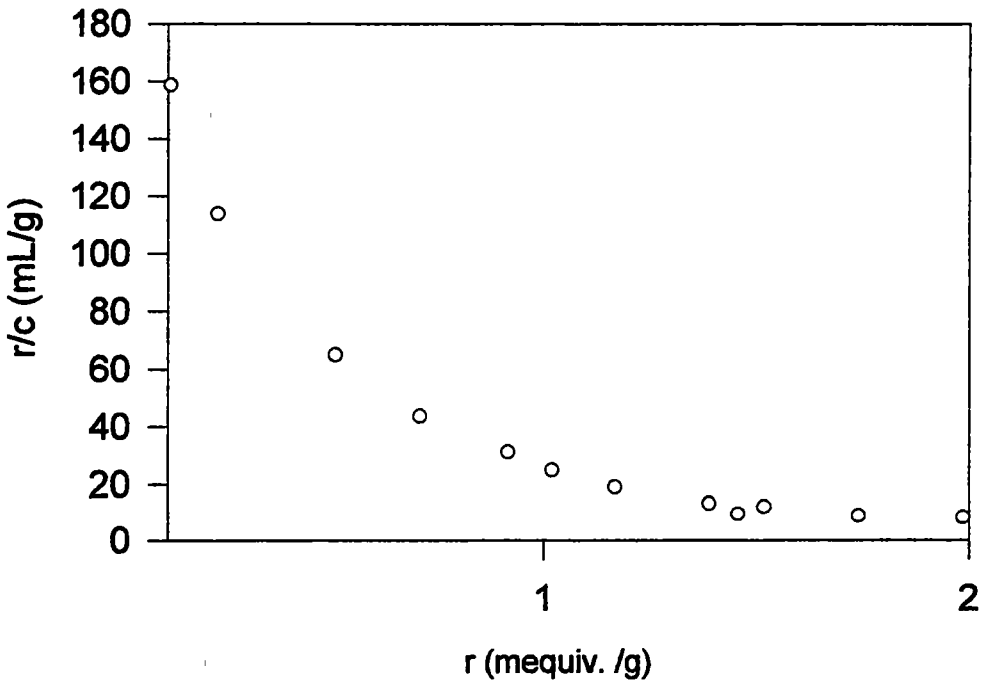

Figure 2.4 Beta-keto Phosphonic Acid (Trial 1)

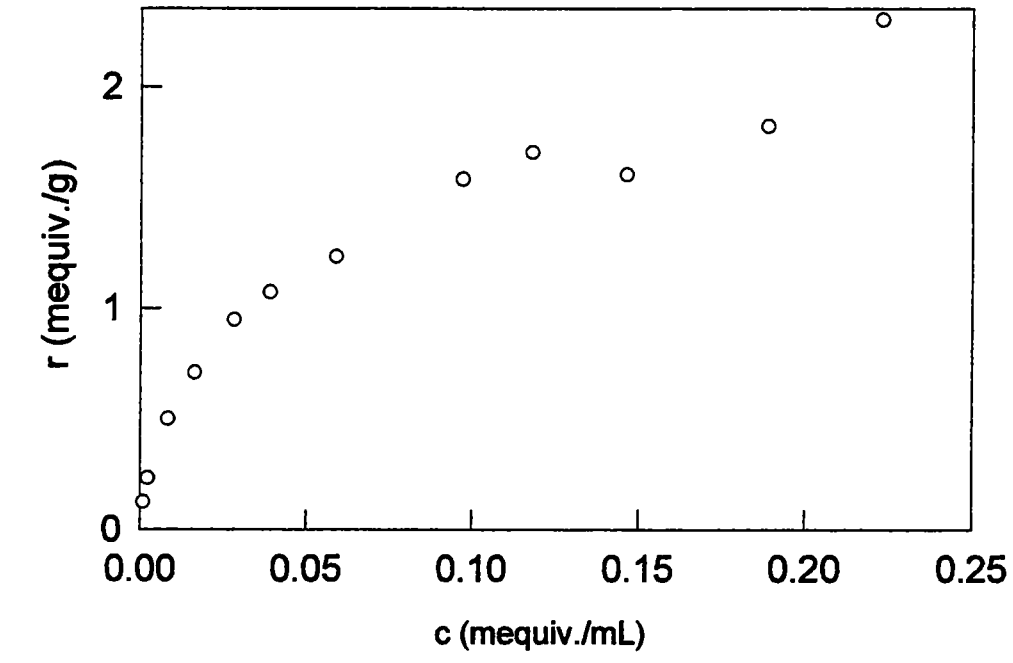

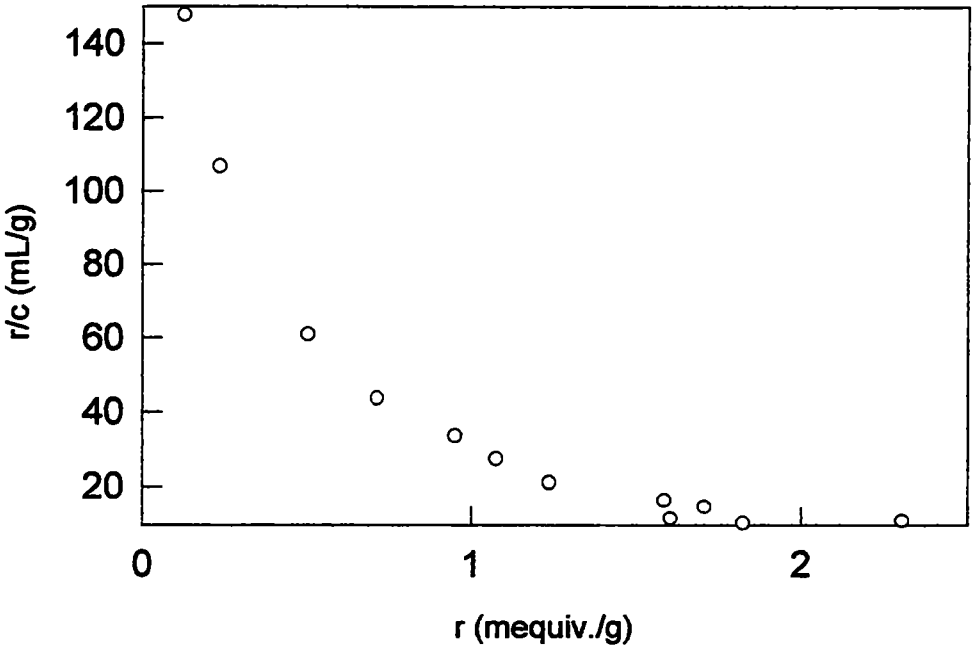

Figure 2.5 Beta-keto Phosphonic Acid (Trial 2)

γ-Ketophosphonic Acid Resin

The introduction of a second methylene moiety within the γ-ketophosphonic acid resin would cause the formation of a seven membered ring upon chelation. This is known to be an unfavorable conformation and leads to coordination solely through the phosphoryl oxygen[27]. Because of this, a decrease in the amount of europium absorbed is expected. Indeed, the percent absorbed (Tables 2.11 and 2.12) ranged from approximately 28 % for the most dilute 0.005 N solution, and 11 % for the most concentrated 0.3 N solution. Reproducibility between trials, in which the same resin was used, gave differences between percent absorbed that were less than 4%. The binding constants and saturation capacities calculated for the γ-ketophosphonic acid resin, regardless of the type of isotherm applied, showed very similar numbers (Tables 2.13 and 2.14). This seems to be due to the low binding strength of all sites within the resin.

Phosphonic Acid Resin

The phosphonic acid resin behaved in a manner comparable to the γ-ketophosphonate resin. A ring cannot be formed upon complexation with the metal, since no carbonyl is present, only the phosphoryl from the phosphonic acid group. Percent absorbed (Table 2.15 and 2.16) ranged from approximately 13 % of the 0.005 N contact solution to 8 % for the 0.3 N solution. The differences in percent absorbed between trials, is less than 13 % which shows reasonable reproducibility, but is not nearly as consistent as the other resins studied. When the trend in percent absorbed is compared

Table 2.11 Raw Data for Gamma-ketophosphonic acid (Trial 1)
Run Code: MK-01-089

initial ratio	dry wt. (g)	% absorbed	r (mequiv./g)	c (mequiv/mL)
0.05	0 3560	28.67	0 0403	3.5665E-03
0 10	0.3558	30 56	0.0859	6.9440E-03
0 25	0.3559	25.66	0 1803	1 8585E-02
0.40	0.3560	22 52	0 2530	0 0310
0 60	0 3559	19 42	0.3274	0.0483
0 75	0 3558	20 64	0 4351	0.0595
1 00	0 3558	18.93	0 5321	0 0811
1 50	0 3560	17.56	0.7398	0 1237
1 75	0.3560	15 12	0 7433	0 1485
2 00	0.3558	19.03	1 0696	0.1619
2.50	0 3560	11.59	0.8138	0 2210
3 00	0 3560	11 76	0 9911	0.2647

Table 2.12 Raw Data for Gamma-ketophosphonic acid (Trial 2)
Run Code: MK-01-090

initial ratio	dry wt. (g)	% absorbed	r (mequiv./g)	c (mequiv/mL)
0.05	0.3558	29 76	0.0418	3.5120E-03
0 10	0 3557	27.81	0.0782	7 2190E-03
0.25	0 3560	23 80	0.1671	1 9050E-02
0 40	0.3559	22 37	0.2514	0.0311
0.60	0.3559	21 21	0.3576	0 0473
0.75	0.3559	21.20	0 4468	0 0591
1.00	0.3560	18.22	0.5117	0.0818
1.50	0.3558	16 22	0 6839	0 1257
1 75	0 3559	12 05	0.5925	0 1539
2.00	0 3558	14 53	0.8168	0 1709
2.50	0.3558	12.11	0 8510	0 2197
3 00	0.3557	10.36	0.8737	0 2689

Table 2.13 Binding Constants and Saturation Capacities of MK-01-090 (Trial 1)

Mathematical Treatment	K_1 (N^{-1})	St_1 (mequiv/ g)	Correlation
Single Langmuir	6.7977	1.5681	0.9368
Double Langmuir	6.7518	1.0028	0.9368

(See Figure 2.6 for Saturation Curves and X-reciprocal Plot)

Table 2.14 Binding Constants and Saturation Capacities of MK-01-090 (Trial 2)

Mathematical Treatment	K_1 (N^{-1})	St_1 (mequiv/ g)	Correlation
Single Langmuir	8.2544	1.2808	0.9769
Double Langmuir	9.2400	0.4024	0.9770

(See Figure 2.7 for Saturation Curves and X-reciprocal Plot)

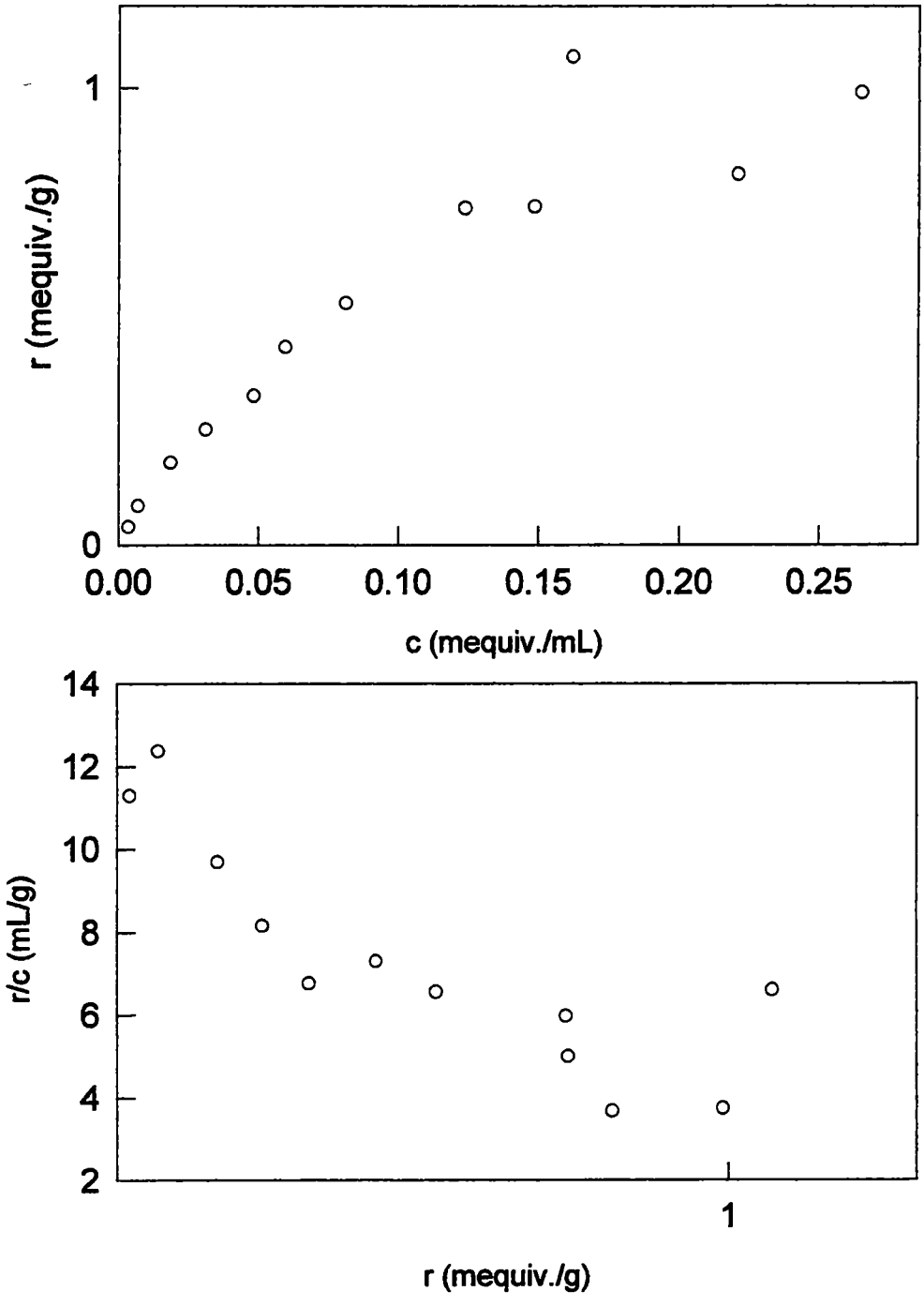

Figure 2.6 Gamma-keto Phosphonic Acid (Trial 1)

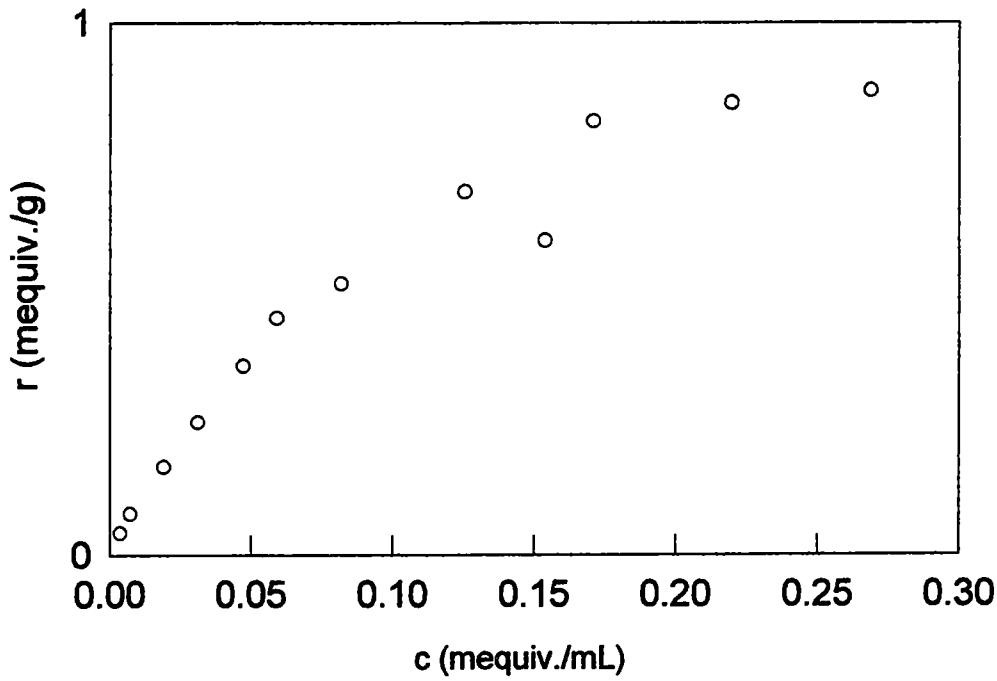

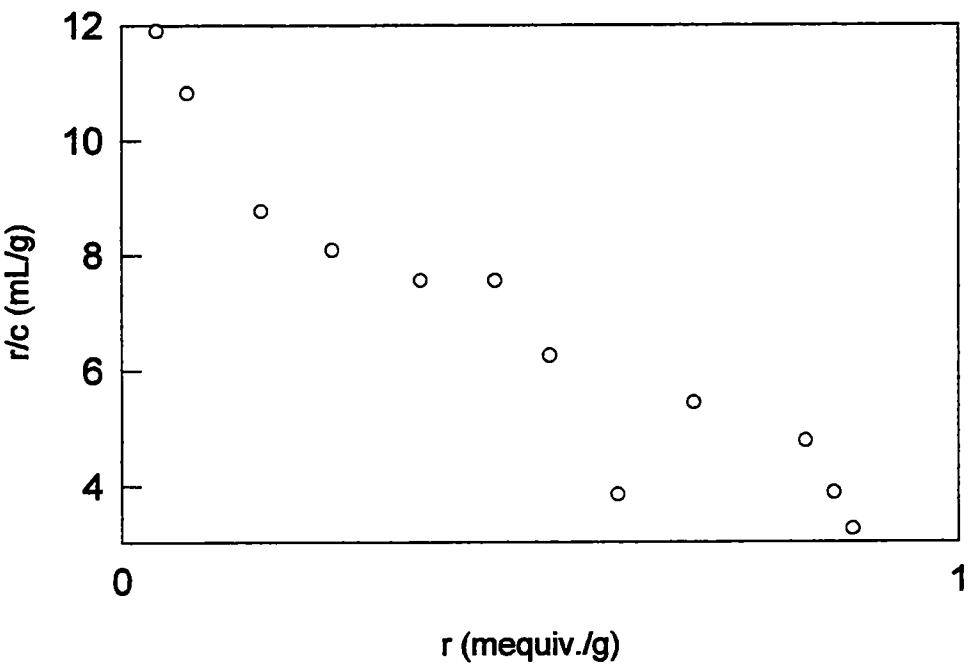

Figure 2.7 Gamma-keto Phosphonic Acid (Trial 2)

Table 2.15 Raw Data for Phosphonic acid (Trial 1)

Run Code: MK-01-048

initial ratio	dry wt. (g)	% absorbed	r (mequiv./g)	c (mequiv/mL)
0 05	0.2293	13.51	0.0557	3.7215E-03
0 10	0 2293	15.61	0 0829	8 0980E-03
0 25	0 2293	14 38	0 1617	2 1290E-02
0 40	0.2293	15.00	0.2760	0.0337
0.60	0.2294	12.91	0 2995	0 0531
0 75	0.2292	14 10	0.2250	0.0698
1.00	0.2293	10 10	0 6290	0.0856
1.50	0.2293	5 33	0 9352	0.1286
1.75	0.2294	9.96	0.9150	0.1540
2.00	0.2293	11 35	0.8258	0.1811
2.50	0.2293	10.00	0.7149	0.2336
3.00	0.2293	8.93	1 1596	0 2734

Table 2.16 Raw Data for Phosphonic acid (Trial 2)

Run Code: MK-01-069

initial ratio	dry wt. (g)	% absorbed	r (mequiv./g)	c (mequiv/mL)
0.05	0.2295	25.57	0.0295	4.3245E-03
0.10	0.2294	19.02	0.0681	8.4390E-03
0.25	0 2294	14.84	0 1568	2 1405E-02
0.40	0.2294	15.83	0.2616	0.0340
0.60	0.2294	11 45	0.3377	0.0523
0 75	0.2294	6 88	0.4613	0 0644
1.00	0.2294	14 43	0.4404	0 0899
1.50	0.2294	14 30	0.3487	0 1420
1.75	0.2293	11 99	0.7596	0.1576
2.00	0.2294	9 47	0 9898	0 1773
2.50	0 2294	6.56	1 0903	0.2250
3.00	0 2295	8 87	1.1681	0.2732

from resin to resin, the α, β, and γ-ketophosphonic acid resins all showed decreasing percent absorbed as the concentration of the metal ion increased. The results with the phosphonic acid resin do not show a trend, instead behaving in a sporadic, inconsistent manner as seen in the x-reciprocal plot. This is due to the overall poor ability of the phosphonic acid resin to coordinate the europium from solution.

Table 2.17 and 2.18 show the binding constants, saturation capacities, and correlations calculated when the various isotherm treatments are applied. Trial 1 results show very similar binding constants regardless of the isotherm used, but the saturation capacities vary considerably. A poor correlation of 0.8609 was also achieved for all calculations. Trial 2 results give low saturation capacities for all treatments with the exception of the single Langmuir isotherm. While lower saturation capacities are seen, higher binding constants are found due to the steeper tangent that is drawn to the portion of the curve in the x-reciprocal plot that represents the stronger binding sites. With this data set, there appears to be a problem with consistency in how the tangent representing the strongest binding sites is drawn. This is believed to be due to the increased scatter when compared to other resins. As with trial 1, correlations were still poor indicated by the scatter in the data.

Table 2.17 Binding Constants and Saturation Capacities of MK-01-026 (Trial 1)

Mathematical Treatment	K_1 (N^{-1})	St_1 (mequiv/ g)	Correlation
Single Langmuir	4.86	1.84	0.861
Double Langmuir	4.75	0.884	0.861
Triple Langmuir	5.09 *	0.306 *	0.861
Quadruple Langmuir	5.01 *	0.317 *	0.861

* Non-converging value.
(See Figure 2.8 for Saturation Curves and X-reciprocal Plot)

Table 2.18 Binding Constants and Saturation Capacities of MK-01-026 (Trial 2)

Mathematical Treatment	K_1 (N^{-1})	St_1 (mequiv/ g)	Correlation
Single Langmuir	1.10	5.15	0.890
Double Langmuir	116	0.113	0.908
Triple Langmuir	85.4	0.125	0.909
Quadruple Langmuir	89.1	0.124	0.909

(See Figure 2.9 for Saturation Curves and X-reciprocal Plot)

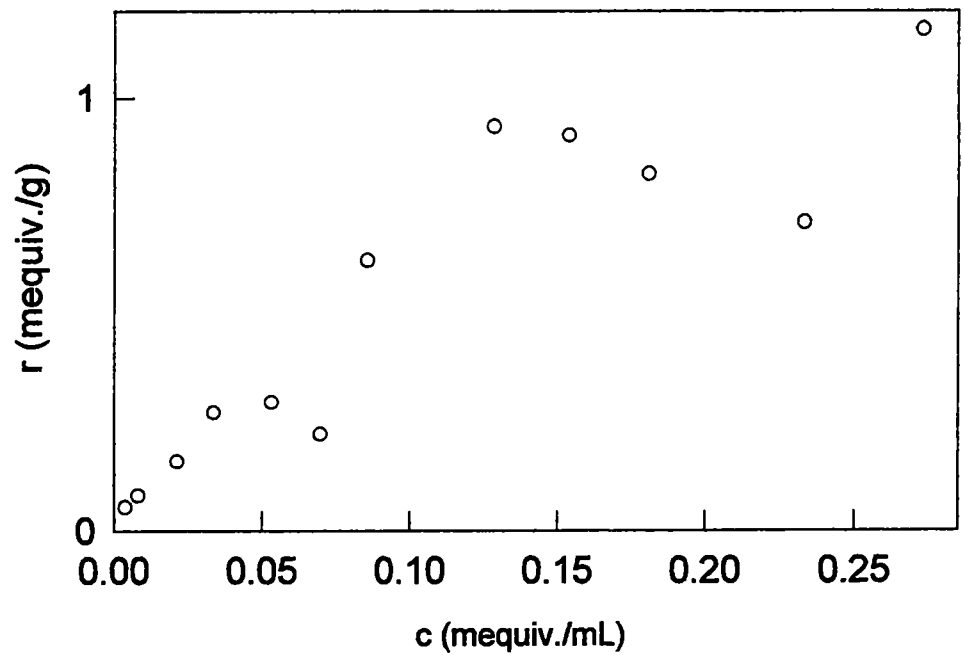

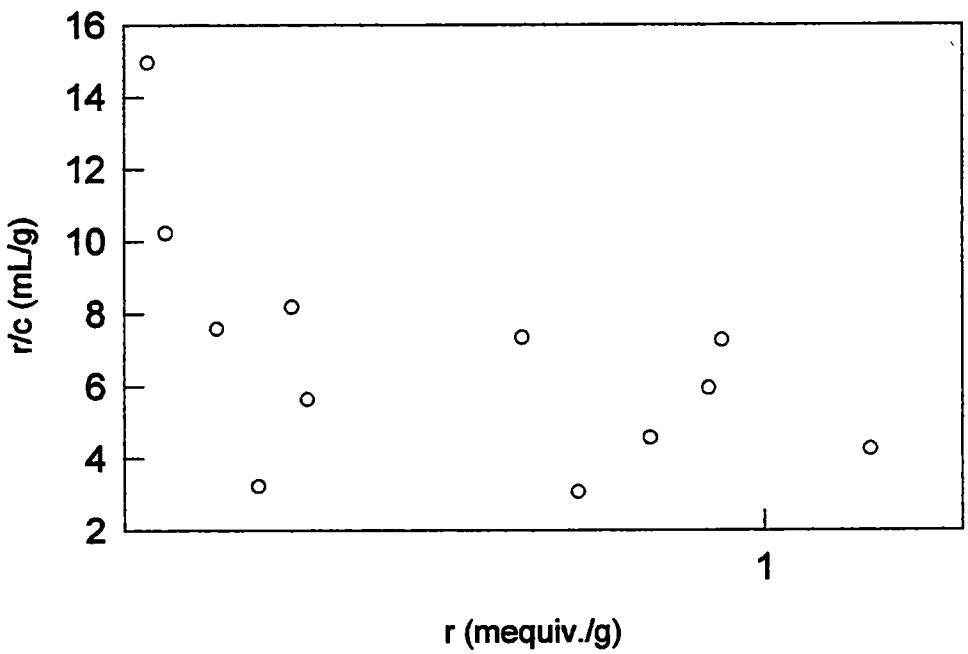

Figure 2.8 Phosphonic Acid (Trial 1)

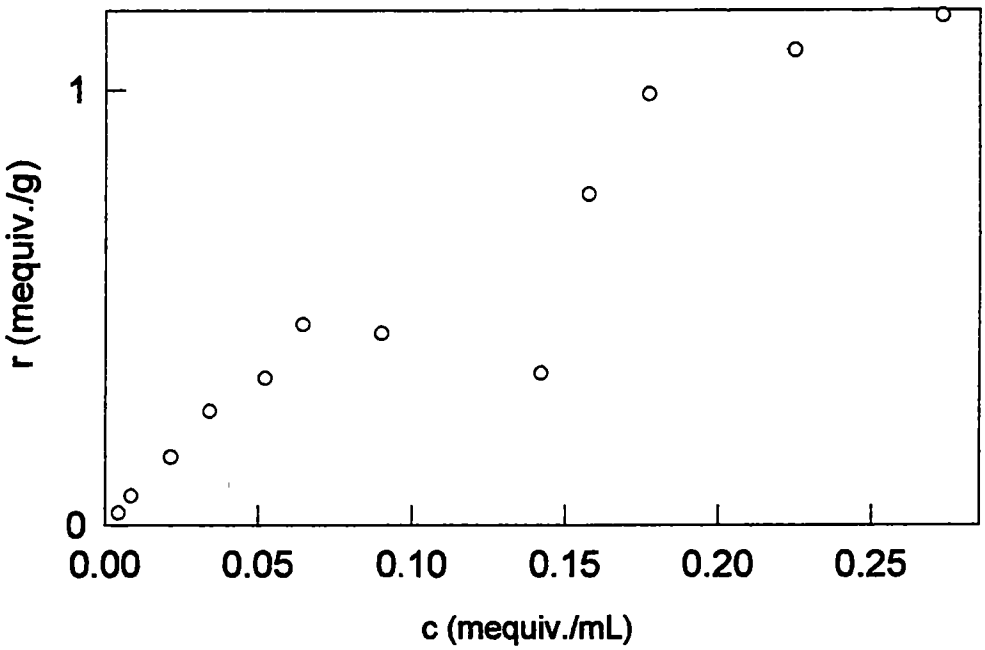

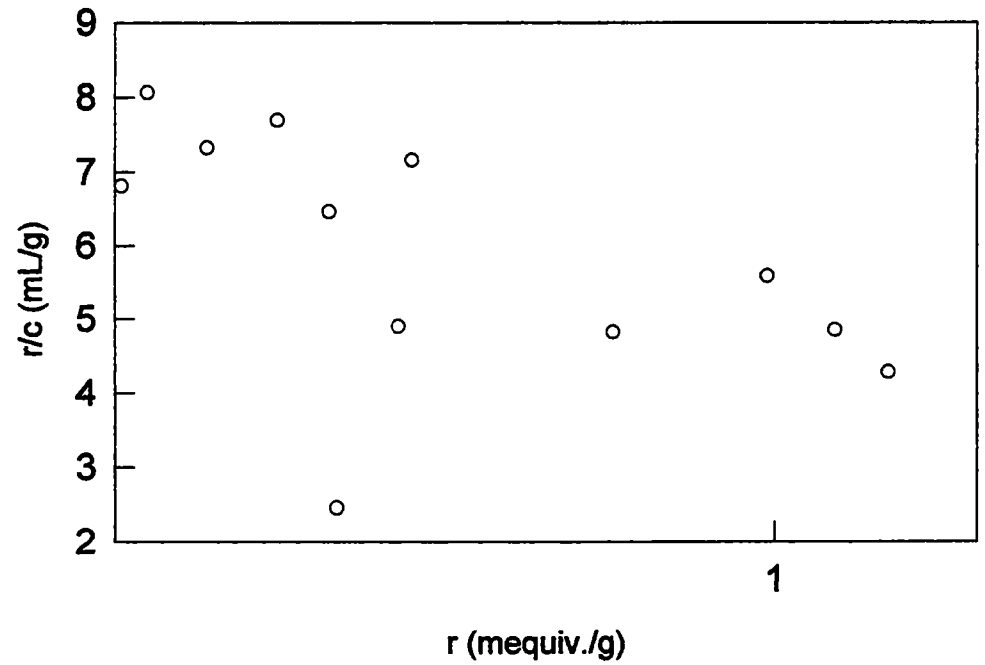

Figure 2.9 Phosphonic Acid (Trial 2)

Discussion

Comparison of percent absorbed values for the different resins show an obvious trend in the resin's ability to complex Eu (III) from solution. The order in terms of ability to coordinate the europium cation from a 1 N nitric acid solution decreases in the following order:

$$\alpha\text{-keto} > \beta\text{-keto} > \gamma\text{-keto} > \text{phosphonic acid}$$

The same trend is seen when comparing the different europium binding strengths (binding constants) of the resins, regardless of the type of isotherm applied. It must be mentioned again that the binding constants and saturation capacities cannot be analyzed independently from one another. If this is done, false interpretation of the resins performance may be made. It is found, though, that when comparing the various isotherm treatments, that improvement of the correlations does not occur with the triple and quadruple Langmuir treatments. The first binding constants and saturation capacities values of the triple and quadruple Langmuir isotherms are consistent with those found with the double Langmuir treatment. The double Langmuir treatment may thus best represent the data, since it is the simplest treatment and suggests that dividing the ligands into strong and weak sites may be sufficient.

Upon inspection of the saturation curves (r vs. c), it can be seen that in most instances, the inflection of the curve occurs around the fourth or fifth point in the series, indicating that all the active sites that are capable of coordination have interacted with the europium metal. These first four points in the saturation curve correspond with the first

four points that make up the first tangent drawn to the curve in the x-reciprocal plot. This is known since one can follow the r, c, and r/c values between the two plots. This indicates that these points play the biggest role in determining the binding constant of the most capable sites. Because of these statements, the following treatment has been devised to determine the binding constant and saturation capacities of the resins.

Initially, each trial is treated individually. The first four percent absorbed values for each of the resins are entered into the spreadsheet and their respective r and c values calculated. The r and c values from the two trials are then averaged together to give an r and c value that represents the two trials together. These new r and c values are then plotted to give a new saturation curve (r vs. c). A single Langmuir isotherm is then applied to the curve, or in this case, nearly a straight line. Table 2.19 shows the calculated values when this treatment is applied to the data.

Table 2.19 Binding Constants and Saturation Capacities Using Revised Treatment

Resin	K_1 (N^{-1})	St_1 (mequiv/ g)	Correlation
α-ketophosphonic	718.9254	0.9286	0.9802
β-ketophosphonic	137.0868	1.0144	0.9938
γ-ketophosphonic	17.5463	0.7116	0.9991
Phosphonic acid	1.7051	4.8551	0.9903

It was found that when this treatment was applied to the four resins, an obvious trend was found for the binding constants. The binding constant and saturation capacity cannot be looked at individually, since as before, a misinterpretation of the resin's performance will be made. The binding constant follows the order of the resin's ability to coordinate the europium species. The correlations found also are very good as compared

to others when other treatments were applied. It is also important to note, that when this treatment is applied, no indications of non-converging values were received from the computer program indicating the convergence to a final value during the iterative evaluations of the Langmuir equations.

A potential drawback in using this treatment is the trend seen in the saturation capacities. While the binding constants decrease as the carbon spacer is increased, the saturation capacity does not decrease respectively. A potential explanation for this is the general ability of the alpha-keto and beta-keto resins to coordinate the europium from solution. In the most dilute solutions, the beta-keto only showed approximately a 10 % decrease in uptake. This compared to the gamma-keto and phosphonic acid resin that showed dramatic decreases. The saturation capacity trend for the alpha and beta resins seems reasonable, since as stated before, the binding constants and saturation capacities cannot be looked at individually. The coordinating ability is similar, but the binding strength is greater for the alpha-keto resin due to the formation of the more stable ring.

An alternative approach can be used to reiterate the previously mentioned binding series. If one compares the computed binding constants at similar saturation capacities for the resins, the same trend is found. Table 2.20 shows the binding constants found for each of the resins at similar saturation capacities.

As stated before, the same trend can be seen indicating that the alpha-ketophosphonate resin binds europium the strongest followed by the beta, gamma and finally the phosphonic acid resin.

Table 2.20 Binding Constant Trend at Similar Saturation Capacities

Resin	K_1 (N^{-1})	S_t (mequiv/ g)	Correlation	Treatment Used
α-ketophosphonic	253.8202	1.1396	0.9047	Triple Langmuir
β-ketophosphonic	86.7704	1.1475	0.9809	Triple Langmuir
γ-ketophosphonic	6.7518	1.0028	0.9368	Double Langmuir
Phosphonic acid	4.7521	0.8837	0.8609	Double Langmuir

While this second method of comparing binding constants at similar saturation capacities is sufficient in showing the binding trend, the alternative data analysis technique which averages the first four r and c values together is preferred. This is because a consistent isotherm treatment can be applied to all of the resins; whereas, binding constants must be taken from both the double and triple Langmuir treatments in the second method in order to work with a converging value. An additional reason in which the first method is preferred is the correlations found. Better correlations are found when the first four r and c values are averaged and then subjected to the single Langmuir treatment. Averaging the r and c values also omits the problem of having varying binding constants and saturation capacities from trial to trial.

Conclusion

The calculation of binding constants and saturation capacities for the novel family of ketophosphonate resins has proven to be difficult. Single, double, triple and quadruple Langmuir isotherms have been applied to the data for each of the systems. It appears that the double Langmuir treatment is sufficient and the higher order isotherms are not required since little if any increase in correlation is seen. Insufficient correlations are also

seen with the single Langmuir isotherm indicating a poor representation of the data. The binding constants and saturation capacities for individual trials and resins showed a trend indicating that as the carbon spacer between the carbonyl and phosphoryl moieties is increased, the stability of the ligand metal ion complex decreases.

We have developed an alternative data analysis technique that utilizes data from two separate trials. The first four points are isolated from the twelve, with the respective r and c values determined. These r and c values for the individual trials are then averaged together, re-plotted to give a new saturation curve and x-reciprocal plot, and then subjected to a single Langmuir treatment. Using this method, decreasing binding constants and saturation capacities are seen for the resins in the following order:

$$\alpha\text{-keto} > \beta\text{-keto} > \gamma\text{-keto} > \text{phosphonic acid}$$

once again, indicating that as the carbon spacer between the carbonyl and phosphoryl moieties increases, the complex stability decreases. The method also showed good correlations with none showing less than 0.98 also with no indication of non-converging values encountered during the calculations.

CHAPTER 3

Interaction of Anions with a Novel Class of Quaternary Ammonium Resins

Introduction

The resins described in the work are strong base type anion exchange resins that utilize quaternary ammonium groups. The following monofunctional resins have been synthesized: trimethyl, triethyl, tributyl, and trihexyl. A bifunctional resin has also synthesized which utilizes both triethyl and trihexyl ammonium groups. (See Figure 3.1 for structures.) The bifunctional resin designed has been found to be selective for the removal of technetium, a byproduct of uranium processing.[33] When in an oxidizing environment, technetium is found as pertechnetate (TcO_4^-),[34] a highly mobile groundwater contaminant. The pertechnetate ion has been found at Department of Energy (DOE) sites in both Paducah Kentucky and Portsmouth Ohio. Due to the radioactive nature of the ion, the DOE has made it a top priority in terms of remediation. The bifunctional amine resin synthesized has been found to be superior to any resin that is commercially available.[33] The commercially available resins commonly used include Reillex™ HPQ, Amberlite™ IRA-900 and IRA-904, Purolite™ A-520E, and Sybron Ionac™ SR-6. Table 3.1 shows the composition of each of these resins.

A common problem with ion exchange resins when increasing the length of alkyl chains within the active site is poor kinetics.[35] While kinetics of the resins synthesized were not studied directly in this work, it must be noted why the bifunctional resin developed out performs all other commercial resins. As stated before, it is well known

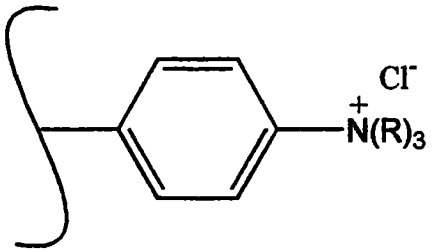

R= $(Me)_3$, $(Et)_3$, $(Bu)_3$, $(Hex)_3$

Monofunctional Quaternary Ammonium Resins

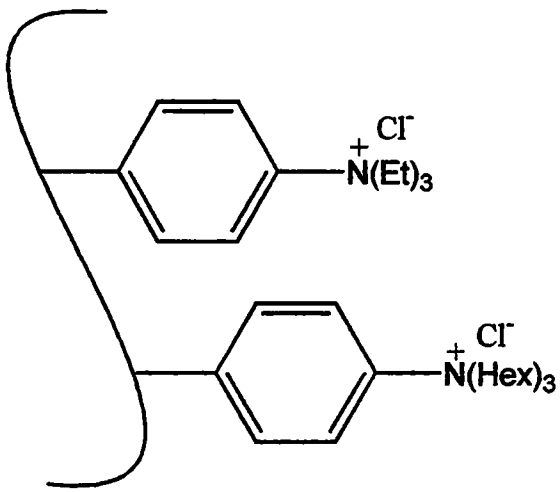

Bifunctional Quaternary Ammonium Resin

Figure 3.1 Structures of Quaternary Ammonium Resins (Chloride Form)

Table 3.1 Common Commercially Available Resins for Pertechnetate Removal

Resin	Manufacturer	Copolymer	Cross-linking	Ligand
Reillex HPQ	Reilly Industries	DVB (25%) 4-vinyl pyridine (75%)	NS	methylated 4-vinyl pyridine
Amberlite IRA-900	Rohm and Haas Company	STY/ DVB	5%	trimethyl ammonium
Amberlite IRA-904	Rohm and Haas Company	STY/ DVB	20%	trimethyl ammonium
Purolite A-520E	Purolite Industries	STY/ DVB	NS	trimethyl ammonium
Sybron Ionac SR-6	Sybron Chemical Inc.	STY/ DVB	NS	tributyl ammonium

NS= not specified in literature.
STY=styrene
PS=polystyrene
DVB=divinylbenzene

that as the length of the alkyl chain within the active site increases, not only do kinetics decrease, but the selectivity of the resin increases for softer, less hydrated anions. When compared to other ligands that contain short alkyl chains, namely the trimethyl and triethyl amine resins, the opposite trend is seen. While these resins show favorable kinetics due to their hydrophilic nature, their selectivity towards softer, less hydrated anions decreases and in turn exchange for harder anions. The shorter alkyl chains would rather interact with more hydrated anions such as chloride or bromide rather than soft anions such as pertechnetate or perrhenate. The bifunctional amine designed incorporates both long alkyl chains (trihexyl groups) and short alkyl chains (triethyl groups). The combination of these two groups allows for selectivity of less hydrated anions due to the presence of the trihexyl groups and favorable kinetics due to the triethyl groups.[35]

The favorable interaction that has been seen with the bifunctional resin and the pertechnetate anion has sparked interest in determining its interaction with other anions of both monovalent and divalent type. In this study, the monovalent anions tested consist of the following: TcO_4^-, ReO_4^-, NO_3^-, I^-, and Br^-. In terms of divalent species, both SO_4^{2-}, and SeO_4^{2-} were studied. For each of these anions, distribution coefficients, K_d, and distribution coefficients per equivalent of active site, K'_d (eq), will be determined.

Mathematical Representation of Data

If equation 3.1 is allowed to represent the equilibrium between the exchange site of the resin ($R\text{-}Q^+$) and the anion of interest (A^-) and X^- represents the original counter-ion within the resin,

$$R\text{-}Q^+X^- + A^- \Leftrightarrow R\text{-}Q^+A^- + X^- \qquad (3.1)$$

expressions for K_d, and K'_d (eq) can be made accordingly. Kd values gives the absorption of the specified anion per gram of resin, K'_d (eq) gives the absorption ability per exchange site. Equations 3.2 and 3.3 represent how the K_d and K'_d (eq) are determined.[36] The specific case below is a general equation that represents all the anions studied.

$$K_d = \frac{C_{A^-},\ resin}{C_{A^-},\ aq} \qquad (3.2)$$

where C represents the concentration in mmol and K_d has units of mL/g.

$$K'_d\ (eq) = \frac{C_{A^-},\ resin}{C_{A^-},\ aq}\ (Exchange\ Capacity)^{-1} \qquad (3.3)$$

where C, again, is in mmol and K'_d (eq) has the units of mL/ mequiv.

It is important when carrying out these experiments that certain parameters be followed. The percent loading of the resin with the anion of interest must be kept below 10 %. Studies have shown that when loadings exceed 10 %, loading effects can be seen. Loading effects cause the already absorbed ions to play a role in the further absorption of other ions. If low loading conditions are maintained, then this problem is avoided.

Experimental

Synthesis of Quaternary Ammonium Resins

All resins were synthesized from –40 +60 mesh size poly(vinylbenzyl chloride) macroreticular type copolymer beads. Amination of the copolymer, to obtain each of the resins, was carried out using the appropriate amine. See experimental section for a detailed synthesis.

Experimental Design

All experiments were batch type experiments. The amount of resin used was normalized to 0.5 mequiv of active site to accommodate for partially functionalized resins. Equation 3.4 was used to determine the resin mass:

$$\frac{0.5 \text{ mequiv} * (\text{exchange capacity})^{-1}}{(\% \text{ solids}/ 100)} \qquad (3.4)$$

where the exchange capacity is in mequiv/ g and percent solids is the dry to wet mass ratio. Resin was weighed into appropriately labeled 50 mL polypropylene centrifuge tubes.

Individual contact solutions were made from a 1.0×10^{-2} M stock solution. This stock was then used to make 1 L of 1.0×10^{-4} M. Each contact solution was also made to have a specific amount of chloride or nitrate background. Please see Table 3.2 for matrix parameters.

Table 3.2 Matrix Parameters Studied

Anion Studied (all concentrations at 1.0 X 10^{-4} M)	Chloride Background Matrix Studied	Nitrate Background Matrix Studied
Pertechnetate	1 M	60 mM
Perrhenate	1 M	90 mM, 60 mM
Iodide	1 M	---
Nitrate	1 M, 90 mM	---
Bromide	1 M, 90 mM	---
Selenate	---	60 mM
Sulfate	90 mM	60 mM

In all experiments, 25 milliliters of the contact solution was volumetrically pipetted onto the measured resin. The resin and solution was then shaken on an orbital shaker at a rotation rate of 268 rpm for 7 days to allow for exchange to take place. After contact, the contacted solution was removed from the beads and placed into a clean 25 mL centrifuge tube. The removed solutions were then stored in a refrigerator until time of analysis. This procedure was carried out for all solutions with the exception of pertechnetate. Please see aqueous solution analysis for treatment of pertechnetate solutions.

Aqueous Solution Analysis

Three different methods were used for analysis of the contacted metal ion solution. The three methods were inductively coupled plasma (ICP), ion chromatography (IC), and radiotracer techniques. ICP (Thermal Jarrell Ashe) was used chosen for perrhenate, sulfate and selenate due to the ease of analysis. IC could also have been used for analysis of perrhenate, but due to the high chloride background concentration, dilution

would be necessary, which would lower the concentration of perrhenate to well below the IC detection limit. Sulfate, which also could have been determined by IC, was analyzed by ICP, since peak resolution between chloride and sulfate was difficult. When carrying out analysis by ICP, a high solids nebulizer was used rather than the normal cross flow nebulizer. This different nebulizer was used due to the high ionic strength of the samples. After each sample, the nebulizer was thoroughly flushed with water to allow the plasma to return to its original state. A multi-element detector was also used. All blanks and standards used to calibrate the instrument contained the appropriate amount of background chloride to match the amount in the samples.

Since the ICP method was not conducive to the analysis of bromide, iodide, or nitrate, an ion chromatograph (Dionex GP40 with ED40 conductivity detector) was used as the method of analysis. Thousand fold dilutions were carried out, prior to analysis due to the high chloride background. All blanks and standards used to calibrate the instrument contained the appropriate amount of background chloride to match the amount in the samples. To obtain consistent injection volumes, all samples were injected by means of a AS400 autosampling system. A 1000 µl injection loop was also used.

Pertechnetate was analyzed by radiotracer techniques. Pertechnetate undergoes low energy, 0.29 MeV, beta emission, ($t_{1/2} = 2.14 \times 10^5$ yrs)[37,38,39]. Aliquots were analyzed by initially filtering five mL of the contacted solution, followed by removing a 1 mL subsample from the filtered aliquot. This 1 mL subsample was then mixed with 10 mL of Ultima Gold Scintillation Cocktail and allowed to sit in the counting trays (approximately 30 minutes) prior to analysis to allow the sample to darken. The samples

were counted twice in 15 minute intervals. To correct for background, 1 mL of 1 M Cl^- solution was mixed with 10 mL of cocktail and was counted twice in 15 minute intervals.

Interaction with Monovalent Anions

Upon inspection of the K_d and K'_d (eq) values (see appendix for tabulated data), three trends can be seen with the monovalent anions. The first trend indicates that regardless of the anion and background anion being studied, the following order in terms of affinity is found:

$$(Hex)_3 > \text{Bifunctional} > (But)_3 > (Et)_3 > (Me)_3$$

K_d and K'_d (eq) values decrease as the alkyl chain length is decreased. The presence of this trend reiterates the fact that as the length of the alkyl chain within the ligand is increased, the selectivity of the resin is increased. The fact that the bifunctional resin still performs well indicates that the presence of the hydrophilic triethyl groups does not diminish the overall selectivity of the resin to a great extent.

A second trend can be seen when comparing the monovalent anion interaction with the resins. It can be seen that as the size of the anion is increased, the resin's affinity for the anion is increased. (See appendix for tabulated Kd values and Table 3.3 for thermochemical radii.) (Thermochemical radii are derived from lattice energies (U), the dissociation of one mole of a substance into its structural components. When the radius of an anion is lacking, they can be calculated from thermodynamic data of other similar species. As long as the lattice energy is known due to the Born-Haber cycle , by

backtracking through a series of equations, the unknown radius can be derived. They are termed "thermochemical" since they are derived from known thermochemical values of other species.[40]) The following trend can be seen in terms of the resins affinity:

$$TcO_4^- > ReO_4^- > I^- > NO_3^- > Br^-$$

This is evident by the larger K_d and K'_d (eq) values for the larger anions.

Table 3.3 Thermochemical Radii and Gibb's Free Energy of Hydration Values (Monovalent Anions)

Anion	Thermochemical Radius (nm)	ΔG_H (calculated) (kJ/mol)
TcO_4^-	.252	-245
ReO_4^-	.260	-240
I^-	.210	-282
NO_3^-	.196	-314
Br^-	.188	-314
Cl^-	.172	-338

A property of the anion that follows its size is the degree of hydration. Table 3.3 shows the thermochemical radius and the Gibb's free energy of hydration (ΔG_H)[41]. As can be seen from the ΔG_H for each of the anions, as the value becomes less negative, its affinity for water is decreased. This is due, in part, to the radius of the anion. As the radius is increased, and the charge is held constant, the charge to size ratio is decreased, therefore, allowing for a weaker ion-dipole interaction with water molecules. Also, as the size of the anion is increased, the amount of energy associated with the hydrogen bond between the anion and a water molecule decreases, due to the more diffuse negative charge. This allows for a poorly hydrated anion, which as a result, has a greater affinity for the less hydrated, long alkyl chains of the active site. It is this interaction that

explains why the trihexyl resin has a much higher affinity for the larger anions than the more hydrophilic active sites, namely the trimethyl and triethyl ligands. It also explains why the trihexyl resin's affinity for the more hydrated anions such as bromide is minimal.

Table 3.3 data indicates a trend for the series of anions studied in terms of their radii and Gibb's free energy of hydration. By strictly following the rule that as the anion radius increases, one would expect that perrhenate would have a greater uptake than that of pertechnetate. While this rule is generally true, another aspect can govern selectivity. This other governing trend is the basicity of the anion.

For oxoacids of the type HMO_4 and others, where M is a series of metals within a group, it is found that the acidity decreases with increasing atomic weight, in turn, increasing the conjugate base strength. The basicity of the anion increases within the column, which in turn allows for greater interaction with water molecules. It is this reason that pertechnetate is removed more favorably than perrhenate due to its lower degree of basicity. It in turn is less hydrated and is therefore preferred[41].

A third trend can be seen when comparing the K_d and K'_d (eq) values. If one compares the values obtained in a 1 M chloride background to those obtained in a 90 mM chloride background for a specific anion, it can be seen that the values change by an approximate factor of ten, the approximate factor difference between chloride concentrations. This is seen for all of the values regardless of what chloride concentrations and anions are compared. This trend is also seen when the nitrate counter ion is considered. This is significant since it represents the fact that simple ion exchange is occurring. Another phenomenon that may occur is called ion intrusion in which

proportionality in values for varying background concentrations would not be seen. The fact that proportionality is seen, indicates that the exchange for the anion and original counter-ion is stoichiometric.

Interaction with Divalent Anions

Studies with the divalent anions, sulfate and selenate, showed a reversal in trends when compared to the monovalent anions. To explain the low sorption of these anions, it must be noted that two adjacent active sites must be utilized when exchanging for these anions. This in turn, allows for a lower degree of sorption when compared to monovalent anion uptake, which only requires one active site. If the trend in uptake is analyzed, it can be seen that very little of either species is sorbed by the more hydrophobic trihexyl, bifunctional, and tributyl resins. However, some uptake is seen for the more hydrophilic trimethyl and triethyl ligands. This is due again to the relationship of the ΔG_H values and the relative size of the anions. Both sulfate and selenate are relatively hard anions. This is due to their high charge to size ratio. This higher concentration of charge density thus allows for greater interaction with water molecules, in turn creating a well hydrated ion. The hydrated nature of the anions then allows for greater interaction with the more hydrophilic trimethyl and triethyl groups and less interaction with the more hydrophobic trihexyl, bifunctional, and tributyl ligands. Table 3.4 shows the thermochemical radii and ΔG_H values for selenate and sulfate[40].

Table 3.4 Thermochemical Radii and Gibb's Free Energy of Hydration Values (Divalent Anions)

Anion	Thermochemical Radius (nm)	ΔG_H (calculated) (kJ/mol)
SeO_4^{2-}	.243	-1047
SO_4^{2-}	.230	-1103

Comparison of Resins

In addition to the trends stated previously, a plot can be produced that shows the increased affinity for the anions as the length of the alkyl chain is increased within the active site. The plot shows the relationship between K'_d (eq) and the length of the alkyl chain. Figures 3.2 and 3.3 show this relationship. The data sets are represented in two separate plots to show the data sets more clearly.

If the two graphs were combined, it would be seen that the trend line slope of each data set varies with respect to the cation radius of the ligand. The slope is important since it describes the uptake dependence on the length of alkyl chain. The slopes are found to decrease in the following order, which follows the decreasing affinity for the anions.

$$(Hex)_3 > (Bu)_3 > (Et)_3 > (Me)_3$$

If the same plots were carried out for the divalent anions, the trend lines would be reversed since the hydrophilic trimethyl ligand has a greater affinity for the well hydrated sulfate and selenate anions, than does the hydrophobic trihexyl groups.

A second plot can be made which makes the correlation of the K'_d (eq) to the number of carbons within the alkyl chain of the ligand. Figure 3.4 shows this relationship for pertechnetate, perrhenate and iodide. Nitrate and bromide were omitted for clarity.

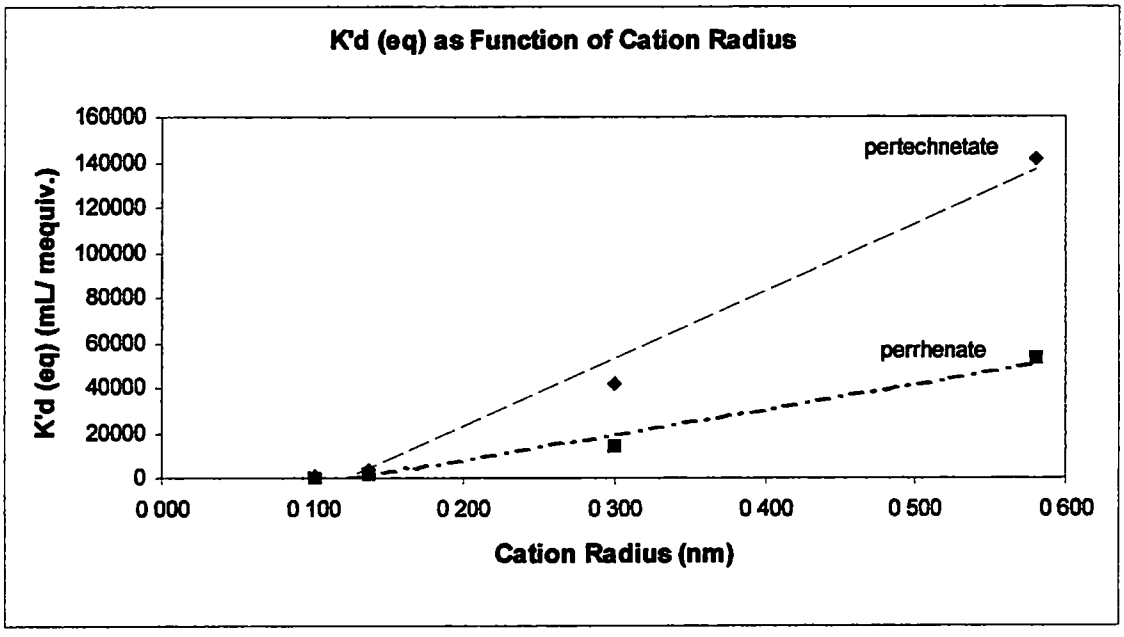

Figure 3.2 K'_d (eq) Dependence on Cation (Ligand) Radius; (pertechnetate, perrhenate)

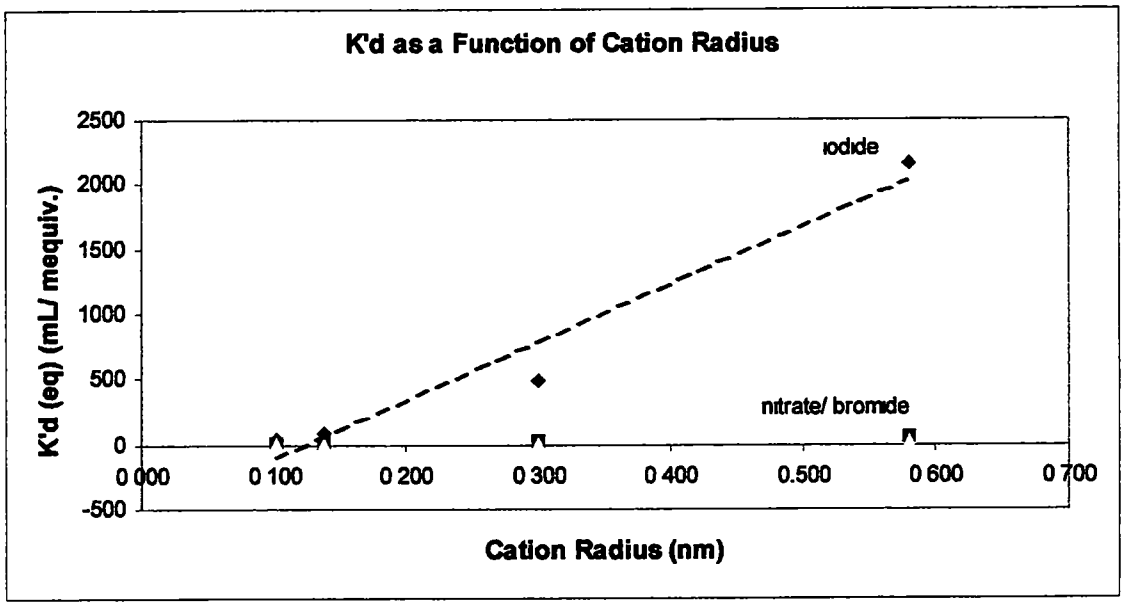

Figure 3.3 K'_d (eq) Dependence on Cation (Ligand) Radius; (iodide, nitrate, bromide)

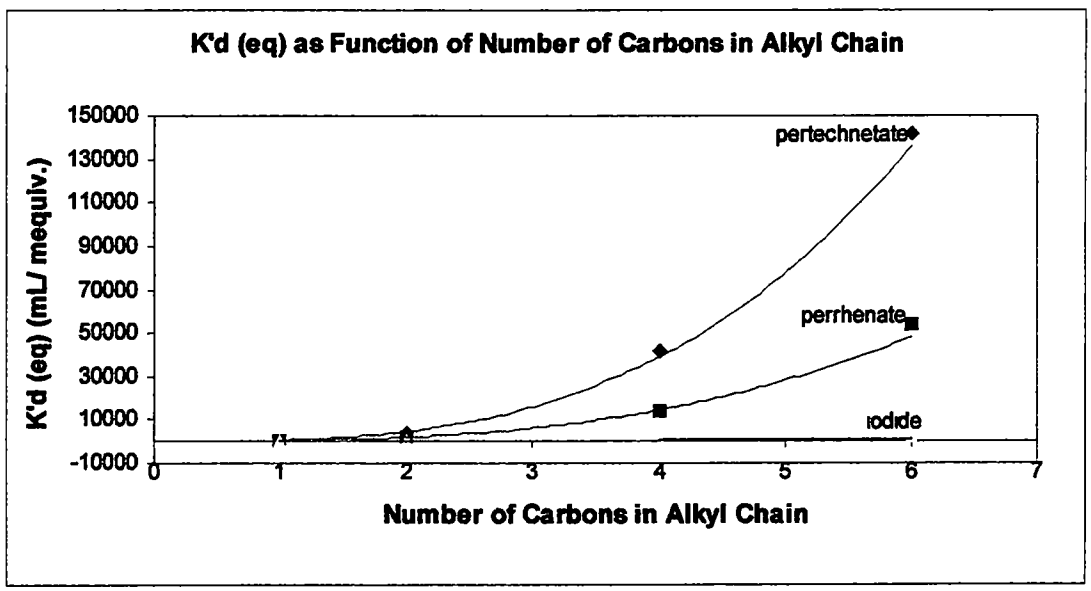

Figure 3.4 Relationship between K'_d (eq) and Number of Carbons in Alkyl Chain

Figure 3.4 shows trend lines when the power equation is applied. The power equation is defined by Equation 3.5:

$$y = cx^b \qquad (3.5)$$

The trend lines indicate a power dependency on the number of carbons within the alkyl chain and the uptake of the resin. The dependency increases for the more hydrophobic anions.

Conclusion

Upon inspection of the K_d and K'_d (eq) values for each of the anions studied, it can be seen that as the alkyl chain length is increased, the affinity for the more poorly hydrated anions increases. This is due to the poorly hydrated active site of the long alkyl chain interacting with the poorly hydrated anions. The uptake of the monovalent anions followed the trend below regardless of the background chloride concentration.

$$TcO_4^- > ReO_4^- > I^- > NO_3^- > Br^-$$

The trend is reversed when studying the divalent anions. Here the hydrophilic divalent anions interact more strongly with the hydrophilic ligands. These include both the trimethyl and triethyl amine ligands. It must be remembered that the uptake of the divalent anions is small to negligible, due to the need of having two adjacent active sites in order for exchange to occur. This is in contrast to the monovalent anions that require only one active site.

It is also seen that as the chloride or nitrate concentration is varied, while holding the anion of interest concentration constant, the K_d and K'_d (eq) values change proportionally. This is an indication that simple ion exchange is occurring and that the process is stoichiometric. It can also be seen that when the hydrophilic triethyl groups are introduced into the trihexyl resin to give the newly designed bifunctional resin, that no loss in selectivity is seen. The bifunctional resin performs better than the tributyl, triethyl and trimethyl amine resins.

While it was mentioned previously that kinetics were not studied directly in these series of experiments, the issue of kinetics is a serious problem that must be addressed when trying to design a resin that exhibits both favorable selectivity and kinetics. Again, to reiterate, as the length of the alkyl chain increases, the kinetics become unfavorable, but when hydrophilic ligands are introduced into a hydrophobic resin, the kinetics improve. Our original hypothesis explaining the decrease in kinetics involves the idea of active site hydration. This idea will be thoroughly explored and discussed in the final part of this work.

CHAPTER 4

A Study of the Water of Hydration in Ion Exchange Resins

Introduction

As stated in the previous portion of this work, the trihexyl amine resin exhibited slow kinetics when compared to the other resins that contained shorter alkyl chains within the active site.[35] It is this problem of slow kinetics that leads us to the investigation described in this work.

The presence of different water types within solid matrices has been well documented. Different water types have been found within hydrocolloids that commonly see use in wound dressings in the medical field. They are used due to their hygroscopic characteristics. It is essential to understand the water structuring within these types of materials to better understand the mechanism of healing, to help determine proper methods to treat skin disorders, and how the bandage works to keep the wound free of moisture and infection. Within these types of materials, multiple types of water have been found when analyzed by differential scanning calorimetry.[42]

Another type of material, such as the mineral sepiolite, has also been found to contain different types of water. Sepiolite is known to possess large channels within its crystalline structure. The mineral has found use as an adsorbant, and as a catalyst support in industrial settings. Studies which utilized thermogravimetric analysis showed the presence of four different types of water within the channels.[43] These different waters were described and named in terms of their interactions with the octahedral sheets of the mineral structure.

Even though the concept of multiple types of water within solids is not new, this is the first study done which makes an effort to quantify the presence of multiple types of water within ion exchange resins. It is believed that at least two different types of water are found within the resins, the first that fills the macropores, and the second that hydrates the active site and the polymeric backbone. It is also hypothesized that as the length of the alkyl chain within the ligand increases, the amount of water associated with the active site will decrease due to the hydrophobicity of the alkyl chains.

To determine the water content of the resin, a general characterization technique, known as percent solids (dry to wet resin mass ratio), can be carried out. This technique normally gives a trend that follows the relative hydrophilicity/ hydrophobicity of the resin. We hoped to make a correlation between percent solids and the water associated with the active site.

We also believe that as the ligand density decreases, the amount of water associated will decrease due to the large spaces between adjacent ligands. The type of counter-ion is also believed to play a role in the structuring of the water due to the ability, or lack thereof, of the ion to undergo an ion-dipole interaction with the water. We plan to study each of these parameters mentioned and their effect on the resins hydration water by thermogravimetric analysis, a technique that monitors mass as a function of temperature and time. Cooling experiments and dehydration/ rehydration experiments will also be carried out to gain a better understanding of the kinetics of water loss and to gain an idea of hysteresis of the resins.

In terms of kinetics, we believe that the trihexyl amine resin which possesses the longest alkyl chains exhibit poor kinetics due to the lack of water that hydrates the active sites[35]. This hydrophobic environment restricts the movement of well hydrated ions within the resin, thus decreasing the rate of exchange. However, this hydrophobic environment allows for selectivity of less hydrated anions over smaller more hydrated anions.[35]

While the effect of crosslinking was not directly studied in this work, it should be noted that by substantially increasing the degree of crosslinking, the resins affinity for less hydrated anions increases. This enhanced selectivity originates from the increased rigidity within the higher crosslinked matrix. The increased crosslinking causes the exchange ligands to become less congregated in hydrated regions, causing the increased selectivity for less hydrated anions. Polymeric backbones that are lightly crosslinked allow for more hydrated regions to form within the resin, thus allowing for more hydrated ions to interact with the active site.[35]

The monofunctional resins studied utilize a quaternary amine group. The amine groups studied before for their properties involve the trimethyl, triethyl, tributyl, and trihexyl type. A bifunctional resin which possesses both trihexyl and triethyl groups was also studied to determine the effect of incorporation of a more hydrophilic ligand. Resins were also studied that had varying degree of functionalization with trimethyl amine. This was done by changing the copolymer support from a pure VBC backbone, to a support that contained varying ratios of VBC and STY. It is believed that the amount of water will change as the amount of functionality decreases. Fluoride, chloride and nitrate

counter-ions were also studied with the trimethyl amine resin to determine how the counter-ion effected the water structuring within the resin. Cooling and dehydration/ rehydration experiments will be carried out on the trimethyl resin, since it should possess the most water due to the hydrophilic nature of the ligand.

Experimental

Resin Preparation

All resins were synthesized and characterized (see experimental section) prior to analysis by thermogravimetric analysis (TGA). All but two resins were macroreticular type, with the others being of gel type. All resins were in their original chloride form unless effect of counter ion was being studied.

To study the effect of counter-ion, a small amount of trimethyl resin was eluted with 1L of 1 M nitric acid for conversion to the nitrate form, or with 1 L of 1 M sodium fluoride solution for conversion to its fluoride form. Both elutions were carried out over a 1 hour period. To test for complete conversion, a small sample of the eluent from each elution was collected into a small vial and tested with aqueous silver nitrate for the presence of insoluble silver chloride. The elution was continued until no precipitate was found. The resin eluted with the acid was then rinsed with nanopure water until a neutral pH was obtained. The pH was tested using simple litmus paper. The resins were then Buchner dried (see experimental) and then transferred to a small glass vial labeled appropriately, and then capped tightly until time of analysis.

Thermogravimetric Analysis Heating Sequence

A Stanton Redcroft Simultaneous Thermal Analysis 780 Series instrument was used for all analyses. Resins were measured into a small crucible and placed within the furnace. The furnace was maintained with a dry air atmosphere. During the analysis, the resin was allowed to progress through its initial weight loss during a long term room temperature hold at 25 ^{0} C. This holding period usually extended overnight and was discontinued once a plateau was reached in the weight loss curve. The resin was then subjected to a heating sequence that progressed at a 10 $^{\circ}$C/min ramp rate. The ramping started at room temperature and ended at 150 $^{\circ}$C. Following the ramping sequence, the resin was then held at 150 $^{\circ}$C for 200 minutes. The resin and furnace were then allowed to cool to room temperature and were then subjected to a ramping sequence from room temperature up to 150 $^{\circ}$C at a 10 $^{\circ}$C/min ramp rate. This final ramping stage was performed to observe the baseline for the system. This heating sequence was carried out on all resins studied. This heating sequence was found to be most suitable for the determination of the resin's water of hydration since if initial heating was carried out, discrimination between water types could not be made.

Cooling Experiment Sequence

The resin was prepared as above and placed into the furnace as with the normal heating sequence. The temperature of the furnace was lowered, to approximately 7 ^{0} C, by cooling the air within the chamber. This was done by lowering the thermostat of the oven, and the addition of antifreeze to prevent the oven from freezing. The resin was

then subjected to this cooled temperature until a plateau was reached in the TGA curve. The remainder of the sequence follows that of the heating sequence mentioned previously.

Dehydration/ Rehydration Sequence

This sequence followed that of the normal heating sequence mentioned previously, but then was followed by a rehydration period. The rehydration was carried out by bubbling water into the air that entered the furnace and sample area. An approximate relative humidity of 75 % was attained. This rehydration was continued until a plateau was reached, followed by another dehydration sequence.

Results

General Observations

The TGA curves (see Appendix) suggest that multiple types of water are present within the resin's pores. This is seen for all resins studied. The long term hold at room temperature shows the largest weight loss indicating that the majority of the water within the resin has no strong interaction with the ligand or polymeric backbone. We define this first type of water as Type I water. Type I water is calculated by determining the percent mass change and comparing it to the starting mass.

Polymeric backbones ranged from 100% VBC to 95% PS/ 5% VBC. Both unfunctionalized VBC and PS resins were analyzed for the control experiments, since these were the precursors for all the resins. Both the VBC and PS resins exhibited no

further weight loss after the room temperature hold. This indicates the presence of only Type I water within the resins. The control resins also exhibited another behavior that was unique from the functionalized resins when subjected to the TGA analysis. If the derivatives of the weight loss curve (DTG) are analyzed, it can be seen that the rate of water removal is not constant. The inconsistent rate of removal is seen by the changing slope within the DTG curve. If the water being removed from the resin was leaving at a constant rate, a constant slope would be observed. This inconsistent rate of water loss leads us to believe that potentially more than one type of water may be removed during this room temperature hold. We define this water as Type II water. This second type of water is once again seen in all the resins studied.

If the DTG curves are analyzed further and compared to the PS control resin, marked differences can be seen in the manner in which the water leaves the resin. The unfunctionalized resin exhibits a sharp break in the DTG curves indicating that the water leaves abruptly. The functionalized resins display a rounded shoulder when approaching the end of the initial water loss. The smooth curve of the functionalized resins indicates a stronger interaction with other water types remaining within the resin. This comparison between unfunctionalized and functionalized resins leads us to the third type of water present, Type III water. This water can only be quantified by extrapolation and deconvolution of the DTG and weight loss curves and is, once again, only seen in the functionalized resins.

The heating stage indicates a final, different type of water that is present within the functionalized resins. This weight loss is usually on the order of 0.5-2 % of the

resin's total water weight. It is believed that this small weight loss corresponds to the last portion of water that is bound to the resin's active site. We define this last water removed from the resin as Type IV water. The amount of Type IV water is calculated by determining the percent mass change and comparing it to the baseline and to the mass at the initial onset of heating. All resins analyzed exhibit this type of behavior, regardless of the degree of functionalization (except for unfunctionalized controls), type of active site, type of counter-ion or type of copolymer.

As stated above, the resins exhibit a small weight loss during the ramping stage indicating the removal of more tightly bound water within the resin. Our TGA results indicate that the amount of bound water is dependent on the type of functionality found within the resin. In our resins, the functionality includes quaternary ammonium groups of the following types: trimethyl, triethyl, tributyl, and trihexyl, with amount of Type IV water decreasing in the respective order. A bifunctional resin was also tested which possessed both triethyl and trihexyl groups. The introduction of triethyl groups gives the functional site greater hydrophilicity which is indicated by the increase in amount of Type IV water present.

The cooling and dehydration/ rehydration experiments failed to yield useful information. The cooling experiments, while allowing the water to be removed at a slower rate, gave no new information that allowed for the quantitation of Type II water. The dehydration/ rehydration experiments did show some weight gain during the rehydration portion of the run, but this water was then easily removed when subjected to a

long term, room temperature hold. This indicates that the absorbed water is not Type IV water, rather some other type due to its ease of removal.

Water Classification System

Using observations from above, we distinctly define each of the different water types, and hence develop a water of hydration classification system for ion exchange resins.

* **Type I** : Bulk water in the macro pores. This water is removed quickly in dry air at room temperature.

* **Type II** : Bulk water in the micro pores of the gel. This water is removed quickly in dry air at room temperature and thereby cannot be distinguished from macro pore water. This water is believed to exist due to the different rate loss seen during the room temperature hold.

* **Type III** : This water makes up approximately 1 water molecule maximum per site. It is removed slowly at room temperature in dry air. This water is measured by extrapolation and by comparison of functionalized resins to DTG curves and unfunctionalized PS DTG curves.

* **Type IV** : This represents the last portion of water that is associated with the active site. This water is only removed upon heating.

We therefore define gel water as the sum of Type II, Type III, and Type IV water.

Results from Fully Functionalized Resins

Table 4.1 shows the amount of Type IV water with respect to exchange capacity and functional group. An increase in the amount of Type IV water is found as the length of the alkyl chain in the functional group is decreased. The least amount of Type IV water is seen in the trihexyl amine resin, which coincides with the functional group's

greater hydrophobicity. The amount of Type IV water within the bifunctional resin shows that the introduction of the more hydrophilic triethyl groups gives the ligand greater hydrophilicity despite the presence of the hydrophobic trihexyl amine groups. The active sites can be placed in the following order based on their Type IV water content:

$$(Hex)_3 < (Bu)_3 < (Hex)_3/(Et)_3 < (Et)_3 < (Me)_3$$

Table 4.1 Effect of Ligand Type on Amount of Type IV Water

Functionality	*Exchange Cap. (meq/g)**	*Moles Type IV Water/ eq*
bifunctional	2.14	0.13
bifunctional	2.23	0.22
trihexyl	1.40	0.040
trihexyl	1.75	0.030
tributyl	2.09	0.13
tributyl	2.08	0.10
triethyl	3.06	0.36
triethyl	3.17	0.54
trimethyl	4.03	0.68
trimethyl	3.70	0.63

*Experimental exchange capacity; based off of nitrogen elemental analysis.
All resins in chloride form.
Different resin batches as indicated by capacity.

Results from Trimethyl Resins with Various Counter-Ions

Varying the counter-ion on the exchange site gave results that indicate that not only does the type of exchange site within the resin play a role in the amount of Type IV water, but also what type of counter-ion is present. All resins studied previously were in their original chloride forms.

Table 4.2 indicates that upon varying the counter-ion from a hard anion such as chloride to a softer anion such as nitrate, it can be seen that the amount of Type IV water

present within the resin decreased dramatically. The diffuse negative charge within the nitrate anion does not allow for sufficient ion-dipole interaction to take place with water molecules within the resin. Switching to a fluoride counter-ion, which is harder than chloride due to its smaller size and greater charge density, the amount of Type IV water increases to nearly one molecule of water per active site. This is most likely due to the greater ion-dipole interaction that is allowed.

Table 4.2 Effect of Counter- Ion on Amount of Type IV Water

Counter-ion	*Exchange Capacity (meq/g)**	*Moles Type IV Water/ eq*
NO_3^-	4.03	0.11
NO_3^-	3.70	0.23
Cl^-	4.03	0.68
Cl^-	3.70	0.66
F^-	4.03	0.98
F^-	3.70	1.01

*Experimental exchange capacity; based off of nitrogen elemental analysis.
**All resins tested of trimethyl type on 100% VBC support.

Results from Partially Functionalized Trimethyl Resins

Table 4.3 shows the amount of Type IV water found when the polymeric backbone was varied from a pure vinylbenzyl chloride matrix to a PS/ VBC copolymer. As expected from the previous results, the amount of Type IV water present within the resins increased with increasing percent of trimethyl amine groups. An interesting result was found though when the amount of Type IV water found was compared to that found in a fully functionalized resin. A fully functionalized tributyl resin possesses approximately 0.12 moles of Type IV water, whereas a 5 % functionalized trimethyl resin has approximately 0.20 moles of Type IV water. A potential explanation of this is the

incorporation of the hydrophobic benzene rings from the styrene monomer. These benzene rings cause Type IV water to rearrange within the resin so as to maximize the amount of water present around the hydrophilic trimethyl groups. Another interesting observation is that while the amount of Type IV water present decreases with the ligand density, the difference between a 5 % functionalized and a 75 % functionalized is only about 0.4 water molecules. This indicates that even though the spacing between adjacent active sites is increased as the PS content is increased, the high hydrophilic nature of the trimethyl ligand still allows for the presence of a considerable amount of water. Also, it can be seen that a maximum amount of Type IV water is reached around the 50/50 support type. This can be interpreted as the exchange sites reaching some critical intersite distance, perhaps allowing for bridging water.

Table 4.3 Effect of Ligand Density on Amount of Type IV Water

mol % VBC/ STY	*Exchange Cap. (meq/g)**	*Moles Type IV Water/ eq*
5/95	0.59	0.43
5/95	0.50	0.48
18/82	1.77	0.45
18/82	1.22	0.38
50/50	3.01	0.54
50/50	2.30	0.70
75/25	3.36	0.66
75/25	3.16	0.81
100/0	4.03	0.68
100/0	3.70	0.63

*Experimental exchange capacity; based off of nitrogen elemental analysis.
VBC=vinyl benzyl chloride, STY=styrene
All resins in chloride form.

Results from Trimethyl Ammonium Gel Type Resins

When the type of resin was changed from macroreticular type to a gel type bead with the same degree of crosslinking (5 %), there was little change in the amount of Type IV water associated with the functional groups. However, the amount of Type III water increased from 3 % to approximately 6 % of the total water weight. If the percentage of Type III water is looked at for macroreticular type resins, the highest percentage found is only 4.5 %. If the definition of gel water is applied, the gel type resin contains more gel water than the macroreticular type resins. Another trimethyl gel type resin was studied, but with 2 % crosslinking of divinylbenzene. Here the amount of Type IV water per active site is consistent with the other gel type resins studied and also with the macroreticular type resins studied. However, if the percentage of Type III water is compared to that of the 5 % crosslinked gel type resin, the percentage decreases by about half. This is believed to be due to lower degree of crosslinking. The 5 % crosslinked copolymer possesses a more hydrophobic backbone that is from the incorporation of the benzene rings from the divinylbenzene crosslinking agent. The introduction of the hydrophobic rings does not allow the exchange sites to find optimal interaction. This may lead to more highly hydrated sites with the sites positioned as in a reverse micelle. The amount of Type IV water remains nearly constant, since the ligand density does not change dramatically upon increasing crosslinking. See Table 4.4 for data.

Table 4.4 Effect of Copolymer Type on Amount of Gel Phase Water (Trimethyl)

Exchange Capacity* (meq/g)	% Crosslinking	Type IV water/ eq	% Type III water
4.12	2	0.54	2.75
3.95	5	0.60	5.50
4.65	5	0.56	6.00

* Experimental exchange capacity; based off of nitrogen elemental analysis.

Figure 4.1 shows the correlation between the amount of Type IV water and exchange capacity of the ion exchange resins for both the monofunctional resins, bifunctional resin, partially functionalized resin and variation of counter ion. By analysis and with the aid of trend lines, it can be seen that a maximum amount of bound water is present within the resins, when holding the counter ion constant. Extrapolation from the graph indicates that approximately 0.60 moles of bound water is the maximum amount of water permitted to exist between neighboring exchange sites.

Discussion

The presence of less than one water molecule per active site for resins in the chloride form presents an interesting scenario to the potential arrangement of these water molecules. The maximum amount of bound water that can be present between exchange sites as seen from Figure 4.1, indicates a potential bridging or similar type of bonding phenomenon between water molecules and adjacent active sites. This phenomenon takes place for the more hydrophilic trimethyl and triethyl groups. Once the carbon chain within the ligand is increased to four, the bridging between two active sites decreases. This may be partially due to the longer, more mobile chains of the tributyl groups in

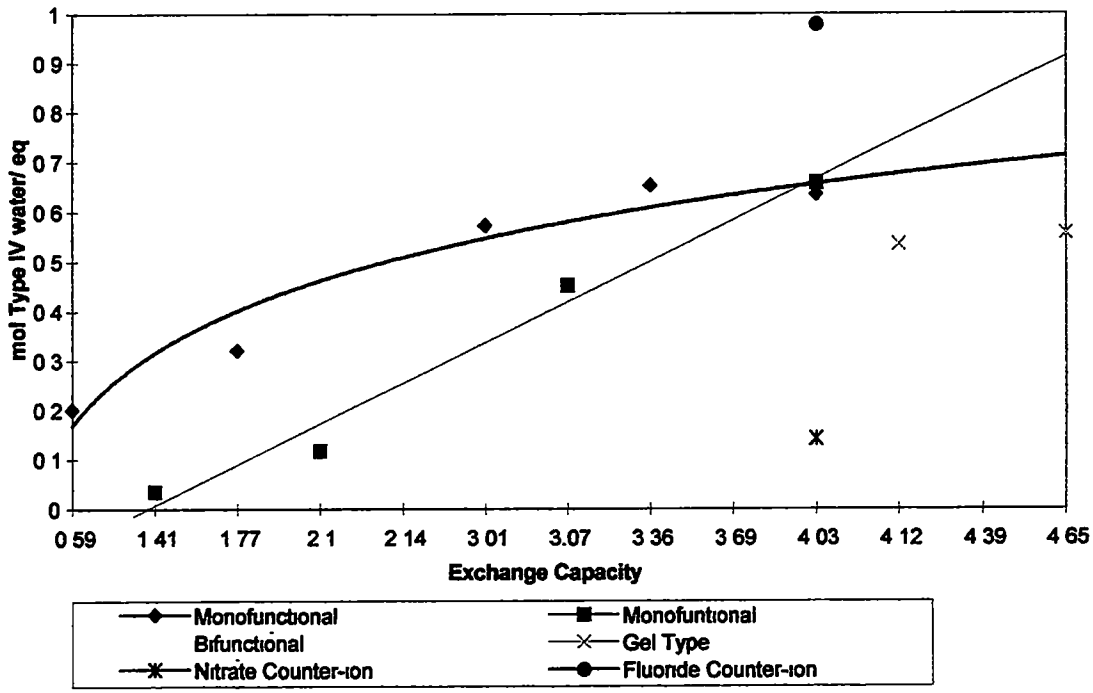

Figure 4.1 Correlation of Type IV Water to Resin Exchange Capacity

addition to their increased hydrophobicity, or potentially increased sharing of a single water molecule between multiple active sites. This is also believed to occur with the trihexyl amine ligand.

Results from the variation of the counter-ion indicate that the water content changes dramatically upon introduction of different anions. While the chloride counter ion seems to permit bridging between adjacent active sites, the introduction of fluoride seems to allow for nearly one water molecule per active site, while the incorporation of the soft nitrate ion allows for only one tenth of a water molecule per active site. This is, once again, due to the poor ion-dipole interaction allowed due to the diffuse negative charge over the anion.

As stated previously, the resins that possess longer alkyl chains within the active site allow for greater selectivity of softer, less hydrated anions. It was also mentioned, that as the carbon chain length is increased, the kinetics decrease dramatically.[35] Natural ground water will contain some nitrate.[42] If the resin is initially used in the chloride form, then over a period of time, the chloride will eventually be exchanged for softer anions such as nitrate. This conversion, in turn, is believed to lead to a dehydration phenomenon within the resin as seen from the TGA results as the counter-ion is varied. This supports our original hypothesis that active site hydration plays a does indeed play a role in resin kinetics. The bifunctional resin, as previously mentioned, possesses both good selectivity and favorable kinetics. It is believed that the introduction of the more hydrophilic triethyl groups within the trihexyl groups counteracts the dehydration effect seen, thus allowing for favorable kinetics.

Kinetic Studies

Experimental Design

All resins were Buchner dried previously and percent solids carried out. Enough resin to give 0.5meq of active site was weighed in a clean, labeled 50 mL polypropylene centrifuge tube. 25 mL of contact solution that consisted of 1.0×10^{-4} M ReO_4^- and 1 M Cl^- was volumetrically pipetted onto the resin in each of the tubes. The samples were then placed on an orbital shaker (approximately 368 rpm) and allowed to exchange for a specified amount of time. Contact time was started at the onset of placement onto the shaker since uniform mixing was not achieved during pipetting of the solution. Kinetic studies were completed with the monofunctional resins in chloride and nitrate form (with chloride and nitrate background respectively), and with the partially functionalized resins in chloride form only. (See individual tables for contact times.)

Upon completion of the contact time, the resin was removed from the orbital shaker and solution was removed and filtered using a single use, disposable syringe equipped with a 0.2 μm filter. Enough solution was filtered to give approximately a 10 mL volume. The samples were then analyzed by inductively coupled plasma (Thermal Jarrell Ash) with the use of a high solids nebulizer, due to the high ionic strength of the solution.

Results

Since the majority of the TGA experiments were carried out with the resins in their chloride form, initial kinetic studies were carried out with the chloride counter-ion

and chloride in the background matrix. Table 4.5 gives the log K'd values for the uptake of perrhenate for each of the resins at the individual contact times. A general trend can be seen that as the length of the alkyl chain is increased in the exchange site, the selectivity increases. However, these results indicate that the extraction power of the tribuytl, trihexyl, and bifunctional resins are nearly equal. The reason behind this phenomenon

Table 4.5
K'd (ReO_4^-) as a Function of Time (Chloride Counter Ion/ Chloride Background)

Time (hrs.)	log K'd $(Me)_3N+$	log K'd $(Et)_3N+$	log K'd $(Bu)_3N+$	log K'd $(Hex)_3N+$	log K'd Bifunctional
0.08	2.20	2.80	3.30	3.64	3.31
0.5	2.46	3.24	3.77	4.06	3.72
1	2.57	3.27	3.94	4.03	3.79
5	2.60	3.33	4.03	4.28	4.02
24	2.60	3.34	4.23	4.46	4.21
96	2.65	3.33	4.51	4.45	4.29
168	2.59	3.33	4.54	4.26	4.26

K'd in (mL/meq)
1×10^{-4} M ReO_4^- / 1M Cl^-

remains unclear. It would be expected that the trihexyl amine resin have the greatest extraction power due to its long alkyl chains.[35] It can also be noticed that equilibrium is nearly reached within the first five hours of contact. This is very surprising since previous kinetic studies in dilute solutions showed equilibration times on the order of weeks for the trihexyl amine resin.[35] The results presented here show little if any difference in time needed for the resins to reach equilibrium.

The TGA results show that when the counter ion is varied within the resin, from a hard anion such as chloride to a soft anion such as nitrate, the amount of Type IV water that is present decreases by more than a half. If the kinetics of the resins are indeed

dependent on the amount of water associated with the active site, then having a poorly hydrated anion such as nitrate present should cause the kinetics to decrease as well. Table 4.6 shows the log K'd for the uptake of perrhenate as a function of time with the nitrate counter-ion and nitrate present within the background matrix. However, as with the chloride experiments, equilibrium was reached almost within the first five hours of contact.

Comparison of the log K'd values show a decrease in uptake when the counter-ion and chloride matrix are switched to that of nitrate. The decrease in uptake is expected since the competition between perrhenate and nitrate for the active site is much greater.

Table 4.6
K'd (ReO_4^-) as a Function of Time (Nitrate Counter Ion/ Nitrate Background)

Time (hrs.)	log K'd $(Me)_3N+$	log K'd $(Et)_3N+$	log K'd $(Bu)_3N+$	log K'd $(Hex)_3N+$	log K'd Bifunctional
1.25	1.64	2.03	2.69	2.32	2.66
4.75	1.65	2.04	2.74	2.86	2.68
24	1.71	2.03	2.70	3.04	2.69
96	1.55	2.00	2.71	3.07	2.69
191	1.52	1.98	2.70	3.07	2.69

K'd in (mL/ meq)
1×10^{-4} M ReO_4^- / 1M NO_3^-

This is due to the presence of the softer nitrate anion and the soft perrhenate as opposed to the presence of the hard chloride anion.

The effect of ligand density was studied by varying the copolymer support from pure VBC to a VBC/ STY mix. It was assumed that ligand density would decrease the rate of uptake of perrhenate; however, this was only true for the 5 % functionalized resin. The log K'd values (Table 4.7) indicate that equilibrium is reached within about the first

hour of contact. Uptake is faster for the partially functionalized resins than for the fully functionalized resin in the first five minutes of contact. This is probably due to the benzene rings from the styrene monomer. As stated before, just as increasing crosslinking increases selectivity for less hydrated anions, the incorporation of hydrophobic styrene units gives the same type of results. After about an hour, the fully functionalized resin uptake is comparable to the others studied in this series.

Table 4.7
K'd (ReO_4^-) as Function of Time (Partially Functionalized Trimethyl Resins)

Time (hrs.)	log K'd 100%	log K'd 75%	log K'd 50%	log K'd 18%	log K'd 5%
0.08	2.20	2.52	2.43	2.31	0.64
0.5	2.46	2.56	2.52	2.56	0.56
1	2.57	2.60	2.56	2.60	0.36
5	2.60	2.59	2.50	2.59	1.28
24	2.60	2.54	2.52	2.65	0.52

*Chloride counter ion and chloride background matrix.
K'd in (mL/ meq)
1×10^{-4} M ReO_4^- / 1M Cl^-

All the kinetic results described previously show equilibrium being reached within the first 5 hours of contact. However, if the rate of uptake is monitored as a function of time, it can be seen that the matrix that contained the nitrate counter-ion and nitrate background matrix is indeed slower than that of chloride. Table 4.8 shows the % completion of uptake as a function of time for the trihexyl resin in both the chloride and nitrate matrices.

Table 4.8
Percent Completion for Trihexyl Ammonium Resin in Nitrate/ Chloride Matrices

Chloride Counter-Ion/ Chloride Background		***Nitrate Counter-Ion/ Nitrate Background***	
Time (hrs.)	**% Completion**	**Time (hrs.)**	**% Completion**
0.08	99.03	1.25	82.56
0.5	99.73	4.75	97.33
1	99.71	24	99.67
5	99.91	96	100.00
24	100.00	191	99.98
96	100.00		
168	99.90		

As can be seen from the data above, the chloride matrix has almost reached equilibrium within the first five minutes of contact. When this is compared to the nitrate matrix, it requires nearly 24 hours to reach equilibrium. This can be attributed to the amount of Type IV water associated with the active site. If the trend of the amount of Type IV water associated with the ligands is recalled, the trihexyl amine ligand possessed the least amount. This is due to the increased hydrophobicity of the ligand. Also, if the effect of changing the counter ion is considered, a relatively large anion such as nitrate does not allow for sufficient ion-dipole interaction. The combination of these two factors dramatically decreases the amount of Type IV water associated with the exchange site. This, in turn, causes the anion capable of exchanging to travel through hydrophobic regions, which in turn, decreases the rate of exchange. This phenomenon is enhanced in dilute solutions, which causes extended periods of time for the trihexyl amine resin to reach equilibrium.

Discussion of Results and Ionic Strength Dependency

In ion exchange, a spherical ion exchanger containing some counter-ion Y^- is placed in a solution of electrolyte AX, where X is another counter-ion and A is some co-ion. As equilibrium is approached, the initial counter ion Y^- must diffuse away from the active site and out of the beads into solution, while ion X^- must diffuse from the bulk solution into the bead and active site. It is accepted that the rate determining step in ion exchange is the diffusion time needed for the counter ions to diffuse out of and into the bead. (This is only true when the sites are non-coordinating.) This phenomenon is believed to occur rather than a "chemical" exchange at the fixed ionic group (active site). This leads to the conclusion that ion exchange is a diffusion phenomenon. Ion exchange is also inherently a stoichiometric process. As a counter-ion leaves the matrix of the bead, an equivalent amount of the other counter-ion must take its place to maintain electroneutrality. As the original counter-ion moves away from the fixed ionic group, an electric charge surplus is created which must be counteracted.[1]

As stated previously, it was believed that the unfavorable kinetics of the trihexyl amine resin was due to the lack of hydration of the active site and incorporation of long alkyl chains into the ligand. This was found to be true with previous studies with the trihexyl resin. The conditions in which the studies were carried out were with a ground water test solution that consisted of sulfate, chloride and nitrate anions. When pertechnetate was introduced into the mixture, uptake was found to be very slow. It would be expected that as the concentration of the background matrix is increased, the

kinetics of the resins would slow considerably. This is due to the greater possibility of the background anion interacting with the active site, rather than the anion of interest, which is present in very dilute concentrations.

However, our results show the opposite of this phenomenon. All the resins were found to be near equilibrium within the first five hours of contact. All parameters were held constant including bead size. It would be expected that if the particle size is decreased, the rate of exchange would increase due to a larger surface area, and a smaller diffusion pathway into the bead and the active site.[1] In the current studies, though, particle size was held constant with those studies done in dilute solutions.

As mentioned briefly before, the rate of exchange appears to depend on the ionic strength of the solution in contact with the beads. Since diffusion into the bead is considered to be the rate determining step,[1] the contact solution must in some way be affecting the diffusion coefficients of the species in solution.

The diffusion coefficients of species within an ion exchange resin are determined by many factors. These factors include size, valence, and chemical nature of the ionic species, along with temperature and composition of the pore liquid.[1] To review, the initial studies done in dilute solutions consisted of 60 μM pertechnetate and a ground water test solution that contained chloride, nitrate, and sulfate. The matrix used for the current experiments consisted of 1.0×10^{-4} M perrhenate and 1 M Cl^-, (sodium salts). The experiments were carried out at 25 ° C. The only factor that is dramatically varied is the composition of the pore liquid. The pore liquid is in turn affected by the concentration of the external solution in which the exchange is taking place. Studies conducted in the

1950's by Schlogl indicated, that as the external solution concentration is increased, the free water within the resin decreases.[1] Naturally, one would expect the rate of diffusion of the counter-ion to decrease, but this is only for the co-ions, which is sodium in these experiments due to the use of sodium salts. The studies indicate that the mobility of the counter-ion (Cl^- or ReO_4^-) actually increases, apparently due to the increased concentration of co-ions within the pores of the resin. The analogy of the active sites and co-ions within the resins acting as potential energy troughs is offered. In order for the anion of interest to move from one energy trough to another, a potential energy barrier must be overcome. The presence of the co-ions within the pores helps facilitate the passage of these barriers.[1] Even though the perrhenate is in such low concentrations as compared to chloride, the resins affinity for perrhenate is much greater than that for chloride or nitrate due to the softness and less hydrated nature of the ion.

Conclusion

The original hypothesis of the presence of multiple types of water within ion exchange resins was found to be true. TGA results show the presence of at least four different types of water within the pores. These include Type I, Type II, Type III and Type IV water, with the amount of interaction with the polymer backbone and active site increasing from Type I water to Type IV water. Cooling experiments and dehydration/ rehydration experiments yield inconclusive results when trying to determine more accurately the amount of Type II water and Type III water present.

Also, as can be seen from the TGA results, the amount of Type IV water associated with the active site decreases as the carbon chain length is increased. This is believed to be mostly due to the increased hydrophobicity of the ligand as the carbon chain length is increased. Also, as the ligand density is decreased, the amount of Type I water decreases as well. This is attributed to the increased spacing between active sites. Finally, the counter-ion also determines the extent of hydration of the active site. The presence of a hard anion such as fluoride or chloride allows for a strong ion-dipole interaction to occur. Relative to these less charge diffuse anions, a softer anion such as nitrate does not favor the ion-dipole interaction due to its diffuse negative charge.

The original hypothesis of the extent of active site hydration and its effect on kinetics does hold true to an extent in concentrated background solutions. While equilibrium was reached with all resins in approximately five hours, the rate of exchange was indeed slower for the nitrate matrix. This is believed to be true due to the less hydrated nature of the active site due to the hydrophobicity of the trihexyl ligand coupled with the poor ion dipole interaction with the nitrate counter-ion.

Results and literature research indicate that as the concentration of the background solution is increased, the diffusion coefficients of the counter-ions (Cl^- or ReO_4^-) are increased. Conversely, the diffusion coefficients of the co-ions (Na^+) are decreased as their concentration within the pores is increased. The high concentration of co-ions within the resin, help facilitate movement of the counter-ions by helping the species overcome energy barriers.[1] Compared to previous work, the time needed to reach

equilibrium is much faster in concentrated background solutions. However, the rate of exchange is indeed slower for nitrate matrices.

CHAPTER 5

Experimental

All materials were obtained from Aldrich Chemical unless otherwise noted and were used without further purification. All solutions were prepared using Class A glass transfer pipettes and volumetric flasks.

List of Reagents Used for Synthesis of Ion Exchange Resins

Copolymer Synthesis

Organic Phase

- benzoyl peroxide; 97%
- divinylbenzene (DVB); 55.4%
- vinylbenzyl chloride (VBC); 97%
- styrene (STY); 99 +%

Aqueous Phase

- polydiallyldimethyl ammonium chloride (PADMAC), Calgon Corp.
- boric acid
- Pharmagel
- 4 – methyl – 2 – pentanol (4M2P) (used for macroreticular copolymer)

Phosphonic Acid Resins Synthesis

Alpha-ketophosphonic acid

- dimethyl sulfoxide 99.9%
- sodium bicarbonate
- 1,4 – dioxane; 99 +%
- 3N nitric acid
- 30 wt % H_2O_2
- thionyl chloride; 99 +%
- triethyl phosphite; 98%
- concentrated hydrochloric acid

Beta-ketophosphonic acid

- carbon disulfide; 99 +%
- aluminum chloride
- bromoacetyl bromide; 98 +%
- triethyl phosphite; 98%
- concentrated hydrochloric acid

Gamma-ketophosphonic acid

- same as beta-keto phosphonic acid with bromopropionyl bromide

(97 +%) substituted for bromoacetyl bromide

Phosphonic acid

- triethyl phosphite; 98%
- concentrated hydrochloric acid

Amine Resins

- all resin syntheses utilize 1,4 – dioxane, water and the respective amine
- trimethyl amine; 23-25 wt. % solution in water
- triethyl amine; 99 +%
- tributyl amine; 99 +%
- trihexyl amine; 96 %

Synthesis of Copolymers

Synthesis of 2% Crosslinked VBC Gel Copolymer

Copolymer was synthesized via suspension polymerization. The organic phase was prepared in the following manner. 3 g of benzoyl peroxide, 10.83 g of DVB and 286.17 g of VBC were weighed into a ground neck Erlenmeyer flask.

The aqueous phase was prepared by dissolving 17.92 g of PADMAC and 9.50 g of boric acid in 316 mL of distilled water in a large beaker. In a separate beaker, 1.44 g of Pharmagel was dissolved with slight heating in 158 mL of distilled water. The two aqueous mixtures are combined and mixed thoroughly. The pH of the resulting mixture is then adjusted to 10.3 with 50% sodium hydroxide.

The aqueous phase was transferred to a 2 L 3-neck round bottom flask fitted with a condenser, stir bearing, stir shaft with Teflon stir paddle, and a Claisen adapter. The Claisen adapter was fitted with a gas inlet and thermometer. Both aqueous and organic phases were sparged for 15 minutes with nitrogen. The organic phase was then

transferred to the round bottom flask with the aqueous phase. The stir paddle was positioned so that the upper edge was just above the interface of the two phases. The stir motor was turned on for two minutes and then stopped to see if separation had occurred. The formation of beads is evident by the observation of sparkling particles in the flask when looked at using a flashlight. The stir motor was then turned on with the stir speed set at 450 rpm. The stirring was stopped at intermittent times to determine if the proper bead size was obtained. Smaller beads are made using faster stir speeds, while larger are made using slower speeds. A bead size of – 40 + 60 mesh size was desired (approximately 460 rpm stir speed). After the proper bead size was made, the stir motor was kept on and the temperature raised in 7 ^{0}C increments in 15 minute intervals. This temperature increase was continued up to 80 ^{0}C over a two hour period. Temperature was monitored using a Thermowatch and heat lamp. The mixture was then held at 80 ^{0}C for 10 hours.

Following the hold at 80^0 C, the Thermowatch is removed and approximately 100 mL of distilled water was added to the round bottom flask followed by a reflux for 2 hours. After reflux, the solution is removed via gas dispersion tube and the beads stirred with 10^{-4} N HCl for 15 minutes. The acid is then removed and the resin washed 3 times with distilled water. The beads were then Buchner dried and soxhlet extracted for 17 hours with toluene. The beads were then air dried. Approximately 300 g of copolymer is obtained from the synthesis. The beads are then sieved to isolate the proper size beads.

Synthesis of 2% Crosslinked STY Gel Copolymer

The synthesis of the polystyrene gel copolymer follows that as previously described for the polyvinyl benzyl chloride gel type beads with the exception that the VBC monomer is replaced with styrene, and one tenth the amount of boric acid is used. The aqueous solution pH is also adjusted to 10.0.

Synthesis of 5% Crosslinked VBC Macroreticular (MR) Copolymer

The synthesis of VBC MR beads follows that of the gel type copolymer previously described with the exception that the following weights be used for the organic phase: 134.95 g VBC, 13.55 g DVB and 1.50 g of benzoyl peroxide. 150 g of 4M2P is also added to the organic phase.

Synthesis of 5 % Crosslinked VBC/ STY MR Copolymer

The syntheses of these copolymers follows the MR procedure previously described with the exception of the monomer weights used in the polymerization. The following indicates the amount of monomer used in each of the polymerizations.

Copolymer (VBC/STY)	Mass of VBC (g)	Mass of STY (g)
5/95	6.75	128.25
75/25	101.33	33.91

Synthesis of Phosphonic Acid Resin Family

Synthesis of Phosphonic Acid Resin

10 g of VBC gel beads cross-linked with 2% DVB by weight were functionalized via the Arbuzov reaction with 100 mL of triethylphosphite at reflux for 24 hours. After

reaction, remaining triethylphosphite was removed via gas dispersion tube. 100 mL of concentrated HCl was then added to the reaction flask and refluxed for an additional 24 hours. The final reflux with acid is used for conversion of the phosphonic ester to the phosphonic acid moiety. Following reflux, the flask was allowed to cool, the remaining acid was removed, and the beads were then washed with distilled water to bring to a neutral pH. The resin was then transferred to an extended frit and conditioned with successive 1 L/hr elutions of deionized water, 4 wt% NaOH, deionized water, 4 wt% HCl, and deionized water. The resin was then Soxhlet extracted with deionized water for 17 hours to further purify the resin followed again by the water/ base/ water/ acid/ water conditioning sequence. The resin was then analyzed for percent solids, phosphorus capacity and acid capacity. See characterization section for procedures. (The conditioning and Soxhlet extraction procedure described above was carried out for all subsequent resins in the phosphonic acid resin family.)

Synthesis of Alpha-ketophosphonic Acid Resin

10 g of VBC MR beads cross-linked with 5 wt% DVB was weighed into a 500 mL round bottom flask. To the resin, 200 mL of dimethylsulfoxide, and 30 g of $NaHCO_3$ was added and then refluxed for 24 hours. Following reflux, the solution was removed and washed with ethanol and water.

The beads were then swollen in 60 mL of a 70% aqueous dioxane solution for an hour. 130 mL of 3N HNO_3 was added and mixture refluxed for 24 hours. The beads were filtered again and swelled in 60mL of dioxane. 130mL of 30% H_2O_2 was added and

heated at 80^0 C for 24 hours. The beads were then filtered and washed with water. The resin was then conditioned in an extended frit with successive 1 L/hr elutions of deionized water, 4 wt% NaOH, deionized water, 4 wt% HCl, and deionized water. The resin was then analyzed for percent solids and acid capacity.

Following characterization, the monocarboxylic acid resin generated above was azeotropically dried with heptane and stirred with 150 mL of thionyl chloride for 48 hours at reflux. The unreacted thionyl chloride was then filtered off and the resin washed three times with dry toluene. The beads were then refluxed with 100 mL of triethylphosphite for 24 hours, followed by hydrolysis with concentrated HCl for 24 hours at reflux. The resin was then filtered and washed with water. After washing, the resin was conditioned, Soxhlet extracted, reconditioned and characterized for percent solids, phosphorus capacity and acid capacity. See characterization section for procedures.

Synthesis of Beta-ketophosphonic Acid Resin

10 g of STY gel beads cross-linked with 2 wt% DVB were swollen overnight in 40 mL of carbon disulfide. In a separate beaker, 40.0 g (300 mmol) of aluminum chloride was accurately weighed out, followed by the addition of 50 mL of carbon disulfide. The mixture was then stirred and quickly transferred to the reaction flask containing the beads. 25.19 g (124.8 mmol) of bromoacetyl bromide was then weighed into the beaker followed by the addition of 10mL of carbon disulfide to prevent hydrolysis. This was then quickly transferred to an addition funnel and added dropwise to the reaction flask. The mixture was stirred for 48 hours at 0^0 C with the an ice-water bath. The flask was

also purged with nitrogen initially, and held with a positive pressure of nitrogen. Following reaction, the resin was washed with ice-ethanol mixtures, water, acetic acid and ethanol. The resin was then dried overnight in a vacuum oven at 70^0 C.

The dried beads were then reacted with 100mL of triethylphosphite for 24 hours at reflux, beads filtered, and then hydrolyzed with concentrated HCl for an additional 24 hours at reflux. The resin was then filtered and washed with water. After washing, the resin was conditioned, Soxhlet extracted, reconditioned and characterized for percent solids, phosphorus capacity and acid capacity. See characterization section for procedures.

Synthesis of Gamma-ketophosphonic Acid Resin

Preparation of the gamma-ketophosphonic acid resin is carried out in the same manner as the beta-ketophosphonic acid resin with the exception that 21.43 g (125 mmol) of bromopropionyl bromide is substituted for bromoacetyl bromide. Conditioning, extraction and characterization is the same as previous resins. See characterization section for procedures.

Synthesis of Amine Resin Family

Synthesis of Trimethyl Ammonium Monofunctional Resin

20 g of VBC MR beads crosslinked with 5% divinylbenzene was weighed into a tared 1000 mL three-neck round bottom flask. The flask was fitted with a stir bearing, stir shaft equipped with Teflon stir paddle, condenser and stopper. A balloon was also

fitted to the opening of the condenser to help keep amine within the system due to the amines high volatility. All joints were also fitted with Teflon tape.

To the resin, 135 mL of dioxane was added and beads allowed to swell overnight. The next day, 135 mL of water was added along with 600 mL of trimethyl amine (excess) and allowed to reflux for 17 hours with the aid of a heating mantle. After reflux, the amine solution was then filtered off with the aid of a gas dispersion tube. The resin was then washed with 4 wt % HCl to neutralize any excess amine and then washed three times with deionized water. After this, the resin was then transferred to an extended frit where it was conditioned with successive 1L/hr elutions of deionized water, 4 wt% NaOH, deionized water, 4 wt% HCl, and deionized water. The resin was then characterized using nitrogen and chlorine elemental analysis, percent solids, and for total anion exchange capacity. See characterization section for procedures. (The conditioning sequence described above is utilized in all amine synthesis procedures.)

Synthesis of Triethyl and Tributyl Ammonium Monofunctional Resins

The above synthesis of the trimethyl ammonium monofunctional resin is followed for both the triethyl ammonium monofunctional and tributyl ammonium monofunctional resins. The exception is that 330 mL of triethyl amine and 280 mL of tributyl amine are substituted for trimethyl amine to create their respective resin. Conditioning and characterization is then carried out. See characterization section for procedures. Reaction flask and dioxane amounts were varied proportionally to the amount of starting material used.

Synthesis of Trihexyl Ammonium Resins

20 g of VBC MR beads crosslinked with 5% DVB was weighed into a tared 500 mL three-neck round bottom flask. The flask was then fitted with a stir bearing, stir shaft equipped with Teflon stir paddle, condenser and stopper. All joints were connected using vacuum grease. The balloon was also omitted from the setup.

320 mL of dioxane is added to the beads and allowed to swell overnight. Following swelling, 320 mL of trihexyl amine, 32 mL of 1,4-dioxane and 36 mL of water was added. After reflux, the excess amine solution was filtered off with the aid of a gas dispersion tube. The resin was then washed with 4 wt % HCl to neutralize any excess amine and washed three times with deionized water. After this, the resin was conditioned and characterized using nitrogen and chlorine elemental analysis, percent solids, and for total anion exchange capacity. See characterization section for procedures.

Synthesis of Trihexyl/ Triethyl Bifunctional Ammonium Resin

The synthesis of the bifunctional amine resin if carried out in two separate steps. The synthesis of the trihexyl ammonium resin is carried out first. Following this part of the synthesis, a small aliquot of resin is removed and characterized using nitrogen elemental analysis and total anion exchange capacity. The remainder of the synthesis can be carried out by following the procedure of the triethyl ammonium resin. Upon completion, the resin is conditioned and characterized in the same manner as other amine resins. See characterization section for procedures.

Synthesis of Partially Functionalized Trimethyl Ammonium Amine

5.00 g of the respective VBC/ STY copolymer was accurately weighed into a tared 500 mL round bottom flask. 150 mL of dioxane was added and the resin was allowed to swell overnight. After swelling, 40 mL of water was added along with 140 mL of trimethyl amine. The remainder of the setup follows that as described earlier for the other amine syntheses. Characterization also follows those as described earlier. See characterization section for procedures.

Characterization

Buchner Drying

The resin is placed into a Buchner funnel which is affixed to a side arm flask. Tubing is placed between the side arm and a vacuum source. A vacuum is applied and for five minutes to remove interstitial water from the beads. The Buchner funnel is covered with a piece of latex to aid in vacuum.

Percent Solids

A 20 mL vial is oven dried for about 2 hours and then allowed to cool in a dessicator. The vial is then accurately weighed, weight recorded, and then tared. One gram of Bucher dried resin is accurately weighed into the vial and then placed into a 110^0 C oven for 17 hours. After cooling, the weight of the oven dried resin and vial is

recorded and mass of dried resin is calculated. The percent solid is calculated using the equation below:

$$\% \text{ solid} = [(\text{dry wt. of sample})/ (\text{wet wt. of sample})] * 100$$

Acid Capacity

1 to 1.5 grams of Buchner dried resin is accurately weighed into a 250 mL ground glass Erlenmeyer flask. A magnetic stir bar is added along with 200.0 mL of standardized 0.1 N NaOH with 5wt% NaCl. The solution and beads are stirred for 17 hours at a rate of 350 rpm. A 50 mL aliquot of the contacted base solution is then titrated using phenolphthalein indicator and standardized 0.1 N HCl. The following equation is used to calculate the acid capacity of the resin.

$$\text{Acid Capacity} = [(\text{mL NaOH})(\text{N NaOH})-(4)(\text{mL HCl})(\text{N HCl})]/(\text{wet wt. of resin} * \% \text{ solids})$$

The NaOH is standardized against dry potassium hydrogen phthalate and the HCl standardized against the standardized NaOH.

Nitrogen Elemental Analysis

0.2 g of dry resin is accurately weighed into a 3-neck round bottom flask. 0.25 g $CuSO_4$, 10g K_2SO_4 , 25 mL of concentrated sulphuric acid, and a few boiling chips are added to the flask. A standard water jacket is placed in the middle neck with stoppers in the remaining two. The mixture is then gently heated (Variac at 50) for 1 hr, followed by

increased heating (Variac at 85) for 8 hours. Dissolution of the resin should be evident, with the solution being a clear, blue color.

The water jacket is then rinsed with distilled water, along with one of the stoppers. 100 mL of distilled water and a magnetic stir bar are added to the flask. A 250 mL addition funnel is placed in one of the joints and distillation apparatus in the other. The distillation apparatus (with water running through it) is then fitted with a funnel on the end. The funnel is then focused into a 600 mL beaker containing 50 mL of standardized 0.1 N HCl. 150 mL of 6 N NaOH is carefully poured into the addition funnel, and a stir plate is placed under the flask. The sodium hydroxide is then added to the flask. The solution should be brown after addition. The solution is distilled at a Variac setting of 94 until the solution distilling over is no longer basic.

After distillation, the HCl solution is then quantitatively transferred to a 250 mL volumetric flask and diluted to the mark with distilled water. Two 50 mL aliquots are then titrated using standardized 0.1 N NaOH with bromocresol green indicator. The following equation is then used to calculate the nitrogen capacity.

$$[(50mL)(N\ HCl) - 5(N\ NaOH)(volume\ of\ NaOH)]/dry\ wt.\ of\ resin$$

Phosphorus Elemental Analysis

20-25 mg of oven dried resin is accurately weighed into a 125 mL Erlenmeyer flask. 400 μL of 0.5 M $CuSO_4$, and 10 mL of concentrated sulphuric acid are added to the flask. The flask is heated vigorously (setting of 5-6) on a hot plate for 3 hours. The

solution is then allowed to cool followed by the addition of 75 mL of distilled water and 2 g of potassium persulfate. The mixture is then gently heated (setting of 3) for 2 hours. The solution is then allowed to cool. 50% NaOH is then added to the sample until a dark brown color is present. 2% H_2SO_4 is added until a clear, neutral solution is obtained. The sample is quantitatively transferred to a 10 mL volumetric flask and diluted to the mark with distilled water. A 25 mL aliquot is transferred to a 50 mL volumetric flask along with 10 mL of a vanadate-molybdate solution and diluted to the mark with distilled water. A blank is prepared using 10 mL of the vanadate-molybdate solution and water in a 50 mL volumetric flask. The samples are allowed to develop for 15 minutes, which is followed by an absorbance reading on a Spec-21 with the wavelength set at 470 nm. The phosphorus capacity is then calculated utilizing the following equations.

$$\text{mg P} = (\text{Absorbance-Intercept})/\ \text{Slope}$$

$$\text{Phosphorus Capacity (meq/g)} = (\text{mg P} * 4)/\ (30.974 * \text{dry resin wt.})$$

Chlorine Elemental Analysis

0.2 g of oven dried resin is accurately weighed into the Parr bomb capsule along with 0.7 g of mineral oil. The capsule is then placed in the holder. 10 cm of nickel alloy fuse wire was then threaded into the bomb stem holes, secured, and positioned just above the oil surface. The holder is placed into the cylinder containing 5 mL of 5% Na_2CO_3 and cap screwed tightly on. The cylinder is then purged 3 times with 30 atm of oxygen followed by bleeding after each purge. The third purge of oxygen is allowed to remain within the cylinder. The wire leads are then connected to the cylinder, and then placed

into a water bath. After insuring that no oxygen leaks are present within the system, the ignition unit is plugged in and the sample ignited. The cylinder is left within the water bath for 5 minutes.

Following combustion, the cylinder is removed and dried scrupulously. The solution is then transferred to 400 mL beaker and cylinder scrubbed with nanopure water and the aid of a rubber policeman. All washing (approximately 200 mL) were placed into the beaker. The solution was filtered using pre-folded paper into a 250 mL volumetric flask and diluted to the mark with nanopure water.

A 25 mL aliquot (duplicate samples) was pipetted into a 125 mL Erlenmeyer flask. Approximately 3 mL of 2 N HNO_3 and 10 mL (volumetrically pipetted) of 0.05 N $AgNO_3$ was added to the sample. The sample was then heated on a hot plate and allowed to come to a boil. Following heating the samples were allowed to cool in a dark place. 10 mL of $AgNO_3$ was also added to a separate flask with no sample but was not heated.

The boiled samples were then filtered into another 125 mL Erlenmeyer flask with the flask washed with a small amount of 0.01 N HNO_3. A 10 mL buret is filled with 0.05 N NH_4SCN which is to be standardized during each use.

Approximately 3 mL of $FeNH_4(SO_4)_2$ in 2 N HNO_3 is added to the flask containing only the $AgNO_3$. The silver nitrate is then titrated until a faint orange color is present. After the silver nitrate samples have been titrated, the average normality of NH_4SCN is calculated. The filtered samples are titrated in the same manner as the silver nitrate samples. The following equation can be used to calculate the chlorine capacity (meq/g) of the resin.

Chlorine Cap. = {[N $AgNO_3$)(mL $AgNO_3$)]-[(N NH_4SCN)(mL NH_4SCN]}* 10/ dry resin wt

Total Anion Exchange Capacity (TAEC)

2 g of Buchner dried resin is placed into an extended glass frit. The resin was then eluted with 250 mL of a 1 M $NaNO_3$ solution over a 1 hour period. This elution was carried out using a separatory funnel. The eluent was collected into a 250 mL volumetric flask. After elution, all the sodium nitrate solution was expelled from the frit by forcing air through it. The volumetric was diluted to the mark if needed.

A 50 mL aliquot (duplicate samples) of the eluent was transferred to a 125 mL Erlenmeyer flask. 3 drops of methyl orange indicator is added followed by 1 drop of concentrated HNO_3 (solution now pink). The solution is then neutralized with dilute NaOH until yellow again. 3 drops of methyl orange is added again followed by 3 mL of 5 wt% K_2CrO_4. The sample is then titrated with 0.05N $AgNO_3$ until a mahogany endpoint is obtained. The following equation can be used to calculate the TAEC (meq/g) of the resin.

(M $AgNO_3$ * 5 * mL $AgNO_3$)/ dry resin wt

CONCLUSION

The binding constants of the α, β, and γ-ketophosphonic acid resins and the parent phosphonic acid resin is dependent on the stability of the ring formed, or lack thereof, upon chelation of the metal ion species. In this case, Eu (III) is most tightly bound with the α-ketophosphonate due to the formation of a stable five membered ring followed by the β-ketophosphonate resin which forms a six membered ring. The γ-ketophosphonate resin along with the phosphonic acid resin both display low binding constants due to the lack of ability to form stable rings upon chelation with the europium. Coordination in these instances is most likely due to the coordination through the phosphoryl moiety. It has been found that the best method for determining these binding constants is by extracting the first four points from the data set. These first four points represent the y-asymptote portion of the x-reciprocal plot and the strongest sites capable of coordination. These four points are then subjected to a single Langmuir isotherm. Using this treatment, a series can be developed that shows the relative binding strengths of the resins. This series reiterates the stability of complexation upon ring formation with the α-keto resin binding Eu (III) the strongest followed by the β-keto, γ-ketophosphonate, and finally the phosphonic acid resin.

The selectivity of the anion exchange resins studied has been found to be dependent on the type of ligand. The following series shows the relative selectivity of the ligands studied, with the trihexyl ligand showing greatest selectivity.

$$(Hex)_3 > (Hex)_3/ (Et)_3 > (Bu)_3 > (Et)_3 > (Me)_3$$

The ligands studied that possess long alkyl chains show greater selectivity for larger anions with low hydration energies. This was found to be true for all the monovalent anions studied. The following series shows the relative affinities for each of the monovalent anions studied.

$$TcO_4^- > ReO_4^- > I^- > NO_3^- > Br^-$$

Uptake of these anions were greater in matrices that possessed chloride as the background ion, rather than nitrate, due to the greater difference in hydration energies of the anion of interest and that of chloride.

The uptake of divalent anions studied was low for all the ligands studied. This is due to the use of two exchange sites rather than one with monovalent anions. The order of the ligand selectivity is reversed due to the hard nature and high hydration energies of the anions. These anions prefer to associate with ligands that possess shorter alkyl chains. The following series can be applied for ligand selectivity with divalent anions.

$$(Me)_3 > (Et)_3 > (Bu)_3 > (Hex)_3/ (Et)_3 > (Hex)_3$$

Upon analysis of these anion exchange resins by thermogravimetric analysis, it was found that at least four types of water are present within the resins. These waters include Type I, Type II, Type III, and Type IV water. The water of greatest interest is Type IV water, since it represents the water that is most closely associated with the active site and is believed to be responsible for the kinetic behavior of the resins. It was found that resins with short, alkyl chains within their ligands possessed more Type IV water

than those with long, alkyl chains. This is due to the more hydrophilic nature of the methyl groups as opposed to the hydrophobic nature of the trihexyl groups. The introduction of triethyl groups into the trihexyl resin (to give the bifunctional resin) was also found to increase the amount of Type IV water. The amount of Type IV water was also found to decrease as the degree of functionality is decreased, and as the counter ion is varied from soft anions such as nitrate to hard anions such as fluoride.

This increased amount of Type IV water present within the bifunctional resin is believed to be the reason for increased kinetics in dilute solutions (μM concentrations). In solutions of high ionic strengths (1 M concentrations), however, kinetics were found to be favorable for all the ligands studied, regardless of the alkyl chain length. All resins regardless of the matrix was near equilibrium within five hours. This is most likely due to the increased presence of co-ions within the pores which helps increase the self-diffusion coefficients of the anion of interest. However, the rate of uptake is slower for nitrate matrices where the amount of Type IV water is decreased.

LIST OF REFERENCES

LIST OF REFERENCES

1 Helferrich, F., "Ion Exchange," McGraw Hill: New York, 1962.

2 LaGrega, M. D. et al., "Hazardous Waste Management," McGraw Hill· New York, 1994, p. 3.

3. Lewis, C. J. In Recent Developments in Separation Science, Vol. 2; Li, N. N., Ed.; CRC Press: Cleveland, 1972; p. 47-57.

4. Rıtcey, G. M.; Ashbrook, A. W. Solvent Extraction: Principles and Applications to Metallurgy, Part 1; Elsevier: Amsterdam, 1984.

5. Rıtcey, G M. *Sep Sci Technol.* **1983**, 18, 1617.

6. Walsh, D J.; Crosby, P ; Dalton, R F. *Polymer* **1983**, 24, 423.

7 Senise, P., Levi, F , *Anal. Chım. Acta.*, **1960**, 30, 509.

8 Koch, K. R., Yates, J E., *Anal Chım Acta* , **1983**, 147, 235.

9 Bicak, N.; Koza, G.; Atay, T *Journ of App Poly Sci.* **1996**, 61, 799.

10 Huang, S P., Franz, K. J.; et al *Polyhedron*, **1996**, 15, 4241.

11. Jang, B. B.; Lee, K.; et al *Journ. of Poly Scı* **1999**, 37, 3169.

12 Trochımczuk, A. W ; et al. *Sep Scı. and Tech* **1999**, 34, 2243

13 Fujiwara, M ; et al.; *Anal. Chım. Acta.*; **1993**, 274, 293.

14 Topp, K. D.; Grote, M. *React and Funct Poly.*; **1996**, 31, 117.

15 Styles, P. M.; Chanda, M.; Rempel, G. L.; *React and Funct Poly.*, **1996**, 31, 89.

16. Marsh, S. F., Jarvınen, R.A. et al ; *Journ of Radioanal. And Nuc Chem* ; **1998**, 235, 37

17. Alexandratos S D.; et al.; *Journ App Poly. Sci.*; **1996**; 61, 273.

18. Ashley, K. R , et al.; *Solv Extract and Ion Exch.*; **1994**, 12, 239.

19. Wu, Y. J.; Williamson, M. A.; *Solv. Extract. and Ion Exch.*; **1996**, 14, 285.

20. Ashley, K. R.; et al.; *Solv. Extract and Ion Exch.*; **1995**, 13, 353.

21. Gaikar, V. G.; et al; *React. and Funct. Poly.*; **1996**; 31(2); 155.

22. Lee, K.; Ku, Y.; *Sep Scı. and Tech.*; **1996**, 31, 2557.

23. Gregory, J., Semmens, M J.; *Journ. Chem. Soc Faraday Trans.*; **1972**, 68, 1045.

24. Brown, G.; Proceedings of the "Efficient Separations and Processing Crosscutting Program 1996 Technical Exchange Meeting." Jan. 16-19, 1996.

25. Triay, I. R.; Rundberg, R. S.; *Journ Phys. Chem.*; **1987**, 91, 5269.

26. Alexandratos, S. D.; et al.; *Journ. of the Amer. Chem. Soc* **1992**, 114, 3078.

27. Alexandratos, S. D.; Hussain, L. A.; *Macromolecules*; **1998**, 31, 3235.

28. Ciaccio, C. G.; M.S. Thesis, University of Tennessee, Knoxville, December 1992.

29. Connors, K. A.; Binding Constants; John Wiley and Sons· New York, 1987.

30 Deranleau, D. A.; *Journ. of Amer Chem. Soc.*, **1969**, 91, 4044.

31 Contor, C. R.; Schimmel, P. R.; *Biophysical Chemistry, pt 3*; W. H. Freeman and Co.. San Francisco, 1980.

32. Chung, C.; *Journ of Chem. Ed* ; **1984**, 61, 1062.

33. Brown, G.; et al.; "Selective Resins for Sorption of Technetium from Ground Water"; FY 1995 Letter Report Oak Ridge National Laboratory. Sept. 17, 1995

34 Pourbaix, M ; "Atlas of Electrochemical Equilibria," Pergamon Press. Oxford **1966**.

35. Hussain, L. M S Thesis, Univerisity of Tennessee, Knoxville, December 1996.

36. Ashley, K. R.; Ball, J.R., *Solv Extract and Ion Exch.* **1994**, 12(2), 239.

37. Garten, C. T., *Environ. Int* , **1987**, 13, 311.

38. Wilddung, R. E.; McFadden, K. M. and Garland, T. R.; *Journ. of Env. Qual.*; **1979**, 8, 156.

39 Robb, P.; Warwick, P ; Malcome-Lawes, D. J., *Radioanal. Nuc. Chem.*; **1985**; 89(2), 323.

40. Kapustinskii, A. F.; *Quarterly Reviews* 1956, 10,283.

41. Moyer, B. A.; Bonnesen, P. V ; *Supramolecular Chemistry of Anions-Chapt. 1* Wiley, **1997**.

42 Bhaskar, G.; Ford, J.; Hollingsbee, D. A.; *Thermochimica Acta*; **1998**, 322, 153.

43. Balci, S.; *Journ. Chem. Tech Biotech.* **1996**, 66, 72.

APPENDICES

A.1. Tabulated Kd and K'd (eq) for Resins Used in this Work

#	Resin Code	Backbone	Functionality (all Cl- form)	x-link %DVB	Exchange Capacity* mequiv/g	Matrix	Kd mL/g) (7-day)	K'd mL/mequiv (7-day)
1	MK-01-141	100 VBC	$(Hex)_3/(Et)_3$	5	2 142	TcO_4^-/ 1M Cl^-	152504	71197
2	MK-01-125	100 VBC	$(Hex)_3$	5	1 406	TcO_4^-/ 1M Cl^-	198822	141410
3	MK-02-261	100 VBC	$(But)_3$	5	2 085	TcO_4^-/ 1M Cl^-	86524	41499
4	MK-01-118	100 VBC	$(Et)_3$	5	3 065	TcO_4^-/ 1M Cl^-	11309	3690
5	MK-01-112	100 VBC	$(Me)_3$	5	4 031	TcO_4^-/ 1M Cl^-	2459	610
6	MK-02-259	100 VBC	$(Hex)_3/(Et)_3$	5	2 230	ReO_4^-/ 1M Cl^-	43456	19487
7	MK-01-141	100 VBC	$(Hex)_3/(Et)_3$	5	2.142	ReO_4^-/ 1M Cl^-	40025	18686
8	MK-01-125	100 VBC	$(Hex)_3$	5	1 406	ReO_4^-/ 1M Cl^-	*75101*	*53415*
9	MK-02-261	100 VBC	$(But)_3$	5	2 085	ReO_4^-/ 1M Cl^-	28967	13893
10	MK-01-118	100 VBC	$(Et)_3$	5	3 065	ReO_4^-/ 1M Cl^-	4932	1609
11	MK-01-112	100 VBC	$(Me)_3$	5	4 031	ReO_4^-/ 1M Cl^-	*1092*	*271*
12	MK-02-259	100 VBC	$(Hex)_3/(Et)_3$	5	2 230	I^-/ 1M Cl^-	*1824*	*818*
13	MK-01-141	100 VBC	$(Hex)_3/(Et)_3$	5	2.142	I^-/ 1M Cl^-	*1191*	*556*
14	MK-01-125	100 VBC	$(Hex)_3$	5	1 406	I^-/ 1M Cl^-	*3043*	*2164*
15	MK-02-261	100 VBC	$(But)_3$	5	2 085	I^-/ 1M Cl^-	1005	482
16	MK-01-118	100 VBC	$(Et)_3$	5	3 065	I^-/ 1M Cl^-	285	93
17	MK-01-112	100 VBC	$(Me)_3$	5	4 031	I^-/ 1M Cl^-	177	44
18	MK-02-259	100 VBC	$(Hex)_3/(Et)_3$	5	2 230	NO_3^-/ 1M Cl^-	58	26
19	MK-01-141	100 VBC	$(Hex)_3/(Et)_3$	5	2 142	NO_3^-/ 1M Cl^-	51	24
20	MK-01-125	100 VBC	$(Hex)_3$	5	1.406	NO_3^-/ 1M Cl^-	73	52
21	MK-02-261	100 VBC	$(But)_3$	5	2 085	NO_3^-/ 1M Cl^-	50	24
22	MK-01-118	100 VBC	$(Et)_3$	5	3 065	NO_3^-/ 1M Cl^-	28	9
23	MK-01-112	100 VBC	$(Me)_3$	5	4.031	NO_3^-/ 1M Cl^-	*16*	*4*

#	Resin Code	Backbone	Functionality (all Cl- form)	x-link %DVB	Exchange Capacity* mequiv/g	Matrix	Kd mL/g) (7-day)	K'd mL/mequiv (7-day)
24	MK-02-259	100 VBC	$(Hex)_3/(Et)_3$	5	2 230	Br^-/ 1M Cl^-	36	16
25	MK-01-141	100 VBC	$(Hex)_3/(Et)_3$	5	2 142	Br^-/ 1M Cl^-	30	14
26	MK-01-125	100 VBC	$(Hex)_3$	5	1 406	Br^-/ 1M Cl^-	35	25
27	MK-02-261	100 VBC	$(But)_3$	5	2 085	Br^-/ 1M Cl^-	23	11
28	MK-01-118	100 VBC	$(Et)_3$	5	3 065	Br^-/ 1M Cl^-	25	8
29	MK-01-112	100 VBC	$(Me)_3$	5	4.031	Br^-/ 1M Cl^-	24	6
30	MK-01-141	100 VBC	$(Hex)_3/(Et)_3$	5	2.142	NO_3^-/ 90mM Cl^-	574	268
31	MK-01-125	100 VBC	$(Hex)_3$	5	1 406	NO_3^-/ 90mM Cl^-	723	514
32	MK-01-136	100 VBC	$(But)_3$	5	2.096	NO_3^-/ 90mM Cl^-	493	235
33	MK-01-118	100 VBC	$(Et)_3$	5	3.065	NO_3^-/ 90mM Cl^-	239	78
34	MK-01-112	100 VBC	$(Me)_3$	5	4 031	NO_3^-/ 90mM Cl^-	169	42
35	MK-01-141	100 VBC	$(Hex)_3/(Et)_3$	5	2.142	Br-/ 90mM Cl^-	413	193
36	MK-01-125	100 VBC	$(Hex)_3$	5	1.406	Br-/ 90mM Cl^-	863	614
37	MK-01-136	100 VBC	$(But)_3$	5	2 096	Br-/ 90mM Cl^-	340	162
38	MK-01-118	100 VBC	$(Et)_3$	5	3.065	Br-/ 90mM Cl^-	227	74
39	MK-01-112	100 VBC	$(Me)_3$	5	4 031	Br-/ 90mM Cl^-	230	57
40	MK-01-141	100 VBC	$(Hex)_3/(Et)_3$	5	2.142	SO_4^{2-}/ 90mM Cl^-	6	3
41	MK-01-125	100 VBC	$(Hex)_3$	5	1.406	SO_4^{2-}/ 90mM Cl^-	3	2
42	MK-01-136	100 VBC	$(But)_3$	5	2 096	SO_4^{2-}/ 90mM Cl^-	10	5
43	MK-01-118	100 VBC	$(Et)_3$	5	3 065	SO_4^{2-}/ 90mM Cl^-	25	8
44	MK-01-112	100 VBC	$(Me)_3$	5	4 031	SO_4^{2-}/ 90mM Cl^-	85	21

*Exchange Capacity based on nitrogen elemental analysis

Conditions 5meq active site, 25 mL contact, $1 * 10^{-4}$M anion of interest

All studies done in duplicate with same resin batch unless otherwise indicated.

All percent differences between trials was 15% or less unless indicated by italics

#	Resin Code	Backbone	Functionality (all NO_3^- form)	x-link %DVB	Exchange Capacity* mequiv/g	Matrix	Kd mL/g) (7-day)	K'd mL/mequiv (7-day)
45	MK-01-141	100 VBC	$(Hex)_3/(Et)_3$	5	2 142	TcO_4^-/ 60mM NO_3^-	48681	22727
46	MK-01-125	100 VBC	$(Hex)_3$	5	1 406	TcO_4^-/ 60mM NO_3^-	58651	41715
47	MK-01-136	100 VBC	$(But)_3$	5	2 096	TcO_4^-/ 60mM NO_3^-	41306	19707
48	MK-01-118	100 VBC	$(Et)_3$	5	3.065	TcO_4^-/ 60mM NO_3^-	10455	3411
49	MK-01-112	100 VBC	$(Me)_3$	5	4 031	TcO_4^-/ 60mM NO_3^-	4087	1014
50	MK-01-141	100 VBC	$(Hex)_3/(Et)_3$	5	2 142	ReO_4^-/ 60mM NO_3^-	18389	8585
51	MK-01-125	100 VBC	$(Hex)_3$	5	1.406	ReO_4^-/ 60mM NO_3^-	23636	16811
52	MK-01-136	100 VBC	$(But)_3$	5	2 096	ReO_4^-/ 60mM NO_3^-	16611	7925
53	MK-01-118	100 VBC	$(Et)_3$	5	3.065	ReO_4^-/ 60mM NO_3^-	4122	1345
53	MK-01-112	100 VBC	$(Me)_3$	5	4 031	ReO_4^-/ 60mM NO_3^-	1600	397
54	MK-01-141	100 VBC	$(Hex)_3/(Et)_3$	5	2 142	ReO_4^-/ 90mM NO_3^-	14646	69
55	MK-01-125	100 VBC	$(Hex)_3$	5	1.406	ReO_4^-/ 90mM NO_3^-	17414	12385
56	MK-01-136	100 VBC	$(But)_3$	5	2.096	ReO_4^-/ 90mM NO_3^-	12187	5814
57	MK-01-118	100 VBC	$(Et)_3$	5	3 065	ReO_4^-/ 90mM NO_3^-	2897	945
58	MK-01-112	100 VBC	$(Me)_3$	5	4.031	ReO_4^-/ 90mM NO_3^-	1102	274
59	MK-01-141	100 VBC	$(Hex)_3/(Et)_3$	5	2 142	SeO_4^{2-}/ 60mM NO_3^-	-4	-2
60	MK-01-125	100 VBC	$(Hex)_3$	5	1 406	SeO_4^{2-}/ 60mM NO_3^-	1	0.5
61	MK-01-136	100 VBC	$(But)_3$	5	2 096	SeO_4^{2-}/ 60mM NO_3^-	2	1
62	MK-01-118	100 VBC	$(Et)_3$	5	3 065	SeO_4^{2-}/ 60mM NO_3^-	9	3
63	MK-01-112	100 VBC	$(Me)_3$	5	4.031	SeO_4^{2-}/ 60mM NO_3^-	40	10

*Exchange Capacity based on nitrogen elemental analysis

Conditions 5meq active site, 25 mL contact, $1 * 10^{-4}$M anion of interest

All studies done in duplicate with same resin batch unless otherwise indicated

All percent differences between trials was 15% or less unless indicated by italics.

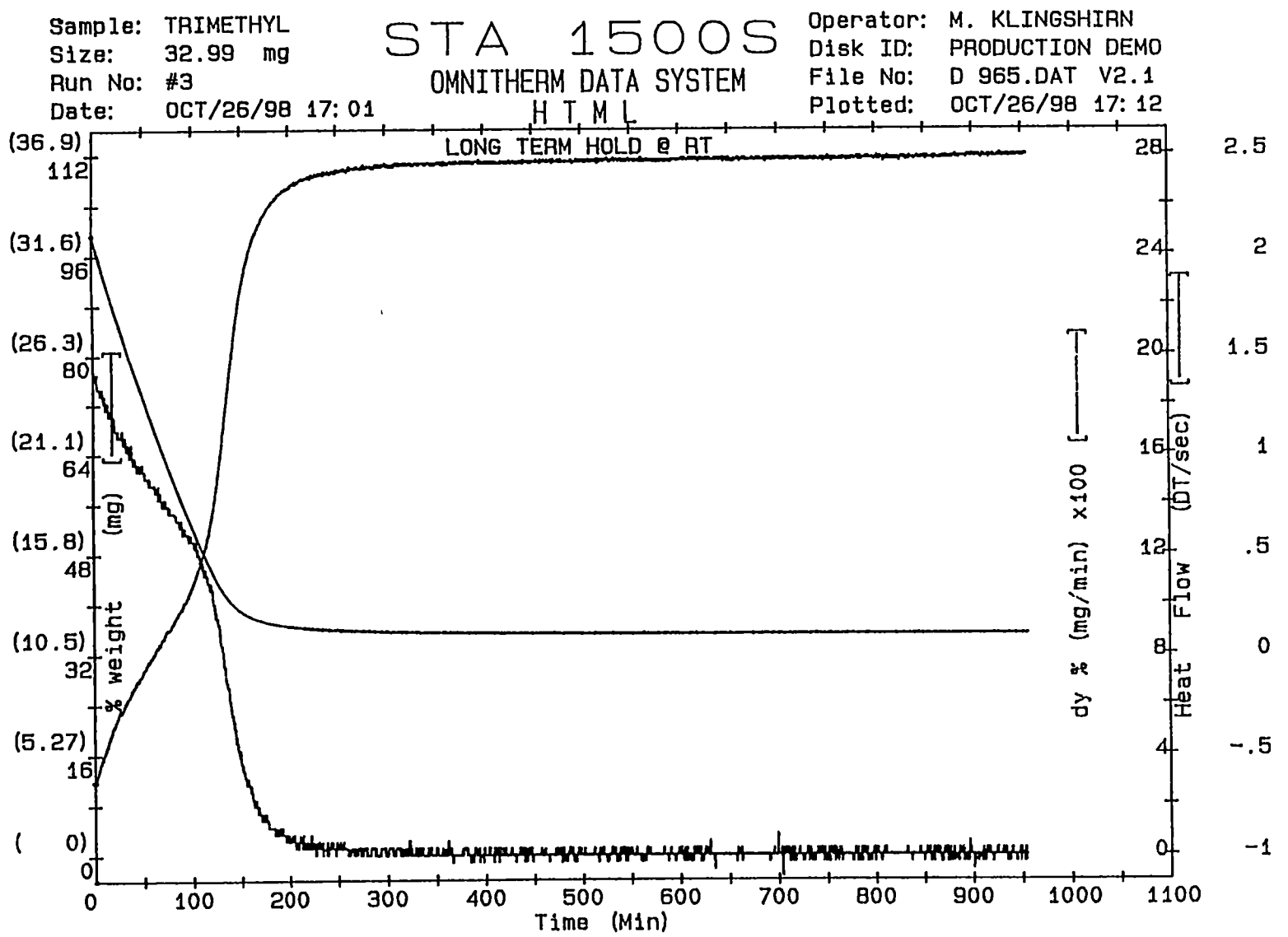
Sample: TRIMETHYL
Size: 32.99 mg
Run No: #3
Date: OCT/26/98 17:01
STA 1500S
OMNITHERM DATA SYSTEM
H T M L
Operator: M. KLINGSHIRN
Disk ID: PRODUCTION DEMO
File No: D 965.DAT V2.1
Plotted: OCT/26/98 17:12
LONG TERM HOLD @ RT
% weight (mg)
dy % (mg/min) x100
Heat Flow (DT/sec)
Time (Min)
(36.9)
112
(31.6)
96
(26.3)
80
(21.1)
64
(15.8)
48
(10.5)
32
(5.27)
16
(0)
0
28
24
20
16
12
8
4
0
2.5
2
1.5
1
.5
0
-.5
-1
0
100
200
300
400
500
600
700
800
900
1000
1100

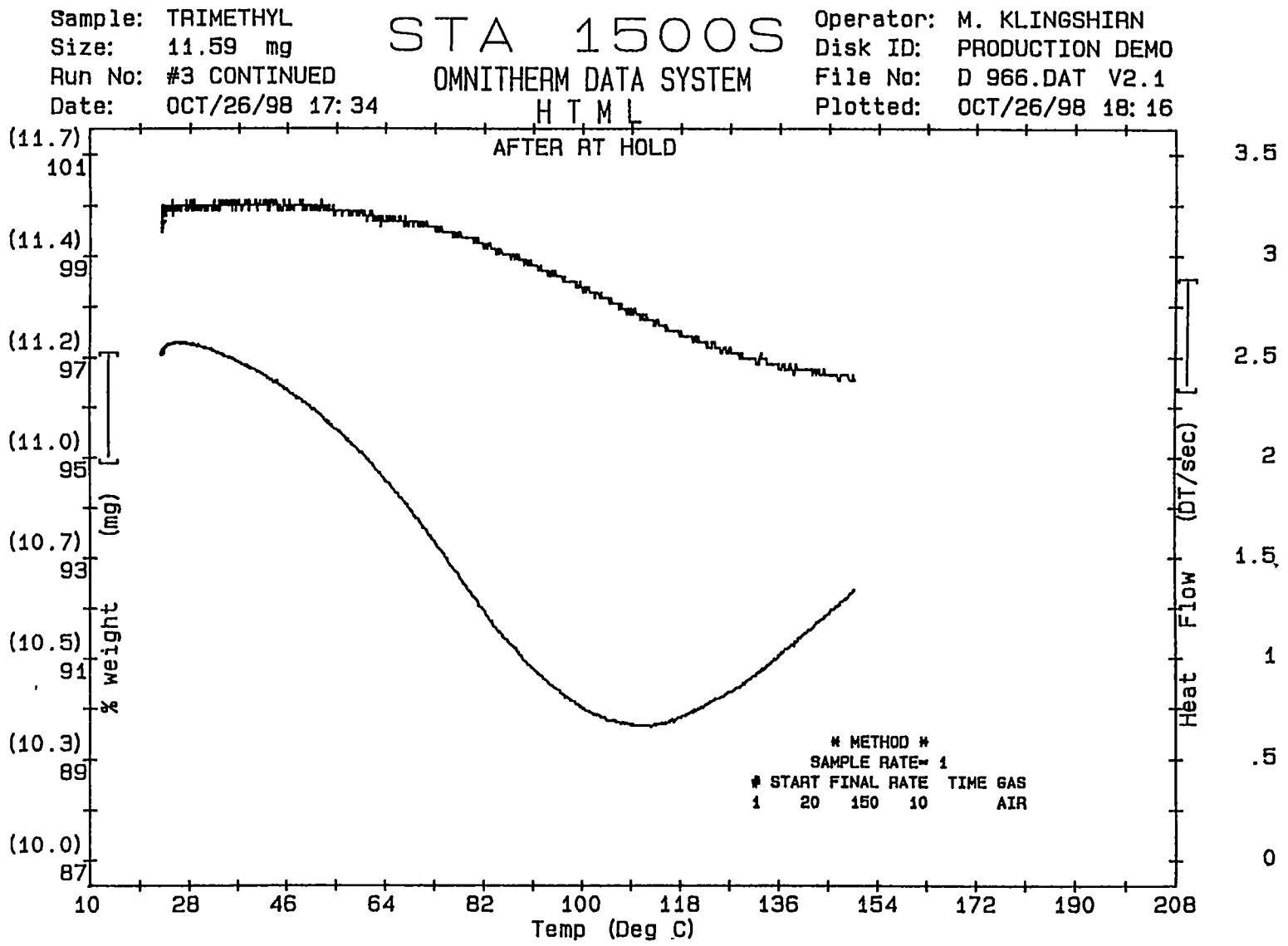
Sample: TRIMETHYL
Size: 11.59 mg
Run No: #3 CONTINUED
Date: OCT/26/98 17:34
STA 1500S
OMNITHERM DATA SYSTEM
H T M L
Operator: M. KLINGSHIRN
Disk ID: PRODUCTION DEMO
File No: D 966.DAT V2.1
Plotted: OCT/26/98 18:16
AFTER RT HOLD
(11.7)
101
(11.4)
99
(11.2)
97
(11.0)
95
(10.7)
93
(10.5)
91
(10.3)
89
(10.0)
87
% weight
(mg)
3.5
3
2.5
2
1.5
1
.5
0
Heat Flow (DT/sec)
10
28
46
64
82
100
118
136
154
172
190
208
Temp (Deg C)
* METHOD *
SAMPLE RATE= 1
START FINAL RATE TIME GAS
1 20 150 10 AIR

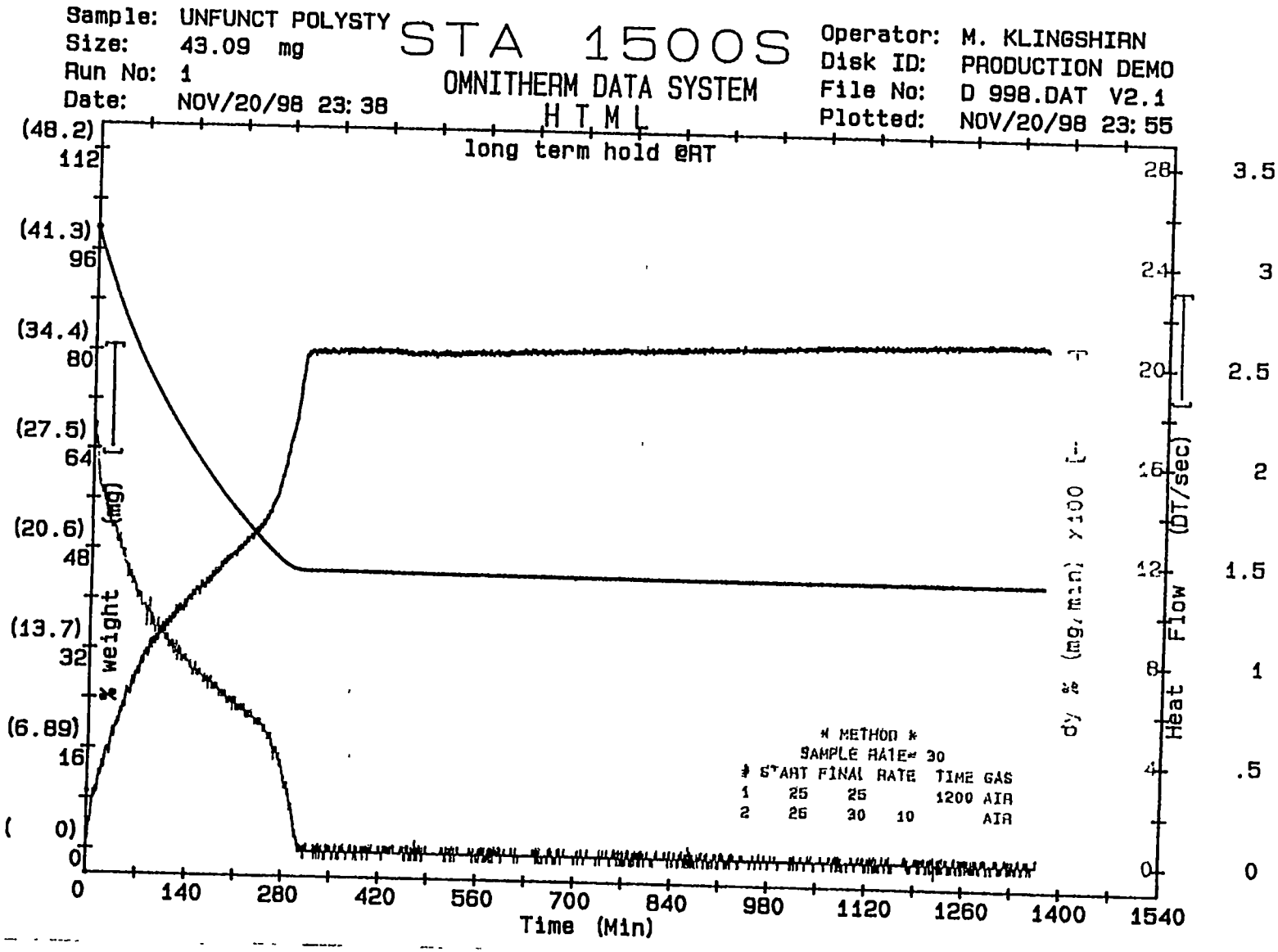
Sample: UNFUNCT POLYSTY
Size: 43.09 mg
Run No: 1
Date: NOV/20/98 23:38
STA 1500S
OMNITHERM DATA SYSTEM
H T M L
long term hold @RT
Operator: M. KLINGSHIRN
Disk ID: PRODUCTION DEMO
File No: D 998.DAT V2.1
Plotted: NOV/20/98 23:55
(48.2)
112
(41.3)
96
(34.4)
80
(27.5)
64
(20.6)
48
(13.7)
32
(6.89)
16
(0)
0
% weight
(mg)
0
140
280
420
560
700
840
980
1120
1260
1400
1540
Time (Min)
28
24
20
16
12
8
4
0
Heat Flow (DT/sec)
3.5
3
2.5
2
1.5
1
.5
0
dy/dt (mg/min) x100
* METHOD *
SAMPLE RATE= 30
START FINAL RATE TIME GAS
1 25 25 1200 AIR
2 25 30 10 AIR

A.2 Characterization Results of Resins Used in this Work (Theoretical Capacities in Parentheses)

Code	Copolymer	%-X-linking	Resin Type	Functionality	%-Solids	N-Capacity	Cl-Capacity	TAEC
MK-01-112	100% VBC	5	macroreticular	trimethyl	28 02	4 03 (4 07)	4 47	3.96
MK-01-118	100% VBC	5	macroreticular	triethyl	30 88	3 06 (3 62)	4 26	2 99
MK-01-136	100% VBC	5	macroreticular	tributyl	26 07	2 1 (2 70)	3 95	2 25
MK-01-125	100% VBC	5	macroreticular	trihexyl	34 71	1 41 2 16)	3 81	1 28
MK-01-141	100% VBC	5	macroreticular	trihexyl/ triethyl	41 64	2 14 (2 38)	3 57	2 13
MK-02-259	100% VBC	5	macroreticular	trimethyl	21 04	3 71 (4 07)	4 25	4 09
MK-02-260	100% VBC	5	macroreticular	triethyl	21 67	3 18 (3 62)	3 89	3 57
MK-02-261	100% VBC	5	macroreticular	tributyl	26 83	2 09 (2 70)	2 78	2 34
MK-02-266	100% VBC	5	macroreticular	trihexyl	40 25	1 75 (2 16)	3 30	1 05
MK-02-269	100% VBC	5	macroreticular	trihexyl/ triethyl	28 61	2 23 (2 38)	3 25	2 48
MK-02-105	100% VBC	5	gel	trimethyl	40 63	4 65 (4 07)	5 18	4 27
MK-02-155	5%VBC/ 95%STY	5	macroreticular	trimethyl	37 62	0 59 (0 42)	1 74	0 15
MK-02-091	18%VBC/ 82%STY	5	macroreticular	trimethyl	31 63	1 77 (1 39)	4 09	1 28
MK-02-092	50%VBC/ 50%STY	5	macroreticular	trimethyl	18 78	3 01 (3 23)	4 86	3 27
MK-02-154	75%VBC/ 25%STY	5	macroreticular	trimethyl	18 75	3 36 (3 67)	4 19	3 72
MK-03-023	100% VBC	5	gel	trimethyl	40 88	3 95 (4 07)	3 19	4 23
MK-03-016	5%VBC/ 95%STY	5	macroreticular	trimethyl	35 99	0 50 (042)	0 99	0 27
MK-03-017	18%VBC/ 82%STY	5	macroreticular	trimethyl	28 56	1 22 (1 39)	1 83	1 35
MK_03-024	50%VBC/ 50%STY	5	macroreticular	trimethyl	19 10	2 30 (3 23)	3 19	3 73
MK-03-019	75%VBC/ 25%STY	5	macroreticular	trimethyl	20 34	3 16 (3 67)	3 69	2 65

Code	Copolymer	%-X-linking	Resin Type	Functionality	%-Solids	P-Capacity	Acid Capacity
MK-01-035	100% VBC	5	macroreticular	alpha-ketophosphonic acid	39 19	3 13 (4 29)	9 14 (8 58)
MK-01-054	100% VBC	5	macroreticular	alpha-ketophosphonic acid	36 57	3 08 (4 29)	9 11 (8 58)
MK-01-094	100% STY	2	gel	beta-ketophosphonic acid	45 62	2 99 (4 02)	6 98 (8 04)
MK-01-083	100% STY	2	gel	gamma-ketophosphonic acid	53 14	2 81(3 79)	6 7 (7 58)
MK-01-026	100% VBC	2	gel	phosphonic acid	53 36	4 36 (4 59)	9 55 (9 18)

VITA

Marc A. Klingshirn was born in Oberlin, Ohio on September 4, 1974. After graduating from Wellington High School in Wellington Ohio in 1992, he continued his education at Ashland University in Ashland, Ohio where he double majored in Chemistry and Environmental Science. He then graduated with his Bachelor of Science degree in May of 1996. In August of 1996, he accepted a teaching and research assistantship from the Department of Chemistry at the University of Tennessee, Knoxville where he began work toward a Master of Science degree in Environmental Chemistry. The degree was awarded in May of 2000.